THE AMERICIUM/LANTHANIDE SEPARATION CONUNDRUM: SELECTIVE

OXIDATION OR SOFT DONOR COMPLEXANTS?

By

THOMAS CHARLES SHEHEE

A dissertation submitted in partial fulfillment of
the requirements for the degree of

Doctor of Philosophy

WASHINGTON STATE UNIVERSITY
Department of Chemistry

May 2010

To the Faculty of Washington State University:

The members of the Committee appointed to examine the dissertation of
THOMAS CHARLES SHEHEE find it satisfactory and recommend that it be accepted.

_____
Kenneth L. Nash, Ph.D., Chair

_____
Sue Clark, Ph.D.

_____
Dean Peterman, Ph.D.

_____
Scot Wherland, Ph.D.

ACKNOWLEDGMENT

THE AMERICIUM/LANTHANIDE SEPARATION CONUNDRUM: SELECTIVE

OXIDATION OR SOFT DONOR COMPLEXANTS?

Abstract

by Thomas Charles Shehee, Ph.D.
Washington State University
May 2010

Chair: Kenneth L. Nash

The key to managing the disposal of used nuclear fuel is not to consider it as a waste but rather as a resource. In a closed nuclear fuel cycle, the removal and transmutation of high specific activity isotopes can be accomplished to reduce the radiation levels of high level wastes to near uranium mineral levels after a few hundred years. Dissolved used nuclear fuel mixtures include U, Np, Pu, trivalent transplutonium actinides and lanthanides and other fission products, representing a total of about 1/3 of the periodic table. Americium, being a long-lived α-emitter, is the greatest contributor to the radiotoxicity of the waste in the 300-70,000 year time frame after removal from the reactor. The lanthanides, representing about 40% of the mass of fission products, are neutron poisons. They interfere with the transmutation process, necessitating removal before transmutation of the waste can be performed. The mutual separation of Am from chemically similar lanthanides remains one of the largest obstacles to the implementation of a closed nuclear fuel cycle in which Am is transmuted.

Two possible pathways exist that could be utilized in the separation Am from Cm and the lanthanides. These pathways make use of selective oxidation of the actinide or soft donor complexants to perform a given separation. This dissertation contains a description of kinetics of

lanthanide complexation and redox adjustment of americium followed by precipitation of the lanthanide to achieve actinide separations. The separations will be based on oxidation states and soft donor effects. Separations that will be performed in an advanced fuel cycle will take advantage of both of these aspects to make a successful reprocessing scheme.

TABLE OF CONTENTS

Appendix

LIST OF FIGURES

Chapter 6

Appendix

DEDICATION

This dissertation is dedicated to multiple people. To my grandparents, Fred and Florence Gilbert and Herbert and Alice Shehee, who taught me the appreciation for hard work and maybe a bit of stubbornness that helped me get through this degree. To my parents, here is another book to adorn your shelves. Thank you for the support you provided on this long and winding road. I also have to dedicate this work to my wife Kelly who helped me get over this mountain and was able to help me maintain sanity through it all. Finally, I would like to dedicate this work to James C. Sullivan, "Sully", whose 60 years in this field was a valuable asset though, the time I had to learn from him was brief, I learned a lot (not just chemistry). He will be missed.

Chapter 1

Introduction

The purpose of this research project is to aid the management of nuclear waste through the removal of americium from used nuclear fuel to reduce the radiation levels of high level waste to near uranium mineral levels. The composition of used fuel varies with burn-up of the fuel as well as the cooling time. Depending on the burn-up of the fuel, americium-241 increases since it is a daughter product of the 14.4yr ^{241}Pu with 579 g/ton being accumulated in ten years. Americium is the greatest contributor to the radiotoxicity of the waste in the 300-70,000 year time frame after removal from the reactor, making it very important to remove and destroy prior to disposal of any waste. The lanthanides, being neutron poisons, must be removed from the actinides before the latter can be burned in a fast spectrum reactor or transmuted.

Many processes have been used throughout the atomic age for plutonium production as well as for recycling purposes. The use of selective oxidation and/or soft donors will be and has been part of any reprocessing scheme. The use of soft donors has been the typical approach, though the alternative approach might be to selectively separate Am from Cm and fission product lanthanides by selectively adjusting the oxidation state of Am to the accessible upper oxidation states, of which the tetra-, penta- and hexavalent oxidation states are known.

This introduction will look at the basic actinide chemistry, features of separations, the fuel cycle (both foreign and domestic), thermodynamic vs. kinetic control, objectives for separation and TALSPEAK and redox/precipitation for Am from Cm/Ln separation.

Basic actinide solution chemistry for aqueous separations

History

      In a relatively short time period, the majority of the elements now known collectively as actinides were synthesized or discovered. The elements U, Th, Pa and Ac had all been discovered in 1789, 1829, 1899 and 1913.[1] The remaining actinides, Np – Lr, were identified from 1940 to 1961.[1] Interestingly, knowing the rich chemistry of the actinides, uranium was described in chemistry books as being used primarily for coloring glass prior to 1940. With the onset of World War II, this all changed.

Chemistry

      In Figure 1 shown below, the redox chemistry of the actinides is demonstrated. Typically the actinides exist in four main oxidation states; tri-, tetra-, penta- and hexavalent – lanthanides are primarily trivalent. Further, in a given oxidation state, actinides behave similarly. At Am the upper oxidation states are still accessible; however, it is also known that oxidized Am species are strong oxidants, thus readily reduced in conventional acidic aqueous solutions.
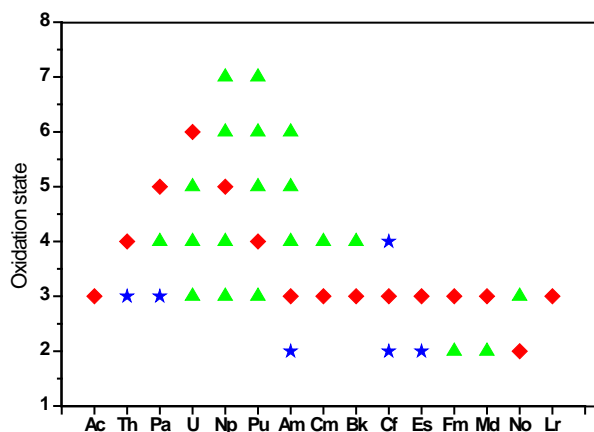
Figure 1: Diamonds depict the most stable oxidation state, triangles represent other oxidation states and stars denote oxidation states only observed in solids

Actinium to americium typically exhibit transition metal-like behavior. Trivalent americium is the most stable oxidation state with penta- and hexavalent states essentially nonexistent in acid solution. As with the lanthanides, an actinide contraction exists wherein the ionic radii of the trivalent cations decrease with an increase in the atomic number. This contraction is generally attributed to the incomplete shielding of the outer electrons, provided by the f electrons, from the steadily increasing nuclear charge. The probability of complex formation and hydrolysis increases with an increase in the atomic number. The complexes formed with the actinides are quite ionic in character yet are more covalent than the lanthanides. Typically the stability of complexes formed with actinides follow the trend $M^{4+} > MO_2^{2+} \geq M^{3+} > MO_2^+$.[2]

Features of an actinide/lanthanide separation

Before a separation can be performed, a method must be found to increase the stability of the oxidized americium species. If their stability could be improved, development of a viable aqueous separation procedure for the selective removal of Am from Cm and the lanthanides becomes possible. Furthermore, there are known approaches that involve (at an analytical scale) solid-liquid separations are known – e.g. oxidized actinides stay in solutions while reduced lanthanides precipitate. Addressing the potential of this approach is the primary goal of this research. How might we stabilize oxidized Am species?

Complexing ligands such as CO_3^{2-} can form strong complexes with the actinides in the order $An^{4+} > AnO_2^{2+} \geq An^{3+} > AnO_2^+$. Compounds containing carbonate have been synthesized and characterized for Am(III) and Am(V) as solids.[3] In aqueous carbonate solutions americium has been shown to form species in all four oxidation states (III, IV, V and VI), whereas only the aquo ions Am^{3+} and AmO_2^{2+} are stable in dilute acid solutions. The actinides typically interact

3

more strongly than the lanthanides with softer donor atoms. The hard soft terminology is based on the hard soft acid base theory. Hard acids and bases are small and non-polarizable whereas soft acids and bases are larger and more polarizable. The overall objective is to determine whether this chemistry can be used to develop fresh approaches to actinide - lanthanide separations.

<u>Redox</u>

Production of the hexavalent americium is paramount in the separations that will be presented in this work. The tetravalent americium is unstable in non-complexing solutions but has been shown to be stable in phosphoric and pyrophosphate media[4] and has been observed as a transient species using pulse radiolysis.[5,6] Pentavalent americium solutions have been prepared through an oxidation of Am(III) in near neutral to alkaline solutions. Solid $NaAmO_2CO_3$ can be precipitated from a solution of 2 M sodium carbonate at 90°C. Also, if a previously prepared Am(VI) solution is heated to 90°C in 2 M Na_2CO_3, the Am will be reduced to Am(V) forming the sodium americyl(V) carbonate.[7] A pure solution of Am(V) free of both Am(III) and Am(VI) can be prepared by dissolving this solid in near neutral conditions.

Am(VI) has been produced in aqueous solution by oxidation of Am(III), Am(IV), or Am(V) with ozone giving an intensely red-brown soluble Am(VI) carbonate complex.[7] The hexavalent complex, $AnO_2(CO_3)_3^{-4}$ ion, has been observed in U, Pu and Np and becomes the dominate species at relatively low carbonate concentrations between pH$\approx$ 7 and about 11.[8-10] At higher pH values, mixed hydroxyl-carbonates of UO_2^{2+},[11,12] NpO_2^{2+} [13] and PuO_2^{2+} [14,15] have been reported. The stability of uranyl triscarbonato ion $UO_2(CO_3)_3^{-4}$ allows its application to in situ leaching with carbonate as an effective mining and decontamination tool.[16-18] It has been shown that the limiting species for Am(VI) in carbonate containing solution is $AmO_2(CO_3)_3^{-4}$.[3,19] To add

to the complexity of this system, a soluble tetra-hydroxide species has been identified as the dominant species at pH 12-14.[20-22]

Curium (III) is difficult to oxidize to the tetravalent oxidation state, Equation 1.

$$Cm^{4+} + e^- \leftrightarrow Cm^{3+} \qquad\qquad E° = 3.1V \qquad\qquad\qquad (1)$$

The penta- or hexavalent oxidation states are not accessible in aqueous solutions as shown in Figure 1. Likewise only a few of the lanthanides, Ce, Pr and Tb, can be oxidized to the tetravalent oxidation state and all Ln(IV) are strong oxidants. Cerium, which is the most stable tetravalent lanthanide, has a standard reduction potential (E° = 1.72V) that would make its presence probable when strong oxidizing agents such as persulfate and ozone are used.

It is conceivable that application of this approach (stabilizing Am(V or VI)) through the introduction of carbonate or sulfate could create new options for efficient separation of the lanthanides plus curium from americium. Though it has been proven to form complexes with the actinides in all oxidation states and allows for oxidation to occur while complexed, carbonate use alone may not lead to a complete separation. Other reagents, such as H_2O_2, may be required to facilitate a complete separation. In the case of H_2O_2, complexes such as $K_3UO_2(CO_3)_2OOH$ have been reported.[22] This study must include a thorough evaluation of conditions: pH, temperature, concentrations or facilitating agents. The pH can be controlled in the range of 9.5 to 11.5 through a change in the ratio of $[HCO_3^-]$ and $[CO_3]^{2-}$. A problem in this system is that the rate the U(VI) peroxo complex formation has been found to be slower in bicarbonate media than in sodium carbonate media possibly due to a pre-equilibrium step prior to addition of H_2O_2.[22] Stability constants for europium and uranyl in carbonate and sulfate containing solutions are presented in Table 1.

Table 1: Stability constants for speciation plots

	Uranium [a,c]		Europium [b,d]	
	$\log \beta\ (CO_3^=)$ [f]	$\log \beta\ (SO_4^=)$ [h]	$\log \beta\ (CO_3^=)$ [e]	$\log \beta\ (SO_4^=)$ [g]
ML	9.68	3.2	5.88	2.63
ML_2	16.94	4.3	10.4	3.71
ML_3	21.6	6.3	13.1	-
ML_4			14.95	
M_2L_3			-31.8 (s) ($\mu = 0.1$) [i]	-5.4 (s) (μ = unk) [i,23]
NaML(s)				-5.8 (s) [i]

	Uranium [d]		Europium [d]	
	$\log \beta$ (EDTA)	$\log \beta$ (DTPA)	$\log \beta$ (EDTA)	$\log \beta$ (DTPA)
ML ($\mu = 0.1$)	9.28	-	17.25	22.39

a) Values for UO_2^{2+} - $\mu = 0$ and T = 25°C - All aqueous unless otherwise noted

b) All values for Eu speciation - $\mu = 1$ and T = 25°C unless otherwise noted

c) Stability constants found in Chemical Thermodynamics of Uranium [26]

d) Stability constants found in the Martell and Smith Database [27]

e) Eu carbonate products - $xM^{3+} + yCO_3^{2-} \leftrightarrow M_x(CO_3)_y^{3x-2y}$

f) UO_2^{2+} carbonate products – $xM^{2+} + yCO_3^{2-} \leftrightarrow M_x(CO_3)_y^{2x-2y}$

g) Eu sulfate products - $xM^{3+} + ySO_4^{2-} \leftrightarrow M_x(SO_4)_y^{3x-2y}$

h) UO_2^{2+} sulfate products – $xM^{2+} + ySO_4^{2-} \leftrightarrow M_x(SO_4)_y^{2x-2y}$

i) Solubility product general form: ML(s) $\leftrightarrow$ M + L

Soft donors

Successful aqueous processing options for separation of fission product lanthanides (radioactive lanthanides produced during fission) from trivalent actinides rely on the use of the ligand donor atoms N, S, and Cl⁻, which are softer than oxygen.[23] Early separation success using cation exchange resins was attributed to the enhanced covalency of An(III) bonds relative to Ln(III) bonds. An even better separation was achieved through the use of soft donor ligands such as thiocyanate.[24] This increased separation ability rests on the small covalency that exist between

the soft ligand donor atoms and trivalent actinides.[24] This increase in covalency provides a slightly greater strength of complexation of trivalent actinides over lanthanides and provides enough thermodynamic driving force for a separation to occur. Stability constants for europium and uranyl in EDTA and DTPA containing solutions are presented in Table 1.

Nuclear Fuel Cycle

General Fuel Cycle characteristics

The term "fuel cycle" was originally coined for the steps in which fertile and fissile material would be recovered from used fuel and returned to the front end of the cycle for use in new fuel elements. Creating a nuclear fuel cycle is very important to the future of the nuclear industry as well as the energy needs of the world. Some countries with nuclear power capability, France, Japan, Russia, India and the UK are interested in and actively pursuing reprocessing of their used nuclear fuel. Canada, the US, Sweden, Germany, and Finland do not reprocess used fuel. The US and Canada use a uranium once-through cycle (UOT) which leads to the placing of un-reprocessed used fuel in final storage. On February 5, 2009, the Swedish government announced in a statement that it intends to reverse the country's long-standing ban on nuclear energy, which was to shut down its fleet by 2010, and allow the building of new nuclear reactors to gradually replace its existing nuclear fleet.[28] Sweden also has well-developed plans to build a repository for the waste that has been accumulated to date.[29] Germany now sends all of its waste to France to be reprocessed. To create closed fuel cycle capability in the U.S., several aspects must be evaluated: the cooling time prior to reprocessing of freshly discharged fuel, the burn-up of the fuel, the original make-up of the fuel, the methods used for reprocessing, the location of reprocessing facilities, and what types of reactors will be used in the future. The main purposes of reprocessing commercially are: 1) to increase utilization of the available energy from fissile

7

and fertile atoms; 2) to reduce long term hazards and cost for handling high level wastes as it relates to repository space; 3) to reduce overall cost of the thermal reactor fuel cycle; 4) to extract valuable byproducts from the high active waste.[29]

Prior to 1975 some countries applied direct disposal to ground waters or the oceans as a way to deal with low level waste (LLW) generated in nuclear power plants, reprocessing plants, and fuel fabrication plants, believing that natural dilution would lower radionuclide concentrations to below the maximum permissible values for general population exposure.[30] High level waste (HLW) was sent to some type of interim storage, either waste tanks or cooling pools. It is reasonable to accept the level of radioactivity of the uranium when mined should be taken as the "de minimis" level of radioactivity for establishing an adequate reduction of radiotoxicity. The total amount of time that is required for the waste to reach the radioactivity level of natural uranium will be more than 10 million years with no reprocessing, as shown in Figure 2.
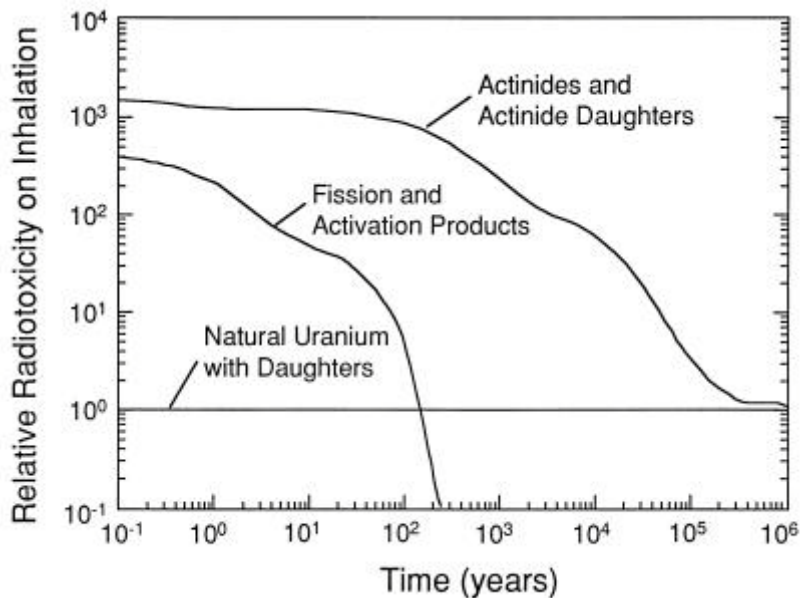
Figure 2: Toxicity from ingestion as a function of decay time for several nuclides in spent LWR fuel.[31]

Fission products such as cesium, strontium and the rare earths are the dominant sources of radioactivity and heat in used fuel for ~300 years.[32] The radionuclides ^{239}Pu, ^{240}Pu, ^{238}Pu, ^{241}Am, ^{151}Sm, ^{237}Np, and ^{99}Tc are major sources after 300 years.[32] After 10,000 years ^{239}Pu, ^{240}Pu, ^{243}Am, ^{237}Np, and ^{99}Tc are the main radionuclides of concern and after 100,000 years ^{242}Pu, ^{237}Np, ^{99}Tc, ^{234,235,238}U and their decay daughters.[32] Some countries are actively recycling the waste that is produced through energy production for civilian use. In France, 1100 MtHM/yr of used fuel is discharged from the French PWRs and 1600 metric tons of used fuel, are being reprocessed each year from both French and foreign sources.[33] The current US policy incorporates a once through option for the fuel which sends used fuel to a cooling pool then to a repository, which has yet to be licensed for operation.

Fuel cycle in US

The better means for disposal of used fuel or other waste generated in nuclear facilities should incorporate steps to reprocess, which allows for the recovery of useful isotopes or a preparation for other isotopes to be transmuted. Waste disposal in the current U.S. nuclear fuel cycle allows for the used fuel to cool in a cooling pool before being sent to a more permanent fuel storage site. Unfortunately, despite more than 30 years of study, a permanent storage location has not been commissioned for use. Storage in the cooling pool was only intended to be short-term solution to allow for the waste to cool thermally and reduce the radioactivity. This option for dealing with used nuclear fuel is termed the Uranium Once-Through (UOT) cycle. In this option, the energy content of unused ^{235}U, fertile ^{238}U, and fissile and fertile plutonium is disposed of as waste. At the present, this is considered the cheapest option available. It also withholds plutonium from possible use in weapons, at least for some time. The Nuclear Waste

Policy Act of 1982 outlined the responsibilities of reactor operators and interim waste disposal as follows.[34]

- the persons owning and operating civilian nuclear power reactors have the primary responsibility for providing interim storage of used nuclear fuel from such reactors by maximizing, to the extent practical, the effective use of existing storage facilities at the site of each civilian nuclear power reactor, and by adding new onsite storage capacity in a timely manner where practical;

- the Federal Government has the responsibility to encourage and expedite the effective use of existing storage facilities and the addition of needed new storage capacity at the site of each civilian nuclear power reactor; and

- the Federal Government has the responsibility to provide, in accordance with the provisions of this subtitle, not more than 1900 metric tons of capacity for interim storage of used nuclear fuel for civilian nuclear power reactors that cannot reasonably provide adequate storage capacity at the sites of such reactors when needed to assure the continued, orderly operation of such reactors.

This same act also provided guidelines for the identification of a process for solidifying high level radioactive waste or packaging used nuclear fuel as well as an estimate of

- the total repository capacity required to safely accommodate the disposal of all high-level radioactive waste and used nuclear fuel expected to be generated through December 31, 2020, in the event that no commercial reprocessing of used nuclear fuel occurs, as well as capacity if reprocessing does occur;

- the number and type of repositories required to be constructed to provide such disposal capacity;

- a schedule for the construction of such repositories; and

- an estimate of the period during which each repository listed in such schedule will be accepting high-level radioactive waste or used nuclear fuel for disposal.

Despite having considered the fuel cycle and having provided an outline of what should be done, the U.S. appears to be at a standstill when it comes to developing a closed nuclear fuel cycle. Similar to CO_2 reduction, current consensus has developed in the world that disposal of nuclear waste should be in the country and paid for by the country where the energy was produced. The popular idea for final waste disposal is in geologic formations like rock salt, crystalline rock (granite), volcanic tuff or clay. Key features of these formations that are required include; 1) geologic stability of the region, 2) absence of large fractures or holes, 3) impermeability to surface water, 4) negligible groundwater circulation, 5) good heat conductivity, and 6) remote location.[29] The U.S. national repository that is slated to be opened at Yucca Mountain has been met with considerable opposition. The projected date that the facility will begin to accept nuclear waste should be 2010 if licensing is approved with decommissioning in the year 2110.[35] After being identified by Congress as the first site to be evaluated as a repository, the top priority for Nevada's governors and congressional delegation has been to oppose the sighting of a nuclear waste repository at Yucca Mountain.[36] The key component in the arguments against a repository at Yucca Mountain is the uncertainty of containment. Due to the ongoing attempts to stop the opening of the repository, the proposed opening and decommissioning dates most likely will continue to move further into the future. Present status is that all funding for continued development has been suspended. Therefore, the storage of used fuel at the generating facilities will continue until a solution has been found for the used fuel.

Currently there are two acceptable storage methods for used fuel after it is removed from the reactor core[34]:

- Used fuel Pools - Currently, most used nuclear fuel is safely stored in specially designed pools at individual reactor sites around the country.

- Dry Cask Storage - When pool capacity is reached and supplemental cooling is no longer needed, licensees may move toward use of above-ground dry storage casks.

Figure 3: Locations of Independent Used fuel Storage Installations in the US[34]

Historical and Next Generation Reprocessing Variants

Historical reprocessing systems have focused on removing the fissile or fertile material from used fuel in acidic media. Processes, such as PUREX and TRUEX, rely on the redox differences for mutual partitioning of the actinides from themselves and other fission products. The PUREX (**P**lutonium **U**ranium **R**ecovery by **Ex**traction) process uses a mixture of tributyl phosphate (TBP) shown in Figure 4 and high boiling hydrocarbon diluents such as kerosene or n-dodecane to extract uranyl nitrate [$UO_2(NO_3)_2$] (Equation 2) and tetravalent plutonium nitrate

$[Pu(NO_3)_4]$ (Equation 3) from an aqueous solution containing nitric acid.[30,32,37] Once extracted, the Pu(IV) is stripped to a new aqueous phase by reduction to Pu(III) with U(IV) or Fe(II) sulfamate. The uranium is preferred since it remains in the organic phase creating a pure plutonium product.

$$UO_2^{2+} + 2NO_3^- + 2TBP \leftrightarrow UO_2(NO_3)_2 \cdot 2TBP \qquad (2)$$

$$Pu^{4+} + 4NO_3^- + 2TBP \leftrightarrow Pu(NO_3)_4 \cdot 2TBP \qquad (3)$$
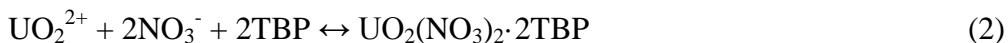
The PUREX process is very selective for U and Pu. PUREX was originally designed to extract Pu for weapons production and is well known due to 60 years experience with this process. The controversy associated with the PUREX process stems from its original use of separating weapons grade plutonium. Due to the concern over weapons proliferation, this process is not considered to be a viable alternative for a commercial U.S. fuel cycle. All neptunium is rejected into the HLW as inextractable Np(V), though oxidation state adjustment is often required to achieve this goal.[3]
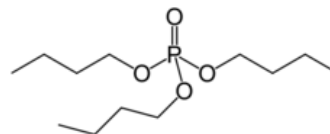
Figure 4: Molecule of Tributyl phosphate (TBP)

The TRUEX (**TR**ans**U**ranic **EX**traction) process, developed at Argonne National Laboratory and designed to remove Am, Cm and the lanthanides from the PUREX raffinate, could be employed to isolate Am/Cm and the lanthanide fission products, or these so-called "minor actinides" could be sent directly to a repository for disposal. If the TRU's are sent to a repository it should not be a permanent disposal, but a secure interim storage that will allow recovery of the plutonium and other transuranics at a later date.

The separation of americium from the lanthanides has proven a challenge in acidic solution. Most approaches to accomplishing this separation have relied on the slightly greater

strength of interaction of trivalent actinides with ligand donor atoms softer than oxygen. The TALSPEAK process, which was developed during the 1960s at Oak Ridge National Laboratory is, at present in the US, considered the best option for the transmutation-enabling separation of trivalent Am and Cm from fission product lanthanides.[38] In the design of proliferation-resistant fuel cycles, a modified PUREX process, UREX, removes uranium and technetium from dissolved used fuel while leaving the plutonium behind with the other transuranics and fission products. The separation begins with the addition of acetohydroxamic acid (AHA) to reduce the Pu to the trivalent state. Pu(III) is not appreciably extracted into TBP from molar concentrations of HNO_3. Uranium (Equation 2) and technetium (Equation 4) are extracted into the TBP (tributyl phosphate) with a separation of ~ 99.9% of the uranium and >95% of technetium from each other and the other fission products and actinides.[32]

$$3TBP + H^+ + TcO_4^- \leftrightarrow (HTcO_4.3TBP) \tag{4}$$
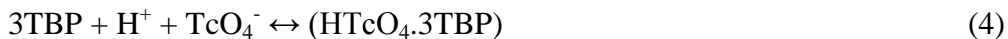
The technetium is stripped using 10 M HNO_3. The uranium is stripped with 0.01M HNO_3. The recovered uranium can then be used to make new fuel elements after re-blending to increase the content of fissile material. Plutonium and the other transuranics (TRU) remain with the fission products, which in the simplest UREX option can be disposed of in a repository as high level waste. The removal of some of the fission products and TRU's will lower the heat and radioactivity of the waste allowing for a more efficient use of a repository. For instance, strontium is a short-term heat generator and cesium is a gamma emitter that adds to the problem of radiolysis. These elements can be extracted as a further separation in UREX using chlorinated cobalt dicarbolide (CCD) and polyethylene glycol (PEG) or an alternative such as a calixarene-based process, FPEX.[39] Much of the research in CCD-based solvent extraction has utilized 0.5 - 1.0 M guanidine carbonate and 0.02 - 0.04 M diethylenetriamine pentaacetic acid (DTPA) to

simultaneously strip the Cs, Sr, actinides, and lanthanides from the solvent. The drawback of this method is that the resulting strip product contains considerable amounts of organic compounds: 90-200 g/L guanidine carbonate and 10-20 g/L DTPA resulting in an increase in the solidified strip products.[40] By combining the processes previously mentioned, removal of the major contributors of the heat load and radiotoxicity of the waste can be achieved. The UREX+1a scheme, which includes each of the processes as separate "unit operations," is shown in Figure 5.[41]
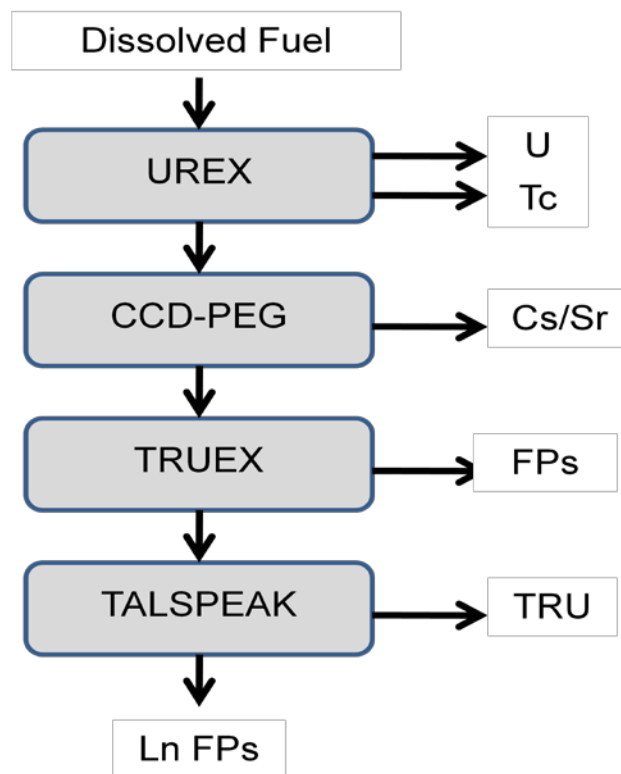
Figure 5: UREX +1a reprocessing scheme

This scheme is a frontrunner for separation of isotopes in used nuclear fuel where the raffinates from each unit operation is treated as a waste, material for new fuel rods, or destined for transmutation then disposal. By retrieving this material when better separation techniques are available or installation of thermal or fast reactors is a reality, most of the TRU inventory will be kept out of the repositories, thus extending the lifetime of a repository.[37] Even with reprocessing,

there will be waste products that will need to be disposed of somewhere though no repository has been commissioned to date.

Legacy waste

Since the beginning of the nuclear age, waste products have been accumulating. The waste is not only in the form of used fuel assemblies, but also aqueous and solid waste forms from early cold war weapons production. An example of this is the waste present in Hanford Tanks that resulted from raffinates of plutonium production processing, which were initially acidic, were made alkaline through addition of excess NaOH prior to disposal to the underground tanks. Alkaline conditions favor the precipitation of the metal species as well as reducing corrosion of the carbon steel liner of the tanks. The wastes in these tanks at the Hanford Site have stratified into three layers over time. A solid crystalline phase that is made predominantly with sodium salts of $CO_3^=$, $SO_4^=$, NO_2^-, NO_3^-, PO_4^{3-}, and OH^- makes up the upper phase. The bottom layer which is considered sludge is composed of oxide, hydroxide, sulfate, phosphate, and silicate solids of metallic fission products, actinides, cladding materials, and tank corrosion products. The supernatant phase in the middle is composed of a saturated aqueous solution/slurry that is defined by the salt cake above, the sludge phase below, and the amount of water present in any given tank.[42] All of this adds to the complexity of the problem before us. This waste remediation must also be considered in scenarios of the development of a closed nuclear fuel cycle.

Thermodynamics vs. kinetic control in separations

Favorable thermodynamic parameters determine whether a reaction will occur as written, but they do not necessarily provide an indication of how fast the reaction will occur. Likewise, mechanistic information cannot be derived from thermodynamic parameters. Studies of the

kinetics of a reaction offer molecular scale insights into the pathway a reaction might take. Activation parameters provide additional insights into these features. Figure 6 demonstrates graphically the reaction path of a simulated reaction. Thermodynamics provides information on starting and ending points of a reaction or whether a reaction occurs or not. It does not however provide any rate data and no molecular level details. Kinetics can define the pathway of the reaction as well as the molecular interactions involved.
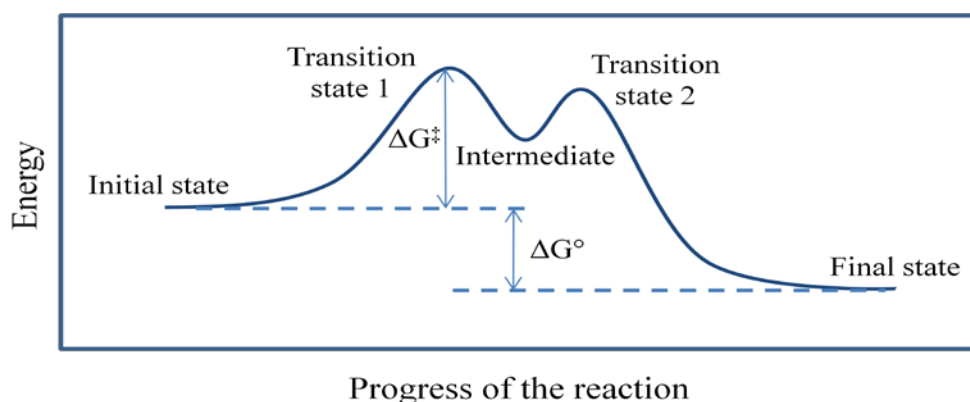
Figure 6: Generic plot showing the advantages of studies of the kinetics of a system.

Knowledge of the rates and mechanism of complexation or decomplexation of DTPA and EDTA with the lanthanides will be productive for understanding the separation potential of the lanthanides from the actinides. Relative to the thermodynamics of actinide and lanthanide complexation, a small number of studies of the complexation kinetics of Ln or An reaction have been completed. Most of the work reported has addressed the complexation of polydentate chelating agents. These studies have relied on a ligand displacement technique that makes use of a highly colored indicator ligand such as chlorophosphonazo III[43,44] or Arsenazo III[45,46]. These studies have all been performed in acidic media, yet little to no work has studied the complexation of EDTA or DTPA with the lanthanides under neutral to basic conditions as found in some tank waste at locations such as the Hanford Site.

Objectives for separations in an advanced fuel cycle

<u>Am and Cm from Ln</u>

The separation of americium from the lanthanides has proven a challenge in acidic solution. Approaches that accomplish the actinide/lanthanide separation have relied on the slightly greater strength of interaction of trivalent actinides with ligand donor atoms softer than oxygen. As previously mentioned, the TALSPEAK process is considered the best option for the separation of trivalent Am and Cm from the fission product lanthanides. This separation enables the destruction of both Am and Cm by transmutation. The lanthanides could then be sent to a low level waste storage site.

<u>Am from Cm and Ln</u>

As an alternative approach, the americium can be separated from curium and the lanthanides. This approach affords one major advantage over the previous approach, the reduction of difficulty in the production of targets for transmutation. This reduction results directly from the removal ^{244}Cm ($t_{1/2}$ = 18.1yrs) with a specific activity of 1.8 x 10^{14} dpm/g. With Cm present, the transmutation targets would have to be produced in a hot cell. With it removed, the targets could be produced in a glove box and ^{244}Cm with its short half life could be held for decay to ^{240}Pu.

TALSPEAK for Am/Cm from Ln – kinetic case

The most widely studied trivalent actinide lanthanide separation is TALSPEAK. In the development of the TALSPEAK separation process, several aminopolycarboxylates were considered with DTPA (diethylenetriamine-N,N,N',N'',N''-pentaacetic acid) determined to be the best.[38] Success in this separation depends on the ability of DTPA to act as a holdback reagent allowing the lanthanides to be extracted by an organophosphate cation exchanging extractant. A study of the rate of complexation or decomplexation of the Ln^{3+} to DTPA or similar EDTA

(ethylenediamine-N,N,N',N'-tetraacetic acid) provides better understanding of the process through the evaluation of mechanisms involved. The kinetics of Ln complexation with DTPA or similar EDTA has been performed with no buffer present, an acetate buffer or at a lactic acid concentration that is much lower than observed in TALSPEAK.[47-49] This is important in that the lactate concentration greatly influences the rate of the reaction.[50] In designing an experiment using these ligands, either the complex formation or the complex dissociation can be measured in a stopped flow spectrophotometer. Depending on the relative strengths of the indicator and the displacing ligand used, a study of formation would have the indicator bound to the metal and being displaced by the ligand being studied. If the indicator was a stronger complex, the ligand would be displaced from the metal-ligand complex providing information on the complex dissociation. The thermodynamics of the chosen method must be favorable.

In a study of lanthanide complexation kinetics with EDTA[45] and with DTPA[46], Arsenazo III was used as the color indicator in a lactic acid buffer. The lanthanide was introduced into the stopped-flow mixing chamber as the Arsenazo III indicator complex which is displaced from the metal by the EDTA or DTPA. Complex kinetics of EDTA or DTPA, reported in the literature and performed in this lab has been done under acidic conditions. Under conditions of the alkaline waste tanks, the kinetics of a lanthanide complexation/decomplexation with EDTA or DTPA would be considerably different. The kinetics of lanthanide-aminopolycarboxylate complexes under alkaline conditions has been examined at pH 9.5 through the use of the non complexing borax buffer. The azo-dye indicator Eriochrome Black T has been employed in the same manner as the Arsenazo study. The lanthanide has been introduced into the stopped flow as the EBT complex where the indicator is displaced by the EDTA or DTPA.

Redox/precipitation for Am from Cm and Ln

Selective oxidation was incorporated into the earliest Pu separations. These studies were used for the first identification of plutonium as a new element. Pu was precipitated in its reduced state along with the other fission products as a fluoride in order to separate these elements from uranium. The solid was then dissolved and the Pu oxidized to the hexavalent state. Trivalent and tetravalent species were then precipitated as fluorides giving a pure plutonium product in solution. This research has looked at the selective oxidation of americium with ozone and persulfate with the complexation by carbonate and sulfate to retain the americium in solution to achieve a solid–liquid separation.

The separation of americium from curium and the lanthanides rests upon the oxidation of Am to its pentavalent or hexavalent oxidation state. The pentavalent state of americium is more stable in acid solution than Am(VI). Previous results indicate that the tetra-, penta- and hexavalent oxidation states of Am are nearly of comparable stability in basic or carbonate media, though there have been only a few observations made.[51] The separation potential of an oxidized actinide from the lanthanides can be studied using the most stable form of uranium in solution, UO_2^{2+}. In most respects, uranium (UO_2^{2+}) has predictive value in describing the solvent extraction chemistry to NpO_2^{2+}, PuO_2^{2+} and AmO_2^{2+}.[52] The hexavalent state of neptunium, plutonium and americium is not the most stable valence for these elements, yet the hexavalent oxidation state is accessible by means of chemical or electrochemical oxidation. The oxidation states available for the actinides have already been shown in Figure 1. Hexavalent neptunium, plutonium, and americium are each strong oxidants, E increases in the order $PuO_2^{2+} < NpO_2^{2+} << AmO_2^{2+}$ respectively 0.9, 1.13 and 1.6 in 1 M $HClO_4$ and 0.3, 0.45 and 0.96 in 1 M $CO_3^{=}$.[50] The oxygen plays an important part in the oxidation and reduction of the actinides due to the

structural changes that must occur upon a change in the oxidation state (Equation 5). The relative kinetics follows:

$$\text{An}^{3+} \xrightarrow{\text{Fast}} \text{An}^{4+} \xrightarrow{\text{Slow}} \text{AnO}_2^{+} \xrightarrow{\text{Fast}} \text{AnO}_2^{2+} \tag{5}$$
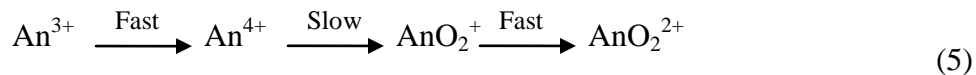
For a successful separation, the comparative slowness of the Am(V/VI) to Am(III/IV) transition could be essential for the ultimate separation.

Literature has demonstrated the preparation of Am(V) and Am(VI) through the use of ozone.[6] Ozone has been chosen as the oxidant for a portion of this work. The chief benefit of ozone use for oxidation is O_3 is a gas therefore no solids are added to the waste. Americium (VI) was quantitatively produced in 0.1 M $NaHCO_3$ containing a suspension of $Am(OH)_3$ when 5% ozone was passed through for one hour.[7] If a solution of 2 M Na_2CO_3 is used, Am(III) is oxidized with ozone to Am(VI) at room and lower temperatures with an accumulation of Am(V) occurring at higher temperatures.[7,53] Without considering the possible complexes that can be formed with americium, the oxidation of Am(III) could be described by the following equations.[53]

$$\text{Am(III)} + \text{O}_3 + 2\text{OH}^- \rightarrow \text{AmO}_2^{+} + \text{O}_2 + \text{H}_2\text{O} \tag{6}$$

$$\text{AmO}_2^{+} + \text{O}_3 \rightarrow \text{AmO}_2^{2+} + \text{O}_3^{-\bullet} \tag{7}$$

$$\text{Am(III)} + \text{O}_3^{-\bullet} \rightarrow \text{Am(IV)} + \text{O}_2 \tag{8}$$

$$\text{Am(IV)} + \text{O}_3 + 2\text{OH}^- \rightarrow \text{AmO}_2^{2+} + \text{O}_2 + \text{H}_2\text{O} \tag{9}$$
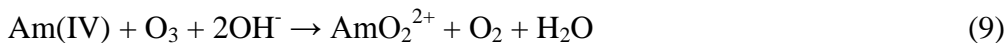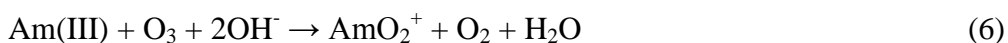
Experiments with 5 M K_2CO_3 verified the reaction mechanism seen in Equation 6 where the oxidation with ozone is accompanied by a replacement of the water molecule in the coordination sphere of the Am(III). However, this experiment also demonstrated that an increased concentration of carbonate can sterically hinder the insertion of ozone resulting in an outer sphere process to form Am(IV).[52] In carbonate media, the carbonate could complex the

americium in the form $AmO_2(CO_3)_3^{4-}$ until an almost complete oxidation of the americium has been performed. The appearance of a burgundy-red color, characteristic of the coordination of AmO_2^{2+} with carbonate ions, could be the indicator of a complete oxidation of the reduced species of americium to AmO_2^{2+}.[3]
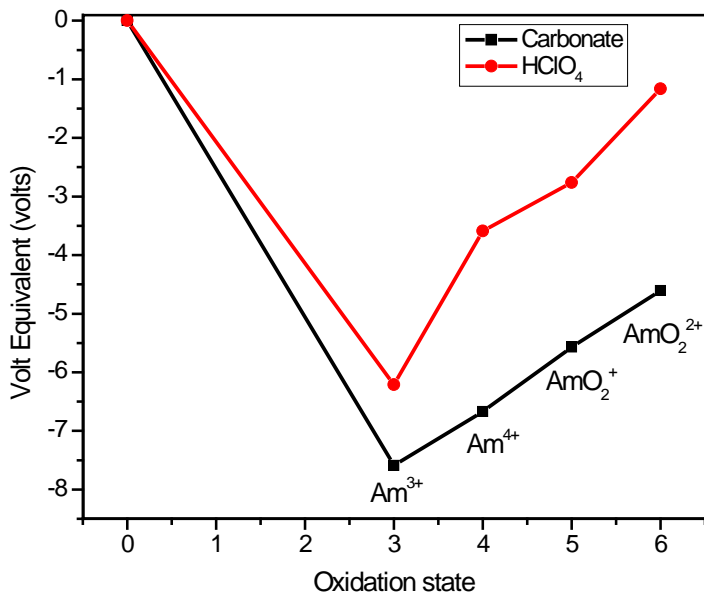
Figure 7: Frost diagram for americium in both acidic and basic media

Oxidations have also been performed in sulfate media using sodium persulfate and potassium monopersulfate as the oxidizing agent. Stability constants have shown that a uranyl tris-sulfato complex has good stability. This species could aid in the separation of americium from the trivalent species. Persulfate provides an unexpected advantage in that once the oxidation of the americium III to VI has occurred, the remaining sulfate ions can complex with the remaining trivalent species whether Cm, remaining Am(III) or the lanthanides resulting in a precipitate. Though most literature usually adds silver to this system as a catalyst, there is some debate on its necessity.[54] A full evaluation of the silver requirement has not been performed but

would be a nice complement in future work that could include other catalysts that may already be found in used fuel such as rhodium or palladium. The main advantage in the use of persulfate as the oxidant is in its dual role as oxidant and complexing ligand. In its role as a complexing ligand, $SO_4^=$ will complex the hexavalent actinide forming $AnO_2(SO_4)_3^{4-}$ as a major soluble product over a wide range of acidic pH. Sulfate complexes the trivalent species as well, forming a precipitate. Precipitation type separations had been abandoned in the drive to produce Pu as quickly as possible. A solvent extraction separation generally has a high throughput and good separation ability. Several advantages can be had by switching to a precipitation style separation. Intrinsically higher single-stage separation factors are possible in a solid liquid separation with the waste products all going to the solid phase. No readily oxidizable substrates are present, as would be in solvent extraction methods involving Am(V/VI), so oxidized Am can persist for a longer time. Oxidized Np, Pu, Am, U all will behave similarly, so a total TRU/Ln separation can be envisioned. The solid Ln materials should be suitable for easy disposal in a variety of media. Finally, in accordance to the driving force of the world, no expensive reagents are used to add to the cost of reprocessing.

The question of whether to use soft donor complexants or selective oxidation of americium to achieve a separation of americium from curium and the lanthanides has been studied. Soft donor complexants have been studied through the kinetic study of lanthanide complexation with EDTA and DTPA. Selective oxidation of americium includes two separation schemes based on inorganic principles to achieve the separation of americium from curium and the lanthanides.

References

1. *The Chemistry of the Actinide Elements*, 2nd ed.; Katz, J.J., Seaborg, G. T., Morss, L. R., Eds.; Chapman and Hall: New York, NY, 1986.

2. Cotton, F. A.; Wilkinson, G.; Murillo, C. A.; Bochmann, M. *Advanced Inorganic Chemistry*, 6th ed.; John Wiley and Sons, Inc.: New York, NY, 1999, pp 1130-1164.

3. Runde, W. H.; Schulz, W. W. Americium. In *The Chemistry of the Actinide and Transactinide Elements*; 3rd ed.; Morss, L. R., Edelstein, N. M., Fuger, J., Katz, J. J., Eds.; Springer: New York, **2006,** Vol. 2, pp 1265-1395.

4. Yanir, E.; Givon, M.; Marcus, Y. Higher Oxidation States of Americium in Phosphate Solutions. *Inorg. Nucl. Chem. Lett.* **1969**, 5(5), 369-372.

5. Woods, M.; Mitchell, M. L.; Sullivan, J. C. A Determination of the Stability Quotient for the Formation of a Tris(carbonato)plutonate(VI) Complex in Aqueous Solution. *Inorg. Nucl. Chem. Lett.* **1978**, 14(12), 465-467.

6. Sullivan, J.C.; Gordon, S.; Mulac, W.A.; Schmidt, K.H.; Cohen, D.; Sjoblom, R. Pulse Radiolysis Studies of Americium(III) and Curium(III) Ions in Perchlorate Media. The Preparation of Americium(II), Americium(IV), Curium(II) and Curium(IV). *Inorg. Nucl. Chem. Lett.* **1976**, 12(8), 599-601.

7. Coleman, J. S.; Keenan, T. K.; Jones, L. N.; Carnell, W. T.; Penneman, R. A. Preparation and Properties of Americium(VI) in Aqueous Carbonate Solutions. *Inorg. Chem.* **1963**, 2(1), 58-61.

8. Chemical Thermodynamics, Vol.1. *Chemical Thermodynamics of Neptunium and Plutonium*. OECD Nuclear Energy Agency, Ed.; North-Holland, Elsevier Inc.: San Diego, Ca, 2001.

9. Sullivan, J. C. Reactions of Plutonium Ions with the Products of Water Radiolysis. In *Plutonium Chemistry*, Carnall, W. T., Choppin, G. R., Eds.; ACS Symposium Series 216; American Chemical Society: Washington, D.C., 1983; pp 241-249.

10. Clark, D. L.; Hobart, D. H.; Neu, M. P. Actinide Carbonate Complexes and Their Importance in Actinide Environmental Chemistry *Chem. Rev.* **1995,** 95(1), 25-48.

11. Maya, L. Detection of Hydroxo and Carbonato Species of Dioxouranium(VI) in Aqueous Media by Differential Pulse Polarography. *Inorg. Chim. Acta.* **1982**, 65(1), L13-L16.

12. Ciavatta, L.; Ferri, D.; Grenthe, I.; Salvatore, F. The First Acidification Step of the Tris(carbonato)dioxouranate(VI) Ion, $UO_2(CO_3)_3^{4-}$. *Inorg. Chem.* **1981**, 20(2), 463-467.

13. Moskvin, A. I. Complexing of Neptunium (IV, V, VI) in Carbonate Solutions. *Sov. Radiochim.* **1971**, 13, 694-699.

14. Gel'man, A.D.; Moskvin, A. I.; Zaitseva, V. P. The Plutonyl Carbonates. *Sov. Radiochim.* **1962**, 4, 138-145.

15. Sullivan, J. C.; Woods, M.; Bertrand, P. A.; Choppin, G. R. Thermodynamics of Plutonium (VI) Interaction with Bicarbonate. *Radiochim. Acta* **1982**, 31(1-2), 45-50.

16. Guilinger, T. R.; Schechter, R. S.; Lake, L. W.; Price, J. G.; Bobeck, P. Factors Influencing Production Rates in Solution Mining of Uranium Using Basic Lixiviants. *Min. & Metall. Process.* **1985**, 2(1), 60-67.

17. Mason, C. F. V.; Turney, W. R. J. R.; Thomson, B. M.; Lu, N.; Longmire, P. A.; Chisholm-Brause, C. J. Carbonate Leaching from Contaminated Soils. *Environ. Sci. Tech.* **1997**, 31(10), 2707-2711.

18. El-Nadi, Y. A.; Daoud, J. A.; Aly, H. F. Modified leaching and extraction of uranium from hydrous oxide cake of Egyptian monazite. *Int. J. Of Min. Process.* **2005,** 76(1-2), 101-110.

19. Silva, R. J.; Bidoglio, G.; Rand, M. H.; Robouch, P. B.; Wanner, H. and Puigdomenech, I. *Chemical Thermodynamics of Americium*, Elsevier: New York, 1995.

20. Maya, L. Hydrolysis and Carbonate Complexation of Dioxoneptunium(V) in 1.0 M $NaClO_4$ at 25 °C. *Inorg. Chem.* **1983,** 22, 2093-2095.

21. Gelis, A. V.; Vanysek, P.; Jensen, M. P.; Nash, K. L. Electrochemical and Spectroscopic Investigations of Neptunium in Alkaline Media. *Radiochim. Acta* **2001**, 89(9), 565-571.

22. Thompson, M. E.; Nash, K. L.; Sullivan, J. C. Complexes of Hydrogen Peroxide and Dioxoactinide (VI) Species of Aqueous Carbonate and Bicarbonate Media. Formation of An(VI)-H_2O_2 Complexes. *Israel J. of Chem.* **1985**, 25(2), 155-158.

23. Nash, K. L. A Review of the Basic Chemistry and Recent Developments in Trivalent F-Element Separations. *Solvent Extr. Ion Exch.* **1993**, 11, 729-768.

24. Choppin G. Actinide Chemistry: From Weapons to Remediation to Stewardship. *Radiochim. Acta* **2004**, 92, 519–523.

25. Rard, J.A. Aqueous Solubilities of Praseodymium, Europium, and Lutetium Sulfates. *J. of Sol. Chem.* **1988**, 17(6), 499-517.

26. *Chemical Thermodynamics, **1**, Chemical Thermodynamics of Uranium*, Wanner, H., Forrest, I., Eds.; North-Holland: Amsterdam, 1992.

27. Martell, A. E.; Smith, R. M., NIST Standard Reference Database 46. Version 8.0, 2004.

28. New York Times. http://www.nytimes.com/2009/02/06/business/worldbusiness/06nuke.html, (accessed January 25, 2010.

29. Choppin, G.R.; Liljenzin, J.; Rydberg, J. *Radiochemistry and Nuclear Chemistry* 3rd ed. Butterworth-Heinemann: Woburn, MA, 2002.

30. Benedict, M,; Pigford, T. H.; Levi, H. W. *Nuclear Chemical Engineering*, 2nd ed., McGraw-Hill: New York, 1981.

31. Ewing, R. C. Nuclear Waste Forms for Actinides. *Proc. Natl. Acad. Sci. USA* **1999**, *96(7)*, 3432-3439.

32. Rudisill, T. S.; Thompson, M. C.; Norato, M. A.; Kessinger, G. F.; Pierce, R. A., and Johnson, J. D. *Demonstration of the UREX Solvent Extraction Process with Dresden Reactor Fuel*; WSRC-MS-2003-00089, Rev. 1, Technical Report for Westinghouse Savannah River Company: Aiken, SC, 2003.

33. Warin, D. P and T and fuel Cycle Strategies. Presented at the ITU Summer School on Actinide Science and Applications, Karlsruhe, Germany, 2007.

34. Nuclear Waste Policy Act of 1982, Sections 131,135 and 217.

35. http://www.nrc.gov/waste/hlw-disposal/schedule.html, Accessed on January 22, 2010.

36. Greenspun, B., Ed.; Las Vegas SUN: Las Vegas, NV, 2007; Vol. 2007.

37. Todd, T. A., Wigeland, R. A. Advanced Separation Technologies for Processing Used nuclear fuel and the Potential Benefits to a geologic Repository. In *Separations for the Nuclear Fuel Cycle in the 21st Century*, Lumetta, G. L., Nash, K. L., Clark, S. B., Friese, J. I., Eds.; ACS Symposium Series 933, American Chemical Society: Washington, D.C., pp 41-55.

38. Weaver, B.; Kapplemann, F. A. *TALSPEAK: A New Method of Separating Americium and Curium from the Lanthanides by Extraction from an Aqueous Solution of an Aminopolyacetic Acid Complex with a Monoacidic Organophosphate or Phosphonate.* Oak Ridge National Laboratory Report– 3559: Oak Ridge, TN, 1964.

39. Kelly, J.; Savage, C.: *Advanced Fuel Cycle Initiative (AFCI) Program Plan* 2005.

40. Law, J. D.; Herbst, R. S.; Peterman, D. R.; Todd, T. A.; Romanovskiy, V. N.; Babain, V. A.; Smirnov, I. V. Development of a Regenerable Strip Reagent for Treatment of Acidic, Radioactive Waste with Cobalt Dicarbolide-Based Solvent Extraction Processes. *Solvent Extr. Ion Exch.* **2005**, 23(1), 59-83.

41. Cipiti, B.B. et.al. *Fusion Transmutation of Waste: Design and Analysis of the In-Zinerator Concept*, SAND2006-6590, Sandia National Laboratories Albuquerque, NM, 2006.

42. Harrington, R. C.; Martin, L. R.; Nash, K. L. Partitioning of U (VI) and Eu (III) Between Acidic Aqueous Al(NO$_3$)$_3$ and Tributyl phosphate in N-dodecane. *Sep. Sci. Tech.* **2006**, 41(10), 2283-2298.

43. Feil-Jenkins, J. F.; Sullivan, J. C.; Nash, K. L. Kinetics of the Complexation of Dioxouranium(VI) with Chlorophosphonazo III *Radiochem. Acta.* **1995**, 68, 209-213.

44. Fugate, G.; Feil-Jenkins, J. F.; Sullivan, J. C.; Nash, K. L. Actinide Complexation Kinetics: Rate and Mechanism of Dioxoneptunium(V) Reaction with Chlorophosphonazo III. *Radiochem. Acta.* **1996**, 73, 67-72.

45. Martin, A.; Shehee, T. C.; Sullivan, J. C.; Nash, K. L. Kinetics of lanthanide complexation reactions with EDTA (ethylenediaminetetraacetic acid) in lactic acid media. *Dalton Trans.*, too be submitted for publication, 2010.

46. Martin, A.; Shehee, T. C.; Sullivan, J. C.; Nash, K. L. Kinetics of lanthanide complexation reactions with DTPA (diethylene triamine pentaacetic acid) in lactic acid media. *Inorg. Chem. Acta.*, too be submitted for publication, 2010.

47. Brucher, E.; Laurenczy, G. Aminopolycarboxylates of rare earths. VIII. Kinetic study of exchange reactions between europium(3+) ions and lanthanide(III) diethylenetriaminepentaacetate complexes. *J. Inorg. Nucl. Chem.* **1981**, 43(9), 2089-2096.

48. Laurenczy, G.; Brucher, E. Aminopolycarboxylates of rare earths. 12. Determination of formation rate constants of lanthanide(III)-ethylenediaminetetraacetate complexes via a kinetic study of the metal-exchange reactions. *Inorg. Chim. Acta.* **1984**, 95(1), 5-9.

49. Azis, A.; Matsuyama, H.; Teramoto, M. Equilibrium and non-equilibrium extraction separation of rare earth metals in the presence of diethylenetriaminepentaacetic acid in aqueous phase. *J. Chem. Eng. Japan* **1995**, 28(5), 601-608.

50. Kolařík, Z.; Koch, G.; Kuhn, W. The rate of Ln(III) extraction by HDEHP from complexing media. *J. Inorg. Nucl. Chem.* **1974**, 36, 905-909.

51. Newton, T. W.; Sullivan, J. C. Actinide Carbonate Complexes in Aqueous Solutions. In *Handbook on the Physics and Chemistry of the Actinides*; Freeman, A. J., Lander, G. H., Eds.; North-Holland: Amsterdam, 1985; Vol. 3, pp 387-406.

52. Shilov, V. P.; Yusov, A. B.; Gogolev, A. V.; Fedoseev, A. M. Behavior of Np(VI) and Np(V) Ions in NaHCO$_3$ Solutions Containing H$_2$O$_2$. *Radiochem.* **2005,** 47(6). 558-562

53. Shilov, V. P.; Yusov, A. B. Oxidation of Americium(III) in Bicarbonate and Carbonate Solutions of Neptunium(VII). *Radiokhimiya* **1995**, 37(3), 201-202.

54. Ward, M.; Welch, G. A. The oxidation of americium to the sexavalent state. *J. Chem. Soc.* **1954**, 4038.

Notes on Contributing Authors

Aymeric Martin	French intern at Washington State University February - July 2006. Performed many of the kinetic experiments presented in chapters 2 and 3. Work was supported by the Department of Energy University - Nuclear Energy Research Initiative project number DE-FC07-05ID14644.
James C. Sullivan (April 21, 1921 - February 11, 2007)	Staff scientist to senior scientist in the Chemistry Division at Argonne National Lab from 1946-2006. He came to Washington State University in June 2006 to work as a mentor in the Nash group. Assisted in the verification and interpretation of results obtained in early kinetic experiments presented in chapters 2 and 3. Work was supported by the Department of Energy University - Nuclear Energy Research Initiative.
Leigh R. Martin PhD	Staff scientist at the Idaho National Lab (INL) in the Aqueous Separations and Radiochemistry Department and former Post-Doctoral researcher under Kenneth L. Nash. Provided direct oversight as well as technical guidance and mentoring for experiments performed at INL and presented in Chapters 4 and 6.
Peter J. Zalupski PhD.	Staff scientist at the Idaho National Lab (INL) in the Aqueous Separations and Radiochemistry Department and former Post-Doctoral researcher under Kenneth L. Nash. Provided direct oversight as well as technical guidance and mentoring for experiments performed at INL and presented in Chapters 4 and 6.
Prof. Kenneth L. Nash	Ph.D. supervisor at Washington State University. Direct mentor and principle investigator in the University – Nuclear Energy Research Initiative (U-NERI) program of the U.S. Department of Energy Office of Nuclear Energy and Technology at Washington State University, project number DE-FC07-05ID14644.

Chapter 2

Kinetics of lanthanide complexation reactions with DTPA

(diethylene triamine pentaacetatic acid) in lactic acid media

Preface

Chapter 2 evaluates k_{form} and k_{diss} for DTPA with the lanthanide series under TALSPEAK- like conditions. Since DTPA is used as a holdback reagent for the trivalent actinides, the interaction it has with trivalent lanthanides is useful information when trying to optimize the system further. The ligand displacement technique proved good in this particular system allowing for a full evaluation under many sets of conditions. Additional information for this chapter can be found in the Appendix.

This chapter will be submitted to an inorganic chemistry journal. The first choice for submission is to Inorganica Chimica Acta. Formatting of the chapter results from a balance of ACS guidelines and guidelines set forth by WSU. Figures have been inserted into the text near the reference location for ease of reading in this document. They will be removed and placed at the end of the document prior to submitting.

Kinetics of lanthanide complexation reactions with DTPA (diethylene triamine pentaacetic acid) in lactic acid media

Thomas Shehee[1], Aymeric Martin[1], James C. Sullivan[1#], Kenneth L. Nash*[,1]

[1]Chemistry Department, Washington State University, PO Box 644630, Pullman, WA 99164-4630

- deceased

* Author for correspondence

Abstract

An important feature of the chemistry of the TALSPEAK process (for the separation of trivalent actinides from lanthanides) is the interaction of trivalent lanthanide and actinide cations with aminopolycarboxylic acid complexing agents in lactic acid buffer systems. To improve our understanding of the mechanistic details of these processes, an investigation of the kinetics of lanthanide complexation by DTPA in concentrated lactic acid solution used in TALSPEAK has been completed. The reactions studied occur in a time regime suitable for study by stopped-flow spectrophotometric techniques. Progress of the reaction is monitored using the distinctive visible spectral changes attendant to lanthanide complexation by the colorimetric indicator ligand Arsenazo - III (AAIII). Experiments have been conducted as a function of pH, lactic acid concentration, ligand concentration and temperature. The reaction proceeds as a first order approach to equilibrium over a wide range of conditions, allowing the simultaneous determination of complex formation and dissociation rate constants. Experiments containing only a twofold excess of ligand to metal exhibit the same first order behavior as experiments containing 10-fold excess ligand. The rate of the complexation reaction has been determined for the entire lanthanide series except Pm^{3+}. The complex formation rate has been shown to be

proportional to the hydrogen ion concentration. The predominant pathway for lanthanide DTPA dissociation is inversely proportional to lactic acid concentration. The activation entropy has been interpreted as an indication of an associative mechanism for both complex formation and dissociation of the Ln/DTPA complex. The addition of a surfactant did not affect the rate of complex formation and only had a small effect on the rate of complex dissociation.

Introduction

The separation of the actinides, Np, Pu, and Am, from trivalent lanthanides and curium in used nuclear fuel is a significant problem facing developed countries. The lanthanides are produced in relatively high yield through the fission of ^{235}U. Lanthanides are only radioactive for a reasonably short time, but high thermal neutron capture cross-sections of several lanthanide isotopes limit the efficiency of strategies for transmutation of actinides in reactors, as they compete with the actinide targets for the available neutrons. Consequently, it is highly advantageous to separate the relatively small actinide fraction from the relatively large quantities of lanthanide isotopes. One of the most efficient separation processes available to separate the trivalent actinides from the lanthanides is the TALSPEAK process (Trivalent Actinide Lanthanide Separations by Phosphorus reagent Extraction from Aqueous Komplexes).[1] The process operates by extraction of the lanthanides with di(2-ethylhexyl) phosphoric acid (HDEHP, 0.3 M) solution from aqueous phase of lactic acid (1.0 M) and diethylenetriamine - N,N,N',N'',N'' - pentaacetic acid (DTPA, 0.05 M) at pH 2.5 to 3.0. DTPA retains the actinides in the aqueous phase to allow the selective extraction of the trivalent lanthanides. TALSPEAK is an effective method that does not involve high concentrations of any salt or acid and is resistant to the effects of radiation due to the protective effect of lactic acid keeping the distributions ratios of Am^{3+} lower.[2] This helps keep the HDEHP in the organic phase intact for longer time by

31

keeping the americium in the aqueous phase, allowing for better extraction of the trivalent lanthanides.

The rates of complex formation and dissociation of lanthanides with aminopolycarboxylic acid complexants have been investigated using either metal ion or ligand exchange reactions, mainly by spectrophotometric methods.[3,4] Thermodynamic features of complexation reactions of elements in the lanthanide series with DTPA in an acetate buffer have also been investigated in previous studies.[4] In the present study the rate and mechanism of lanthanide-DTPA complexation reactions have been investigated in lactate media of a moderate 0.3 M concentration. This medium is of interest for the integral role it plays in the TALSPEAK solvent extraction separation process. This biphasic solvent extraction is known to demonstrate unusually slow phase transfer kinetics for a lanthanide system which directly impacts the separation process. This study addresses the rate and mechanism of the complexation in 0.3 M lactate buffer solutions.

The octadentate DTPA, shown in Figure 1, has a binding cavity flexible enough to accommodate a variety of metal ions. For Ln (III), DTPA is 7 - 8 coordinate with an average number water molecules coordinated to the metal of 1.1, as determined by luminescence lifetime measurements.[5] The pK_a values for DTPA are - 0.1, 0.7, 1.6, 2.1, 2.7, 4.10, 8.09 and 9.42 for the five carboxylate groups and three amino groups, in order (I = 0.1 M for pK_{a1-3} and 0.5 M for pK_{a4-8}; T = 25 °C). In the pH range 3.2 - 4.2, $H_3(DTPA)^{2-}$ is the predominant free ligand species present. The coordination chemistry of
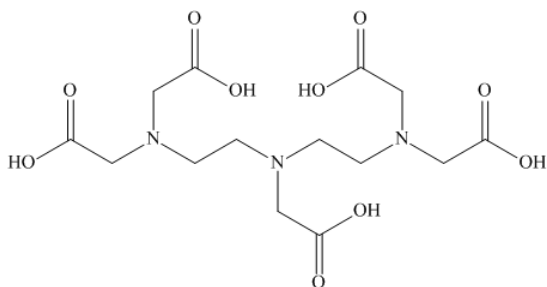
Figure 1: Structure of DTPA

the lanthanide complexes with polyaminocarboxylate ligands, especially DTPA, has been comprehensively reviewed by Moeller.[6-8] The report by Moeller emphasizes that the bonding in lanthanide-polyaminocarboxylate chelates is an electrostatic interaction. As lanthanide series is crossed, charge density increases leading to a stronger interaction.

In exchange type reactions, the metal exchange proceeds through two different pathways where an acid-catalyzed dissociation pathway is the preferred mode at lower pH. [4,9-11] The second was thought to pathway proceeds through a binuclear intermediate that has not been identified. Brücher and coworkers compared the derived rate parameters with order of magnitude estimates of the lanthanide hydration rates, and concluded that the rate determining step of the complex formation between Ln(III) and $H(DTPA)^{3-}$ must be a chelate ring closure reaction.[12] For complex formation reactions between Ln(III) and $H_2(DTPA)^{2-}$, the resolved rates are slower, indicating that proton transfer (deprotonation)[12,13] to convert the ligand to a more kinetically active form becomes rate determining step.

In this investigation the impact of moderate concentrations of lactate buffer solutions on the rate and mechanism of lanthanide complexation by DTPA is investigated. The buffer concentration is maintained at 0.3 M to conform to representative conditions of the TALSPEAK separation system.

Experimental

Reagents

Lanthanide perchlorate stock solutions have been prepared using 99.999% Ln_2O_3 from Arris International Corp. through dissolution of the solid in $HClO_4$. Stock solutions were standardized by ICP-OES analysis. These lab stocks were used to prepare each lanthanide sample in the series. Arsenazo III was added directly to the solutions by weight using material

obtained from Fluka Chemika. Solutions of variable DTPA concentration were prepared by weight using material obtained from Fluka Chemika and using only 99.9% DTPA disodium anhydrous salts because of its better solubility in lactic acid media. Lactic acid is used at different concentrations as a medium constituent. It is prepared by weight using 88.4% w/w material obtained from JT Baker. $NaClO_4 \cdot H_2O$ obtained from Fisher was employed as the supporting electrolyte to maintain constant ionic strength. Triton X-114 surfactant was used in selected studies without further purification using material obtained from Sigma. Adjustment of pH was accomplished by the addition of standardized NaOH or HCl. All solutions were prepared in 18MΩ deionized water.

Procedure

The kinetics of the reaction of lanthanides with chelating agents in lactic acid media have been investigated by stopped-flow spectrophotometry. In stopped-flow spectrophotometry, mixing is essentially complete within a few milliseconds at which time the period of observation of changing absorptivity begins. Rates of reactions that are complete within a range of milliseconds to seconds are accessible using this technique. An OLIS RSM-1000 stopped-flow spectrophotometer was used for data acquisition and the OLIS RSM Robust Global Fitting software package was used for analysis of the absorbance data as a function of time. Data were collected over a wavelength range of 500 nm to 800 nm.

The lanthanide aqua ions are not strongly colored; therefore the application of spectrophotometric techniques like stopped-flow to their complexation kinetics must rely on the use of strongly colored chelating agents, either as the subject ligands or as indicators of the free metal ion in the reaction of interest. Derivatives of chromotropic acid have proven to be quite useful in kinetic investigations of this type and generally do not participate in the kinetics of the

34

reaction of interest. Previous studies[14] investigated in particular the rates of complex formation of a variety of lanthanide cations with Arsenazo III (2,2'-(1,8-dihydroxy-3,6-disulfonaphthylene-2,7-bisazo)bis(benzenearsonic acid, Figure 2).
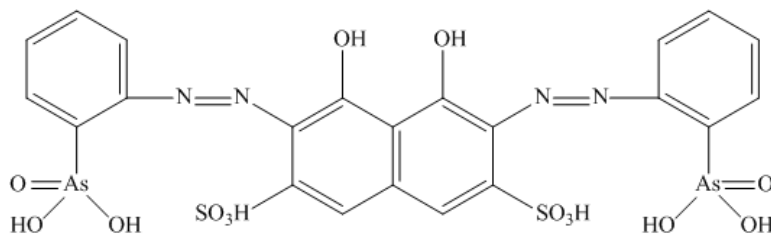
Figure 2: Structure of Arsenazo III

Arsenazo III appears to coordinate the lanthanide cation in a tetradentate manner with one oxygen atom from each arsenate and the phenol groups.[15] The eight pK_a values for Arsenazo III are $pK_1 = -2.5$, $pK_2 = 0$, $pK_3 = pK_4 = 2.5$, $pK_5 = pK_6 = 5.3$, $pK_7 = 7.5$ and $pK_8 = 12.4$.[15] Formation of the complex is accompanied by a significant change in the visible spectrum. Hence, this reagent has been used as an indicator of the free metal ion concentration to study the kinetics of complexation of lanthanide ions with ligands in this work. In most studies, the indicator ligand plays no significant role in the kinetics and mechanism of complex formation of the metal ion with the ligand of interest.[14] The spectrum of the La^{3+}-AAIII complex and free AAIII was measured on an OLIS scanning spectrophotometer and is shown in Figure 3. The λ_{max} for the blue La-AAIII complex is 650 nm, whereas the free AAIII ligand is magenta with a maximum absorbance at 550 nm. The extinction coefficients of the bands at the $\lambda_{max} = 650$ nm are greater than 10^4 $M^{-1}cm^{-1}$, allowing the spectrophotometric monitoring of lanthanide concentration at 10^{-4} M or less. The absorbance band of the La^{3+}-AAIII complex was chosen as the center wavelength, monitoring the disappearance of the peak at 650 nm. Disappearance of this peak would correspond to the complete complexation of the metal ion with DTPA and the appearance of the 550 nm spectrum of free AAIII.

Under most conditions, the DTPA was present in sufficient excess over Ln^{3+} to maintain pseudo-first order conditions. The Ln-AAIII complex concentration was 10^{-4} M with a DTPA concentration in the range of 0.2 - 1.2 mM. The range of concentration of DTPA was dictated in part by its solubility in lactic acid media and does fall to second order conditions on the low end of the range. Even under these conditions, the kinetic trace conformed to a single first order process. Each solution was buffered using a Na/Lactate buffer at pH 3.6. The respective solutions where placed in syringes that are thermostated in a water bath. The solutions were allowed to equilibrate at the desired temperature for 5 minutes before making an injection. Upon injection, the instrument measured the change in absorbance with respect to time. The time interval for evaluation was dependant on the experimental conditions. Five measurements have been made under each set of conditions and averaged to provide k_{obs} for that set of conditions.
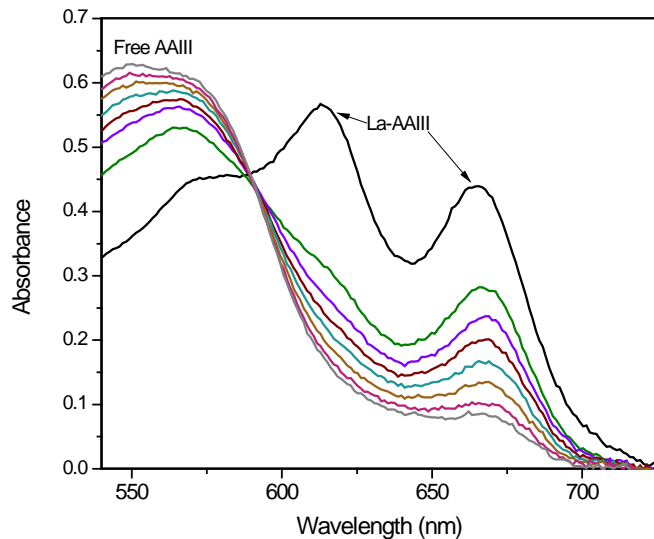
Figure 3: Change in the visible spectrum that occurs upon complex La-AAIII dissociation – [La-AAIII] = 10^{-4} M; [DTPA] = 1.5 x 10^{-3}; [Lac]$_{tot}$ = 0.3 M; pH = 4.2; T = 25 °C.

Results

The observed rate constant for the complexation of every lanthanide ion at several DTPA concentrations was determined at 25 °C. The kinetic traces of absorbance vs. time were seen in all cases to be adequately adjusted using a single exponential fit, i.e. they conform to first order kinetics. Rate constants determined as a function of [DTPA] were plotted to reveal that a linear correlation with finite positive intercept as shown in Figure 4 for La^{3+}. This condition was seen to persist throughout the lanthanide series, though the dissociation rate constants were difficult to determine accurately for ions heavier than Dy. It is also noteworthy in these plots that the first order fits of absorbance vs. time were appropriate even at 0.2 mM DTPA. This implies that the rate determining step is an intramolecular process where a solvent separated forms initially between the lanthanide and the DTPA.
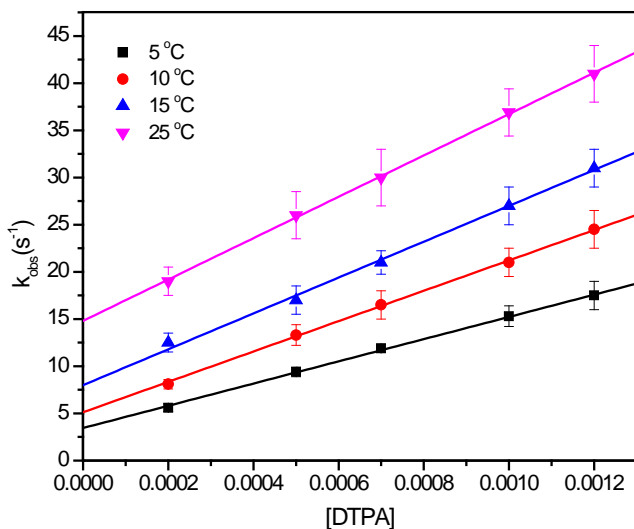
Figure 4: The effect of temperature on the rate of reaction of La with DTPA in lactate solution at pH = 3.5; [La] = [AAIII] = 10^{-4} M, [Lac]$_{tot}$ = 0.3 M.

<u>Determination of k_{form} and k_{diss}</u>

Under present pseudo-first order conditions, excess DTPA, a plot of k_{obs} versus [DTPA] is a straight line with finite positive intercept under most conditions (Equation 1). The slope of this line corresponds to the rate constant for the complex formation k_{form}, which is in $M^{-1}s^{-1}$, while the intercept is the rate constant for the complex dissociation k_{diss} in s^{-1}.

$$k_{obs} = k_{form} [\text{DTPA}] + k_{diss} \tag{1}$$

Figure 4 shows that the first order approach to equilibrium model properly fits the data over the range of temperatures studied.

<u>Acid dependence</u>

Reactions were studied as a function of pH, in the range of pH = 3.3 - 4.3, which allowed examination of the acid dependence for both complex formation and dissociation reactions. In this case, experiments were adjusted to constant ionic strength with sodium perchlorate (0.3 M). Reagent solutions, Ln-AAIII and DTPA were adjusted to the same acidity in any given experiment. For the La-DTPA system in lactate solution, experiments were run, as a function of pH to determine the effect of [H^+] on the rates. Figure 5 shows the plot of the La-DTPA system at varied pH. The rate constants for complex formation are 1.87 ($\pm$ 0.04) x 10^4 $M^{-1}s^{-1}$, 1.45 ($\pm$ 0.03) x 10^4 $M^{-1}s^{-1}$ and 1.03 ($\pm$ 0.02) x 10^4 $M^{-1}s^{-1}$ at pH = 3.3, 3.5 and 4.3 respectively. The rates of complex dissociation are constant, within the accuracy of the measurement, with increasing pH. Complex dissociation constants are 10.6 $\pm$ 0.3, 9.6 $\pm$ 0.3 and 9.1 $\pm$ 0.2 s^{-1} for pH = 3.3, 3.5 and 4.3 respectively.
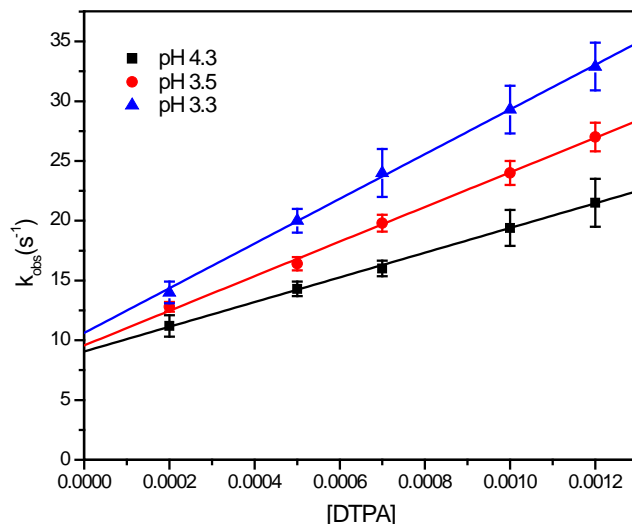
Figure 5: Hydrogen ion dependence of La-DTPA complex for [La] = [AAIII] = 10^{-4} M, T = 25 °C and [Lac]$_{tot}$ = 0.3 M.

Lactate dependence

Influence of lactic acid media was investigated over the concentration a range of 0.1 M to 0.3 M lactic acid. The pH was adjusted using NaOH to pH = 3.6. Ionic strength is maintained to 0.3 M using NaClO$_4$. Lanthanum and AAIII concentrations are held constant at 10^{-4} M. In Figure 6, a plot of k_{obs} vs. [DTPA] demonstrates that first order kinetics are preserved even under second order conditions of [DTPA] = 2 x 10^{-4} M. This observation implies that the rate determining step for the dissociation reaction is probably an intramolecular process. Within the accuracy of the experiments, the complex formation reaction constant is independent of [Lactate]$_{tot}$ at pH 4.0 (k_{form} = 1.93 (± 0.03) x 10^4 M^{-1}·s^{-1}, 2.0 (± 0.1) x 10^4 M^{-1}·s^{-1} and 1.98 (± 0.08) x 10^4 M^{-1}·s^{-1} respectively for lactic acid concentrations 0.1, 0.2 and 0.3 M). The dissociation rate constant (as defined by the intercept) decreases as lactic acid concentration increases with rate constants of 28.6 ± 0.3, 17.6 ± 0.9 and 10.4 ± 0.7 s^{-1} respectively for lactic acid concentrations 0.1, 0.2 and 0.3 M.
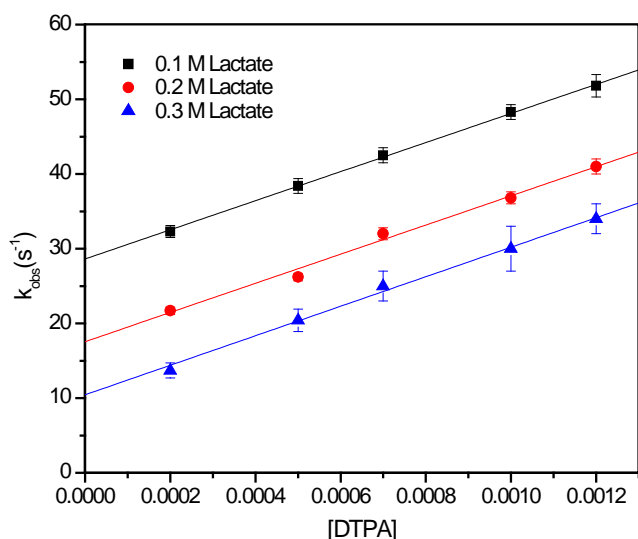
Figure 6: Dependence of reaction rate on lactic acid concentration at T = 25 °C and pH = 3.6 for La-DTPA system with [La] = [AAIII] = 10^{-4} M.

Effects of a surfactant

To simulate reactions that might be occurring at a liquid-liquid interface in the analogous solvent extraction system, the reaction rate was also determined with addition of surfactant Triton X-114. The presence of a surfactant in solution is expected to alter the organization of solvent molecules, which should alter the solvation of the reactants and products and energetic features of their interactions. To complete the study on the role of complex solvation, the rate parameters for complexation reaction were examined in water/Triton X-114 mixed media. The structure of Triton X-114 is shown in Figure 7. The surfactant has been added in the DTPA solution syringe, La solution syringe or both syringes. This allows for possible comparison of interactions of the surfactant with different species.
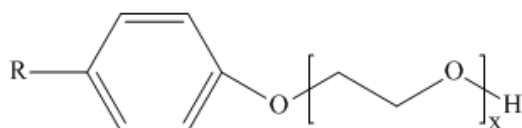
Figure 7: Structure of Triton X-114 – R = octyl (C_8), x = 7.5 (average)

Experiments were run in 0.01 % by weight (10^2 ppm) Triton X-114 aqueous solutions. Increasing the concentration of Triton X-114 from zero to 50% of the critical micelle concentration (350μM) leads to an apparent increase in the rate of complex dissociation but has only a slight effect on the complex formation reaction. Rates for both complex formation and dissociation as a function of Triton X-114 concentration are reported in the Table 1. This table shows that k_{form} is essentially the same through the modifications, i.e. k_{form} is not affected appreciably by surfactant. Upon addition of the surfactant, Table 1 shows an increase in k_{diss} from 2.0 ± 0.1 s^{-1} with no surfactant to 2.7 ± 0.2 s^{-1} when surfactant was present in only one of the reactant solutions to finally 3.51 ± 0.06 s^{-1} when the surfactant was in both reactant solutions.

Table 1: Rate constants for complex formation and dissociation for La-DTPA complex in water/Triton X-114(CMC concentration) mixed media at pH 3.6, T = 25°C and [Lac]$_{tot}$ = 0.3 M.

$k_{form.}$ (M^{-1}s^{-1}) (10^3)	$k_{diss.}$ (s^{-1})	Triton X-114
9.1 $\pm$ 0.1	2.0 $\pm$ 0.1	Without surfactant
9.3 $\pm$ 0.1	2.6 $\pm$ 0.1	With surfactant in DTPA syringe
9.5 $\pm$ 0.2	2.8 $\pm$ 0.2	With surfactant in La syringe
9.4 $\pm$ 0.1	3.5 $\pm$ 0.1	With surfactant in both syringe

Indicator concentration dependence

Though the linear plots of k_{obs} vs. [DTPA] establish the essential validity of the kinetic interpretation, it is also important to demonstrate that AAIII is not a participant in the ligand exchange process. The dependence of the reaction rate on lanthanum and AAIII concentrations has been determined; experiments were run with various concentrations of La at constant pH and lactate concentration. At pH = 3.6, experiments were run at [La^{3+}] = [AAIII] = 1 x 10^{-4} M and [La^{3+}] = 1 x 10^{-4} M and [AAIII] = 2 x 10^{-4} M. In this range of concentrations, La and AAIII concentrations have no influence on the kinetics of La-DTPA complexation. For concentration 1 x 10^{-4} M, k_{form} was 21.7 ($\pm$ 0.3) x 10^3 M^{-1}s^{-1} while k_{diss} was 15 $\pm$ 1 s^{-1}. At 2 x 10^{-4} M, the

corresponding values were $k_{form} = 21.9 \ (\pm 0.4) \ \text{x} \ 10^3 \ \text{M}^{-1}\text{s}^{-1}$ and $k_{diss} = 15 \pm 4 \ \text{s}^{-1}$. These results are interpreted to indicate that AAIII is not involved in the rate determining step of the reaction and further that the reaction rate in independent on the lanthanide cation concentration (thus there are no polynuclear or metal bridged intermediate species involved).

Lanthanide series trends

Differences in the rate constants have been determined in a progression across the lanthanide series (Figure 8, with the exception of promethium). Experiments have been completed in the [DTPA] range from 0.2 - 1.2 mM; [Ln] = [AAIII] = 10^{-4} M; 0.3M Na/Lactate buffer at pH 3.6; [NaClO$_4$] = 0.3 M and 25°C.
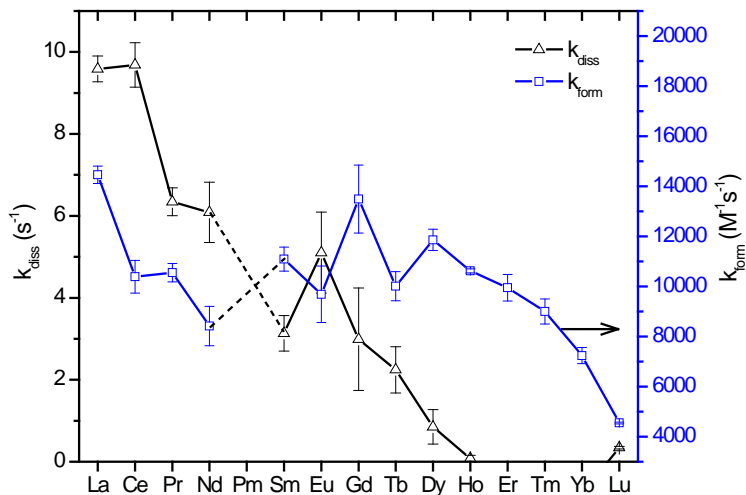
Figure 8: Rate constants for complex formation and dissociation reactions of lanthanides with DTPA at pH 3.6, 25 °C and [Lac]$_{tot}$ = 0.3 M.

As observed in Figure 8, the rate constants vary across the series in an unexpected manner. The apparent anomalies in the complex formation rate appear for elements from the middle of the series, especially for Gd. Initially a decrease can be seen from La to Nd with an increase and leveling from Sm to Dy at which point k_{form} begins to decrease. In general, k_{form}

decreases across the lanthanide series with the lanthanide contraction as demonstrated in previous studies for others ligands.[13] It is seen that k_{diss} decrease more or less regularly across the series. Beyond Dy the complex dissociation rate constants are not discernable, that is the pseudo-first order plots of k_{obs} vs. [DTPA] at constant temperature and ionic strength have zero intercept.

Discussion

It has been shown in earlier studies of lanthanide phase transfer reactions relevant to the TALSPEAK solvent extraction system that the lactate ion (present at significant concentrations) greatly facilitates the rate of the phase transfer reaction.[16,17] A principle objective of this investigation is to establish the role of lactate ion in the rate and mechanism of the complex association and dissociation reaction of lanthanide ions in concentrated lactate media for the present lanthanide-aminopolycarboxylic acid system. It also has been demonstrated previously that the ligand displacement approach utilized in this investigation typically yields information on the rate and mechanism of the reaction of interest generally without direct involvement of the colorimetric indicator in the kinetics of the process.[14,18] The experiments conducted as a function of the concentration of the lanthanide Arsenazo III complex described above confirms that in the present system Arsenazo III is not an active participant in the kinetics of lanthanide - DTPA complexation.

Given that H_3DTPA^{2-} is the dominant free ligand species, the reaction should proceed as follows.

$$\text{La-AAIII} \longrightarrow \text{La}^{3+} + \text{AAIII} \qquad \text{(fast)} \qquad\qquad (2)$$

$$\text{La}^{3+} + \text{H}_3(\text{DTPA})^{2-} \underset{k_{diss}}{\overset{k_{form}}{\rightleftharpoons}} \text{La-DTPA}^{2-} + 3\,\text{H}^+ \qquad\qquad (3)$$

In this standard reversible reaction the observed rate constant will be a sum of the forward and reverse reactions.

The variation of the pseudo-first order rate constants for the dissociation of La^{3+} with [DTPA] and with pH at constant $[Lactate]_{tot}$ (Figure 5) indicates the expected linear plots with finite positive intercepts. The constant intercept value (k_{diss}) indicates that the complex dissociation reaction is nearly independent of pH under these conditions. The complex formation rate increases with increasing $[H^+]$. An increasing rate of complex formation with increasing $[H^+]$ is contrary to what is expected, as the thermodynamic driving force for the reaction of La^{3+} with H_nDTPA^{n-5} increases with decreasing $[H^+]$ due to the increased electrostatic attraction between the presumed reactants Ln^{3+} and H_nDTPA^{n-5} as n decreases.

In Figure 9, the plot of k_{form} and k_{diss} vs. $[H^+]$ shows that both increase with an increase in the $[H^+]$ in the system. From this plot, acid dependent and independent process rate constants can be defined as previously. For k_{form} an $[H^+]$ dependent 3rd order rate constant has been determined to be 1.9 ($\pm$ 0.2) x 10^7 $M^{-2}s^{-1}$ and an $[H^+]$ independent rate constant has been determined to be 9.0 ($\pm$ 0.9) x 10^3 $M^{-1}s^{-1}$ from this data. For k_{diss} the $[H^+]$ dependent 2nd order rate constant has been determined to be 4 ($\pm$ 1) x 10^3 $M^{-1}s^{-1}$ and the $[H^+]$ independent rate constant has been determined to be 8.7 ($\pm$ 0.4) x s^{-1} from this data. In the pH range of this investigation, the predominant protonated form of DTPA remains H_3DTPA^{2-} throughout. This ligand species should exist on average with the three amine nitrogens protonated and all five carboxylates ionized.
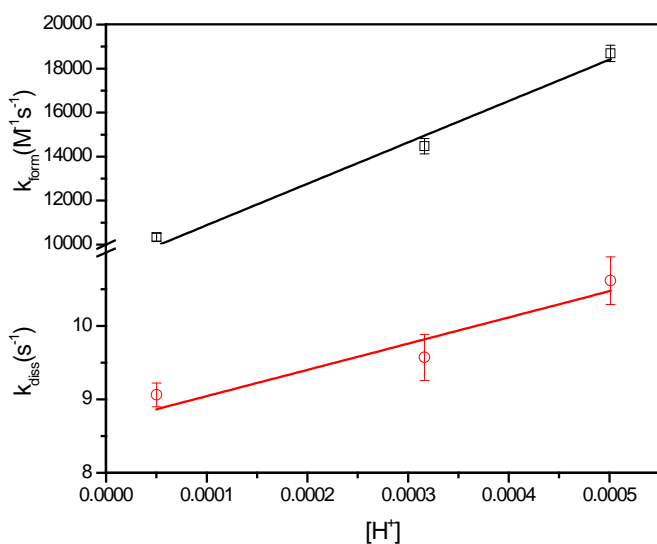
Figure 9: Plots of k_{form} (□) and k_{diss} (○) vs. $[H^+]$; $[La] = [AAIII] = 10^{-4}$ M, T = 25 °C and $[Lac]_{tot}$ = 0.3 M.

Lactate dependence

Previous studies of the kinetics of Ln complexation/dissociation with DTPA and EDTA have been conducted in systems either un-buffered or buffered with acetate by Brucher and Laurency[9,18] or using acetate buffer with EDTA by Ryhl [3,20]. The studies have not been performed with a lactic acid concentration used in the actual TALSPEAK process.[2] In this work, the influence of lactic acid concentration has been studied in the range of 0.1 - 0.3 M. Lactic acid has proven to behave as more than just a buffer in systems where it is present. This can be demonstrated in Figure 10 with a plot of k_{form} and k_{diss} vs. $[Lactate]_{total}$ (Figure 10). The concentration of lactate has negligible effects in the rate of complex formation shown by the average k_{form} of 1.96 ($\pm$ 0.02) x 10^4 $M^{-1} \cdot s^{-1}$ for lactic acid concentrations 0.1, 0.2 and 0.3 M. The dissociation rate constant decreases upon increasing lactic acid concentration with rate constants of 28.6 ($\pm$ 0.3)s^{-1}, 17.6 ($\pm$ 0.9) s^{-1} and 10.4 ($\pm$ 0.7) s^{-1} respectively for lactic acid concentrations 0.1, 0.2 and 0.3 M. The lactate ion thus participates in the rate determining step of the

45

complexation dissociation reaction. A plot of k_{diss} vs. [Lactate]$_{total}$ provides a lactic acid independent rate constant for the complex dissociation of 36 ± 3 s^{-1}(Figure 10).
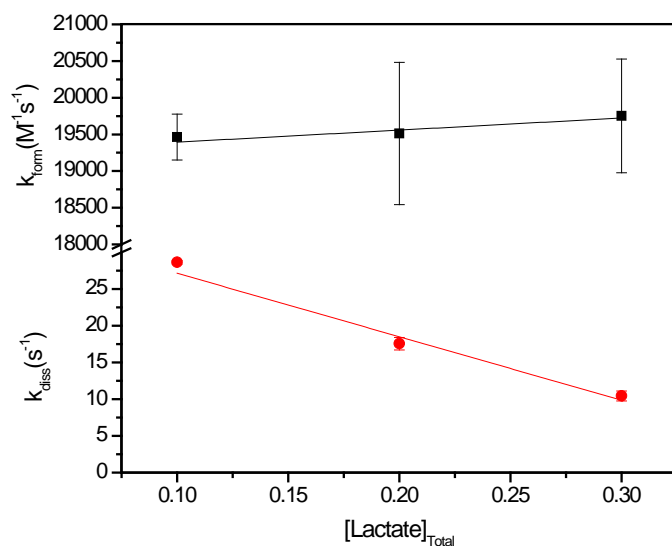
Figure 10: Plots of k_{form} and k_{diss} vs. [Lac]; [La] = [AAIII] = 10^{-4} M, T = 25 °C, pH = 3.6 and I = 0.3M

<u>Activation parameters</u>

Determination of the activation parameters of the Ln/DTPA complexation helps in defining the mechanism of the reaction. To determine activation parameters, reactions were studied as a function of temperature, generally in the range of 5 °C to 35 °C at pH = 3.6, I = 0.3M, [Lac] = 0.3M and [Ln^{3+}] = [AAIII] = 1 x 10^{-4}M. The activation parameters are calculated using the transition state theory equation (TST - Equation 4), using the variable temperature results.

$$k = \kappa(k_b T / h) \exp(\Delta S^* / R) \exp(\Delta H^* / RT) \qquad (4)$$

In this equation, k_b is Boltzmann's constant; h, is Planck's constant; κ, transmission factor (usually κ = 1); and R, the gas constant. The rate constants for complex formation k_{form} and dissociation k_{diss} determined previously were adjusted using the linearized form of Equation 4, shown as Equation 5.

$$\ln(k/T) = \ln(k_b/h) + \Delta S*/R - \Delta H*/RT \qquad (5)$$

A plot of $\ln(k/T)$ vs. $1/T$ produces a straight line from which the enthalpy ($\Delta H*$) is determined from the slope and the entropy ($\Delta S*$) from the intercept (Figure 11). Using the Eyring relation, the enthalpy, entropy and free energy of activation are calculated, for both reverse and forward reaction of the acid catalyzed dissociation process. In the following equations, k_B and h are the Boltzmann and Planck constants respectively, T is the absolute temperature and R is the gas constant. The transition state theory also provides the Gibbs free energy through Equation 6.

$$\Delta G* = \Delta H* - T\Delta S* \qquad (6)$$
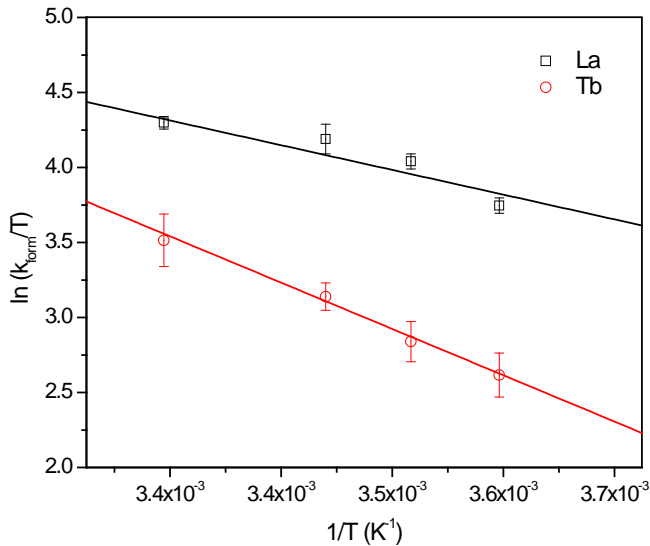
Figure 11: TST plot for complex formation in M-DTPA system (M = La and Tb) (I = 0.3 M). Errors are shown at 3σ.

Activation parameters have been determined for the Ln-DTPA system using La^{3+}, Tb^{3+} and Lu^{3+}. The parameters presented in Table 2 have been determined at pH 3 and 3.5 at temperatures of 5, 15, 20, 25 and 35 °C for the La-DTPA system and 5, 15, 25 and 35 °C for the Tb/Lu-DTPA. To calculate ΔG*, the reference temperature of 25 °C (298 K) was chosen. Comparison of the La^{3+}, Tb^{3+} and Lu^{3+} parameters provides insight into behavior of lanthanides throughout the series (Table 2). The activation entropy for the formation and dissociation of Ln-DPTA is negative. At Tb^{3+}, ΔS* has become less negative for both complex formation, -90 ± 8 J/(mole*K) and complex dissociation, -87 ± 28 J/(mole*K) as compared to La^{3+}. By Lu, the activation entropy for complex formation is effectively equal and complex dissociation has become more negative by 80 J/(mole*K) as compared to La^{3+}. The unfavorable activation entropies are compensated by reduced activation enthalpy barriers (Table 2).

Table 2: Activation parameters for complex formation and dissociation reactions of Ln with DTPA. T = 25 °C, [Lac]$_{tot}$ = 0.3 M and I = 0.3 M.

DTPA	k_{form}			k_{diss}		
	ΔH* (kJ/mol)	ΔS* (J/mol.K)	ΔG* (kJ/mol)	ΔH* (kJ/mol)	ΔS* (J/mol.K)	ΔG* (kJ/mol)
La (pH 3)	39 ± 3	-84 ± 8	64 ± 6	26 ± 3	-191 ± 39	83 ± 14
La (pH 3.5)	18 ± 2	-160 ± 11	65 ± 6	48 ± 3	-117 ± 12	83 ± 7
La w/X-114 (pH 3.5)	26 ± 3	-131 ± 14	65 ± 8	14 ± 3	-239 ± 21	85 ± 9
Tb (pH 3.5)	40 ± 2	-90 ± 8	67 ± 5	61 ± 5	-87 ± 28	87 ± 13
Lu (pH 3.5)	24 ± 2	-150 ± 10	69 ± 5	37 ± 3	-187 ± 15	92 ± 7

The negative ΔS* indicates that both complex formation and dissociation pathways are associative in nature. One possible sequence consistent with the parameters would be for the incoming DTPA to interact with the metal as an outer sphere complex (per the Eigen

mechanism). Water will get pushed out of the coordination sphere as the DTPA carboxylate oxygen atoms begin to bond to the Ln^{3+}. The Ln^{3+}-carboxylate interaction reduces the freedom of movement of the DTPA carboxylates, reducing the entropy of the system. A significant interaction with the softer nitrogen occurs when complexants sterically forces the interaction.[8] The formation of the metal/nitrogen bond has generally been considered to be the slow step in the reaction.

<u>Effects of a surfactant</u>

A surfactant is expected to alter the properties of hydration and solvation, both major factors in kinetics of complexation, modifying the rates for both complex formation and dissociation reactions. Surfactants lower the surface tension of a liquid and the interfacial tension between two liquids. They are usually amphipathic organic compounds, meaning they contain both hydrophobic groups ("tails") and hydrophilic groups ("heads"). They are typically sparingly soluble in both organic solvents and water. Triton X-114, a nonionic surfactant, was chosen as the surfactant in this set of experiments.

Many surfactants can also assemble in the bulk solution into aggregates that are known as micelles. The concentration at which surfactants begin to form micelles is known as the critical micelle concentration or CMC. When micelles form in water, their tails form a core that is like an oil droplet, and their heads form an outer shell, or corona, that maintains favorable contact with water. For Triton X-114, the CMC in distilled water is 0.2 mM at 20 - 25 °C according to Sigma Aldrich. To determine the effect of adding a surfactant on the activation parameters, the experiment was run at the CMC for La-DTPA. As earlier, the ligand concentration was changed at each temperature producing a similar plot to Figure 4.

Activation parameters for complex formation and dissociation reactions in the presence of surfactant were determined using the Arrhenius and Eyring relations. To have access to activation parameters, the condition of surfactant in both syringes has been chosen and run for many temperatures. The critical micelle concentration (CMC) is reached, resulting in the formation of non ionic micelles in solution. Presumably, with non ionic Triton X-114, lanthanide cation is neither attracted nor repulsed by micelles. As a result, the concentrations and thus rates in both micelles and bulk solution should not be significantly affected by the presence of the surfactant. However, the complex dissociation rate constant is increased slightly by the presence of a micelle. We believe that the increase in rates results from an increase in concentration of each reactant in the surface region of the micelle as compared with the bulk solution. The most profound effect on activation parameters is for ΔS^*. This difference can be explained by the change of chemical activity in solution provoked by addition of surfactant. The increase in viscosity that occurs with adding surfactant in solution could also have affected the change in entropy within the system.

Rate Law

Summation of the results and observations provide the overall rate law shown in Equation 9 below.

$$\text{Rate} = k_{form}[\text{Ln}][\text{DTPA}](k_1 + k_2[\text{H}^+])$$

$$- k_{diss}[\text{Ln-DTPA}](k_3 + k_4[\text{H}^+])/(1 + k'[\text{Lactate}]_{tot}) \qquad (9)$$

The [H^+] dependence was accessed in the range of pH from 3.3-4.3. The TALSPEAK process requires a tight control on pH which is corroborated by this work that shows an increase in pH slows the rate of complex formation. The k_{diss} has been demonstrated to be inversely dependent

on the total lactate concentration (k_{diss} decreases as [Lactate]$_{total}$ increases). Increasing lactic acid concentration therefore slows the rate of dissociation.

The finite positive intercept of the plot of k_{diss} vs. [Lactate]$_{Total}$ indicates that there is also a lactate independent dissociation pathway. It is known that the thermodynamic stability of lanthanide-DTPA complexes increases steadily from La^{3+} to Eu^{3+} then remains more or less constant from Gd^{3+} to Lu^{3+}, perhaps indicating lower denticity in the heavier lanthanides.[21] This pattern is not seen to be replicated in the k_{form}, k_{diss} or k_{form}/k_{diss} values shown in Figure 8. It is likely that this disconnect arises from the complexity of the media and mechanism implicit in Equation 9.These observations are important to TALSPEAK since DTPA used is a holdback reagent for Am^{3+} and Cm^{3+} and counterbalances lanthanide extraction by HDEHP. This study shows that a lower [Lactate] would increase dissociation of Ln-DTPA complexes thereby potentially increasing release rate of the lanthanide from Ln-DTPA thus allowing faster release of the lanthanide into the organic phase.

Conclusion

The rates of complexation of lanthanides by DTPA in lactate media have been investigated by stopped-flow spectrophotometry using the ligand displacement technique. The reaction proceeds as a first-order approach to equilibrium under all conditions. The results of this study provide addition evidence that solvation and geometric constraints are major factors in the kinetics of lanthanide complexation by amino-carboxylate ligands. Both complex formation and dissociation rates are directly proportional to hydrogen ion concentration. Interestingly, the predominant pathway for lanthanide-DTPA dissociation is inversely proportional to lactic acid concentration. An associative mechanism appears to govern both complex formation and dissociation of the Ln/DTPA complex. The addition of surfactant did not affect the rate of

complex formation and only had a small effect on the rate of complex dissociation. Not unexpectedly, the mechanism of lanthanide complexation by DTPA in concentrated lactate media is complex. Furthermore, the trans-lanthanide patterns of complex formation and dissociation do not correlate directly with the thermodynamic driving force for the reaction.

Acknowledgements

References

1. Weaver, B.; Kapplemann, F. A. *TALSPEAK: A New Method of Separating Americium and Curium from the Lanthanides by Extraction from an Aqueous Solution of an Aminopolyacetic Acid Complex with a Monoacidic Organophosphate or Phosphonate.* Oak Ridge National Laboratory Report– 3559: Oak Ridge, TN, 1964.

2. Nilsson, M; Nash, K. L. A Review of the Development and Operational Characteristics of the TALSPEAK Process. *Solvent Extr. Ion Exch.* **2007**, 25, 665-701.

3. Ryhl, T. Kinetic Studies of Lanthanoid Carboxylate Complexes. III. Dissociation Rates of Praseodymium, Neodymium, Europium, and Erbium EDTA Complexes. *Acta Chem. Scand.* **1973**, 27(1), 303-314.

4. Glentworth, P.; Wiseall, B.; Wright, C. L.; Mahmood, A. J. A Kinetic Study of Isotopic Exchange Reactions Between Lanthanide Ions and Lanthanide Polyaminopolycarboxylic Acid Complex Ions. I. Isotopic Exchange Reactions of Ce(III) with Ce(HEDTA), Ce(EDTA)$^-$, Ce(DCTA)$^-$, and Ce(DTPA)$^{2-}$. *J. Inorg. Nucl. Chem.* **1968**, 30(4), 967-986.

5. Choppin, G. R. A Half Century of Lanthanide Aminopolycarboxylates. *J. Alloys Compd.*, **1993**, 192, 256-261.

6. Moeller, T.; Martin, D. F.; Thompson, L. C.; Ferrus, R.; Fiestel, G. R.; Randall, W. J. The coordination chemistry of yttrium and the rare earth metal ions. *Chem. Rev*. **1965**, *65(1)*, 1-50.

7. Lincoln, S. F. Solvation, Solvent Exchange, and Ligand Substitution Reactions of the Trivalent Lanthanide Ions. *Adv. Inorg. Bioinorg. Mech.* **1986**, *4*, 217-287.

8. Nash, K. L; Sullivan, J. C. Kinetics of Complexation and Redox Reactions of the Lanthanides in Aqueous Solutions. In *Handbook on the Physics and Chemistry of Rare Earths*, Gscheidner, K. A., Eyring, L. Eds.; Elsevier Science Publishers B.V.: San Diego, CA, 1991, Vol. 15, pp 341-391.

9. Asano, T.; Okada, S.; Taniguchi, S. Kinetic studies on isotopic exchange between neodymium ion and its diethylenetriaminepentaacid complex. *J. Inorg. Nucl. Chem.* **1970**, 32(4), 1287-1293.

10. Brücher, E.; Laurenczy, G. Kinetic Study of Exchange Reactions between Eu^{3+} Ions and Lanthanide III DTPA Complexes. *J. Inorg. Nucl. Chem* **1981**, 43, 2089-2096.

11. Choppin, G. R.; Williams, K. R. Kinetics of Exchange Between Americium (III) and Europium Ethylenediaminetetraacetate. *J. Inorg. Nucl. Chem.* **1973**, 35(12), 4255-4269.

12. Brucher, E.; Banyai, I.; Krusper, L. Aminopolycarboxylates of rare earths, XI. Kinetics of metal ion-exchange and ligand exchange reactions of the (ethylene glycol)bis(2-aminoethylether)tetraacetate complex of cerium(III). *Acta Chim. Hung.,* **1984**, 116(1), 39-50.

13. Kumar, K.; Tweedle, M. F. Macrocyclic Polyaminocarboxylate Complexes of Lanthanides as Magnetic Resonance Imaging Contrast Agents. *Pure Appl. Chem.* **1993**, 65(3), 515-520.

14. Nash, K. L.; Sullivan, J. C. Kinetics of Actinde Complexation Reactions. *J. Alloys Compd.* **1998**, 271-273, 712-718.

15. Rowatt, E.; Williams, J.P. The Interaction of Cations with the Dye Arsenazo III. *Biochem.J.* **1999**, *259*, 295-298.

16. Kolařík, Z.; Koch, G.; Kuhn, W. The Rate of Ln(III) Extraction by HDEHP From Complexing Media. *J. Inorg. Nucl. Chem.* **1974**, 36, 905-909.

17. Nilsson, M.; Nash, K. L. Trans-Lanthanide Extraction Studies in the TALSPEAK System; Investigating the Effect of Acidity and Temperature. *Solvent Extr. Ion Exch.* **2009**, 27(3), 354-377.

18. Fugate, G.; Feil-Jenkins, J. F.; Sullivan, J. C.; Nash, K. L. Actinide Complexation Kinetics: Rate and Mechanism of Dioxoneptunium(V) Reaction with Chlorophosphonazo III. *Radiochim. Acta*, **1996**, 73(2), 67-72.

19. Laurenczy, G.; Brucher, E.. Aminopolycarboxylates of Rare Earths. 12. Determination of Formation Rate Constants of Lanthanide(III)-Ethylenediaminetetraacetate Complexes Via a Kinetic Study of the Metal-Exchange Reactions. *Inorg. Chim. Acta.* **1984**, 95(1), 5-9.

20. Ryhl, T. The Dissociation of Yb, La and Cu EDTA Complexes. *Acta Chem. Scand.* **1972**, 26, 3955-3968.

21. Martell, A. E.; Smith, R. M.: NIST Standard Reference Database 46 version 8.0, 2004.

Chapter 3

Kinetics of lanthanide complexation reactions with EDTA

(ethylenediaminetetraacetic acid) in lactic acid media

Preface

In Chapter 3 the kinetics of lanthanide interaction with EDTA under TALSPEAK-like conditions were examined to evaluate k_{form} and k_{diss} for the lanthanide series. The change in complexing agent provides some information on how changes in the backbone of the holdback reagent affect the rates of complexation under the same conditions as studied in chapter 2. The ligand displacement technique proved good in this particular system allowing for a full evaluation under many sets of conditions. Additional information for this chapter can be found in the Appendix.

This chapter will be submitted to an inorganic chemistry journal. The first choice for submission is to Dalton Transactions. Formatting of the chapter results from a balance of ACS guidelines and guidelines set forth by WSU. Figures have been inserted into the text near the reference location for ease of reading in this document. They will be removed and placed at the end of the document prior to submitting.

Kinetics of lanthanide complexation reactions with EDTA (ethylenediaminetetraacetic acid) in lactic acid media

Thomas Shehee[1], Aymeric Martin[1], James C. Sullivan[1, #], Kenneth L. Nash*, [1]

[1]Chemistry Department, Washington State University, PO Box 644630, Pullman, WA 99164-

4630

- deceased

* Author for correspondence

Abstract

An important feature of the chemistry of the TALSPEAK process (for the separation of trivalent actinides from lanthanides) is the interaction of trivalent lanthanide and actinide cations with aminopolycarboxylic acid complexing agents in lactic acid buffer systems. To improve our understanding of the mechanistic details of these processes, an investigation of the kinetics of lanthanide complexation by EDTA in concentrated lactic acid solution has been completed. The reactions studied occur in a time regime suitable for study by stopped-flow spectrophotometric techniques. Progress of the reaction is monitored using the distinctive visible spectral changes attendant to lanthanide complexation by the colorimetric indicator ligand Arsenazo III (AAIII). Experiments have been conducted as a function of pH, lactic acid concentration, EDTA concentration and temperature. Under all conditions the kinetic traces are adequately adjusted using the rate law appropriate for a single exponential decay. The reaction proceeds as a first order approach to equilibrium over a wide range of conditions, allowing the simultaneous determination of complex formation and dissociation rate constants. The rate of the complexation reaction has been determined for the entire lanthanide series except Pm^{3+}. The complex formation rate has been shown to be proportional to hydrogen ion concentration. The

predominant pathway for lanthanide EDTA dissociation is inversely proportional to lactic acid concentration. Activation entropy has been interpreted as an indication of an associative mechanism for both complex formation and dissociation of the Ln/EDTA complex. The addition of surfactant did not affect the rate of complex formation but had a small effect on the rate of complex dissociation.

Introduction

The separation of actinides from trivalent lanthanides and curium in used nuclear fuel is a significant problem facing developed countries. The lanthanides are produced in relatively high yield through the fission of ^{235}U. Almost all the lanthanide isotopes decay to stable nonradioactive lanthanide isotopes in a relatively short time. Consequently, it is highly advantageous to separate the relatively small actinide fraction from the relatively large quantities of lanthanide isotopes. One of the most efficient separation processes available to separate the trivalent actinides from the lanthanides is the TALSPEAK process (Trivalent Actinide Lanthanide Separations by Phosphorus reagent Extraction from Aqueous Komplexes).[1] TALSPEAK is an effective method which does not involve high concentrations of any salt or acid and is resistant to the effects of irradiation. The process operates by extraction of the lanthanides with di(2-ethylhexyl) phosphoric acid (HDEHP) solution from aqueous phase of lactic acid and diethylenetriamine-N,N,N',N'',N''-pentaacetic acid(DTPA) at pH 2.5 to 3.0. DTPA retains the actinides in the aqueous phase to allow the selective extraction of the trivalent lanthanides.

The rates of complex formation and dissociation of lanthanides with aminopolycarboxylic acid complexants have been previously investigated using either metal ion or ligand exchange reactions, using mainly spectrophotometric methods.[2,3] It is reported that both the dissociative

and interchange mechanisms operate often simultaneously. Thermodynamic features of complexation reactions of elements in the lanthanide series with EDTA (ethylenediamine-N,N,N',N'-tetraacetic acid) in an acetate buffer have also been investigated in these previous studies.[3] In the present study, the rate and mechanism of lanthanide-EDTA complexation reactions have been investigated in lactate media of moderate concentration. This medium is of interest for the integral role it plays in the TALSPEAK solvent extraction separation process. This biphasic reaction is known to demonstrate unusually slow phase transfer kinetics for a lanthanide system. This study addresses the rate and mechanism of the complexation of lanthanides by EDTA in concentrated lactate buffer solutions.

The hexadentate EDTA, shown in Figure 1, coordinates to metal ions by forming five five-member chelate rings. The binding cavity is flexible enough to accommodate a variety of metal ions, but the large Ln (III) appears to be well suited to the hexadentate coordination mode.
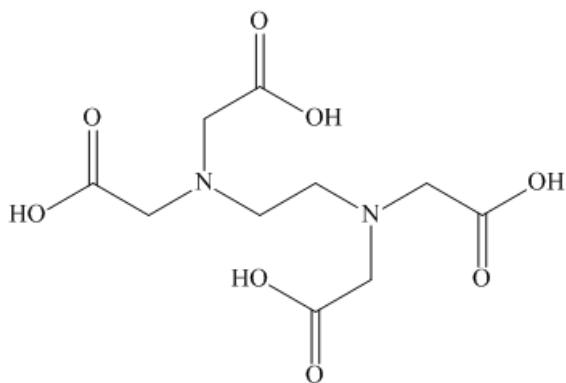
Figure 1: Structure of EDTA

The pK_a values for EDTA are 0.0, 1.4, 2.02, 2.52, 6.19 and 8.73 for the four carboxylate groups and two amino groups, in order at I = 1.0 M and T = 25 °C.[4] In the pH range studied, $H_2(EDTA)^{2-}$ is the predominant free ligand species present. The coordination chemistry of the lanthanide complexes with polyaminocarboxylate ligands, especially EDTA, has been comprehensively reviewed.[5-7] The report by Moeller emphasizes that the bonding in lanthanide-polyaminocarboxylate chelates may be considered as involving fundamentally an electrostatic interaction. In addition to the evidence of this structure and bonding, there is an

additional investigation reported in literature that is relevant of this type of metal chelate. Hoard et al.[8] have reported an X-ray crystallographic study of solid lanthanide chelates, $Ln(H_2O)_3X^-$ where $X = EDTA^{4-}$, in which it is proposed that the polyaminocarboxylate chelates of the light lanthanide elements are nine-coordinate. The proposed structure shows that the entire chelating ligand is contained in one hemisphere, leaving ample space for three water molecules in the other hemisphere.[3] As shown in Figure 2, the complex is composed of five five-member chelate rings. In four rings, the metal cation is bound by one oxygen atom and one nitrogen atom. The fifth is composed of the metal cation bound to both nitrogen atoms of EDTA.
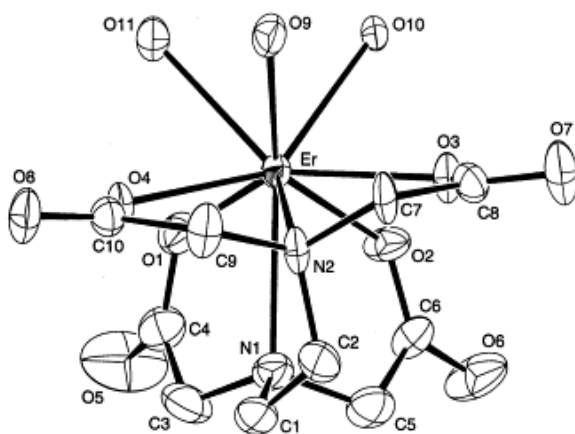
Figure 2: Crystalline structure of $[C]^+$ [(Sakagama 1999)] In the structure, erbium (CN = 9), is coordinated by EDTA six times and coordinated to three water molecules.

An earlier stopped flow kinetics complexation reaction investigation of cation exchange kinetics between Tb^{3+} and $Ca(EDTA)^{2-}$ monitored the progress of the reaction by Tb(III) luminescence.[9] The data obtained was interpreted to indicate that metal ion exchange occurs via acid-catalyzed dissociation of the $Ca(EDTA)^{2-}$ complex with rapid formation of the Tb(III)-EDTA complex, and through a parallel process involving a dinuclear intermediate. The acid-catalyzed dissociation pathway was concluded to be the preferred mode.[9] Brücher and coworkers, compared the derived rate parameters with order of magnitude estimates of the lanthanide hydration rates, conclude that the rate determining step of the complex formation

between Ln(III) and $H(EDTA)^{3-}$ must be a ring closure reaction in agreement with previous data interpretations.[10] For complex formation reactions between Ln(III) and $H_2(EDTA)^{2-}$, the resolved rates are slower, indicating that proton transfer to convert the ligand to a more kinetically active form becomes the limiting process.

In this investigation the impact of moderate concentrations of lactate buffer solutions on the rate and mechanism of lanthanide complexation by EDTA is investigated. The buffer concentration is maintained at a moderate concentration to conform to representative conditions of the TALSPEAK separation system.

Experimental

Reagents

Lanthanide perchlorate stock solutions have been prepared using 99.999% Ln_2O_3 from Arris International Corp. through dissolution of the solid in $HClO_4$. Stock solutions were standardized by ICP-OES analysis. These lab stocks were used to prepare each lanthanide sample in the series. Arsenazo III was added directly to the solutions by weight using material obtained from Fluka Chemika. Solutions of variable EDTA concentration were prepared by weight using material obtained from JT Baker and using only 99.9% disodium EDTA anhydrous salts because of its better solubility in lactic acid media. Lactic acid is used at different concentrations as a media constituent. It is prepared by weight using 88.4% w/w material obtained from JT Baker. The $NaClO_4 \cdot H_2O$ obtained from Fisher was employed as the supporting electrolyte to maintain constant ionic strength. Triton X-114 surfactant was used in selected studies without further purification using material obtained from Sigma. Adjustment of pH was accomplished by the addition of standardized NaOH or HCl. All solutions were prepared in 18 $M\Omega$ deionized water.

Procedure

The kinetics of the reaction of lanthanides with chelating agents in lactic acid media have been investigated by stopped-flow spectrophotometry. In stopped-flow spectrophotometry, mixing is essentially complete within few milliseconds at which time the period of observation of changing absorptivity begins. Rates of reactions that are complete within a range of milliseconds to seconds are accessible using this technique. An OLIS RSM-1000 stopped-flow spectrophotometer was used for data acquisition and the OLIS RSM Robust Global Fitting software package for analysis of the absorbance data as a function of time. Data were collected over a wavelength range of 500 nm to 800 nm.

The lanthanide aqueous ions are not strongly colored; therefore the application of spectrophotometric techniques like stopped-flow to their complexation kinetics must rely on the use of strongly colorimetric chelating agent, either as the subject ligands or as indicators of the free metal ion in the reaction of interest. Derivatives of chromotropic acid have proven to be quite useful in kinetic investigations of this type and generally do not participant in the kinetics of the reaction of interest. Previous studies[11] investigated in particular the rates of complex formation of a variety of lanthanide cations with Arsenazo III (2,2'-(1,8-dihydroxy-3,6-disulfonaphthylene-2,7-bisazo)bis(benzenearsonic acid, Figure 3).
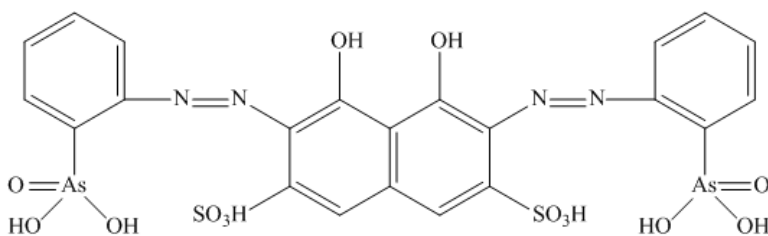
Figure 3: Structure of Arsenazo III (2,2'-(1,8-dihydroxy-3,6-disulfonaphthylene-2,7-bisazo)bis(benzenearsonic acid)

Arsenazo III appears to coordinate the lanthanide cation in a tetradentate manner with one oxygen atom from each arsenate and the phenol groups.[12] The eight pK_a values for Arsenazo III are $pK_1 = -2.5$, $pK_2 = 0$, $pK_3 = pK_4 = 2.5$, $pK_5 = pK_6 = 5.3$, $pK_7 = 7.5$ and $pK_8 = 12.4$.[11] Formation of the complex is accompanied by a significant change in the visible spectrum. Hence, this reagent has been used as indicator of the free metal ion concentration to study the kinetic of complexation of lanthanide ions with ligands in this work. In most previous studies, the indicator ligand plays no significant role in the kinetics and mechanism of complex formation of the metal ion with the ligand of interest. The spectrum of the La^{3+}-AAIII complex and free AAIII was measured on an OLIS scanning spectrophotometer and is shown in Figure 4. The λ_{max} for the blue La-AAIII complex is 650 nm, whereas the free AAIII ligand is magenta with a maximum absorbance at 550 nm. The extinction coefficients of the bands at the $\lambda_{max}= 650$ nm are greater than 10^4 $M^{-1}cm^{-1}$, allowing the spectrophotometric monitoring of lanthanide concentration at 10^{-4} M or less. The absorbance band of the La-AAIII complex was chosen as the center wavelength, monitoring the disappearance of the peak at 650 nm. Disappearance of this peak would correspond to the complete complexation of the metal ion with EDTA and the appearance of the 550 nm spectrum of free AAIII.

Under most conditions, the EDTA was present in sufficient excess over Ln^{3+} to maintain pseudo-first order conditions. The Ln-AAIII complex concentration was 10^{-4} M with an EDTA concentration in the range of 0.2 - 1.2 mM. The range of concentration of EDTA was dictated in part by its solubility in lactic acid media. At the lower concentration range, pseudo first order conditions are not maintained with only a twofold excess of EDTA as opposed to 10-fold excess for pseudo first order. Even under these conditions, the kinetic trace conformed to a single first order process. Each solution was buffered using a Na/Lactate buffer at pH 3.6. The respective

solutions where placed in syringes that are thermostated in a water bath. The solutions were allowed to equilibrate at the desired temperature for 5 minutes before making an injection. Upon injection, the instrument measured the change in absorbance with respect to time. The time interval for evaluation was dependant on the experimental conditions. Five measurements have been made under each set of conditions and averaged to provide k_{obs} for that set of conditions.
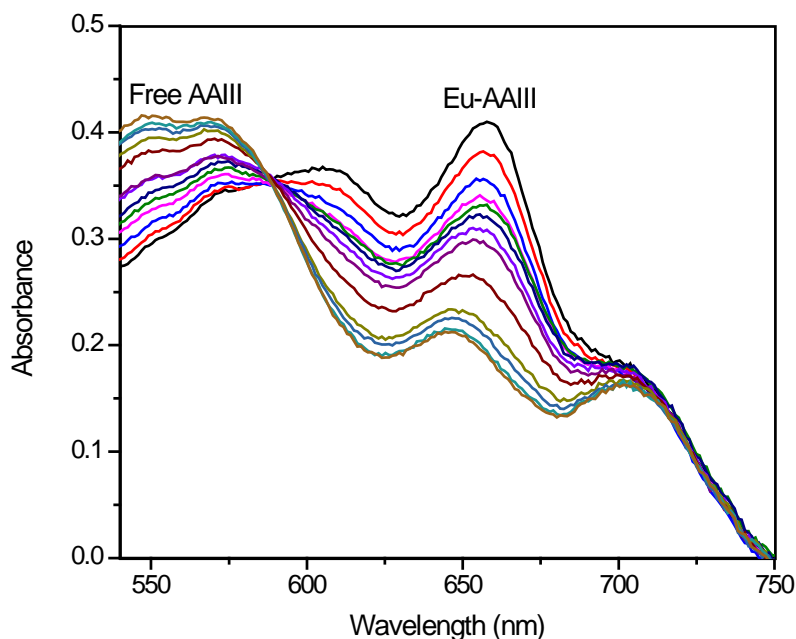
Figure 4: Change in the visible spectrum that occurs upon complex Eu-AAIII dissociation – [Eu-AAIII] = 10^{-4} M; [EDTA] = 2.4 x 10^{-3}; [Lac]$_{tot}$ = 0.3 M; T = 25 °C

Results

The observed rate constant for the complexation of every lanthanide ion at several EDTA concentrations was determined at 25 °C. The raw data is shown in Figure 4. Olis Globalworks used this data to produce the kinetic traces of absorbance vs. time, which were observed in all cases to be adequately adjusted using a single exponential fit, i.e. they conform to first order kinetics. Rate constants determined as a function of [EDTA] were plotted to reveal that a linear correlation with finite positive intercept as shown in Figure 5 for La^{3+}. This condition was seen

to persist throughout the lanthanide series. It is also noteworthy in these plots that the first order fits of absorbance vs. time were appropriate even at 0.2 mM EDTA. This implies that the rate determining step is an intramolecular process.

Determination of k_{form} and k_{diss}

Under present pseudo-first order conditions, excess EDTA, a plot of k_{obs} versus [EDTA] is a straight line with finite positive intercept (Equation 1), except at 5 °C. The slope of this line corresponds to the rate constant for the complex formation k_{form}, which is in $M^{-1}\cdot s^{-1}$, while the intercept is the rate constant for the complex dissociation k_{diss} in s^{-1}.

$$k_{obs} = k_{form} [EDTA] + k_{diss} \qquad (1)$$

Figure 5 shows that the first order approach to equilibrium model properly adjusts the data over the range of temperatures studied.
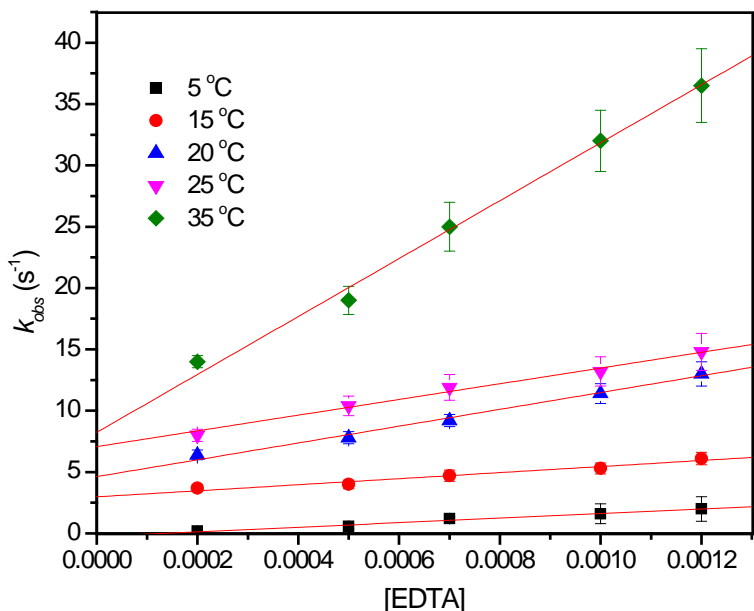
Figure 5: The effect of temperature on the rate of reaction of La with EDTA in lactate solution at pH = 3.6, $[Lac]_{tot} = 0.3$ M and I = 0.3M.

<u>Acid dependence</u>

Reactions were studied as a function of pH, in the range of pH = 3 - 4.7, which allowed examination of the acid dependence for both complex formation and dissociation reactions (Figure 6). In this case, experiments were adjusted to constant ionic strength with sodium perchlorate (0.3 M). Reagent solutions, Ln-AAIII and EDTA were adjusted to the same acidity in any given experiment. For the La-EDTA system, experiments were run, in lactate solution, as a function of pH to determine the effect of $[H^+]$ on the rates. The complex formation constants are 1.20 ($\pm$ 0.02) x 10^4 $M^{-1}s^{-1}$, 9.1 ($\pm$ 0.1) x 10^3 $M^{-1}s^{-1}$, 7.0 ($\pm$ 0.2) x 10^3 $M^{-1}s^{-1}$ and 4.6 ($\pm$ 0.1) x 10^3 $M^{-1}s^{-1}$ at pH = 3, 3.5, 4 and 4.7 respectively. The rates of complex dissociation are; however, constant with increasing pH. Complex dissociation constants are 2.5 ($\pm$ 0.1) s^{-1}, 2.0 ($\pm$ 0.1) s^{-1}, 2.0 ($\pm$ 0.2) s^{-1} and 2.24 ($\pm$ 0.09) s^{-1} for pH 3, 3.5, 4 and 4.7 respectively.
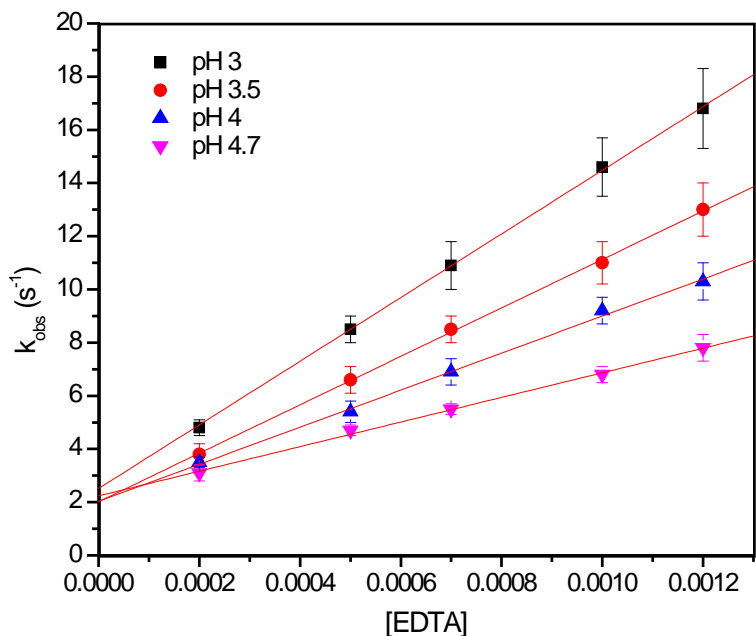
Figure 6: Hydrogen ion dependence of La-EDTA complex for [La] = [AAIII] = 10^{-4} M, T = 25 °C and $[Lac]_{tot}$ = 0.3 M.

<u>Lactate dependence</u>

Influence of lactic acid media was investigated over the concentration range of 0.1 M to 0.3 M in lactic acid (Figure 7). The pH was adjusted using NaOH to pH = 4. Ionic strength is maintained to 0.3 M using $NaClO_4$. Lanthanum and AAIII concentrations are held constant at 10^{-4} M. A plot of k_{obs} vs. [EDTA] demonstrates that first order kinetics are preserved even under second order conditions of [EDTA] = 2 x 10^{-4} M. This observation implies that the rate determining step for the dissociation reaction is probably an intramolecular process. Within the accuracy of the experiments, the complex formation reaction constant is independent of $[Lactate]_{tot}$ at pH 4.0 (k_{form} = 6.6 (± 0.3) x 10^3, 6.7 (± 0.8) x 10^3 and 7.0 (± 0.2) x 10^3 $M^{-1} \cdot s^{-1}$ at $[Lactate]_{tot}$ 0.1, 0.2 and 0.3 M). The dissociation rate constant decreases as lactic acid concentration increases with rate constants of 6.9 ± 0.2, 3.8 ± 0.6 and 2.0 ± 0.2 s^{-1} respectively for lactic acid concentrations 0.1, 0.2 and 0.3 M.

Figure 7: Dependence of reaction rate on lactic acid concentration at T = 25 °C and pH=4 for La-EDTA system with [La] = [AAIII] = 10^{-4} M.

To simulate reactions that might be occurring at a liquid-liquid interface in the analogous solvent extraction system, the reaction rate was also determined with addition of surfactant Triton X-114. The presence of a surfactant in solution is expected to alter the organization of solvent molecules, which should alter the solvation of the reactants and products and energetic features of their interactions. To complete the study on the role of complex solvation, the rate parameters for complexation reaction were examined in water/Triton X-114 mixed media. The structure of Triton X-114 is shown in Figure 8. The surfactant has been added in the EDTA solution syringe, La solution syringe or both syringes. This allows for possible comparison of interactions of the surfactant with different species. The critical micelle concentration for Triton X-114 is 0.2 mM at 20 - 25 °C according to Sigma Aldrich.

Experiments were run in 0.01 % by weight (10^2 ppm) Triton X-114 aqueous solutions. Increasing the concentration of Triton X-114 from zero to 50% of the critical micelle concentration leads to an apparent increase in the rate of complex dissociation but has a minimal effect on the complex formation reaction. Rates for both complex formation and dissociation as a function of Triton X-114 concentration are reported in the Table 1. This table shows that k_{form} is essentially the same through the modifications, i.e. k_{form} is not affected by surfactant. There is an increase in k_{diss} from no surfactant to surfactant in either EDTA or Ln syringe to surfactant in both syringes, though the overall effect is not dramatic.
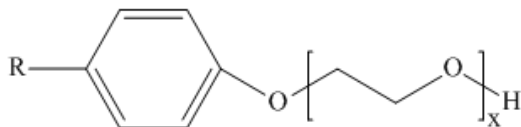
Figure 8: Structure of Triton X-114 – R = octyl (C_8), x = 7.5 (average)

Table 1: Rate constants for complex formation and dissociation for La-EDTA complex in water/Triton X-114(CMC concentration) mixed media at pH 3.5, T = 25°C and $[Lac]_{tot} = 0.3$ M.

$k_{form.}$ (M⁻¹s⁻¹)	$k_{diss.}$ (s⁻¹)	Triton X-114
$9.1 \pm 0.6 \times 10^3$	2.00 ± 0.05	Without surfactant
$9 \pm 1 \times 10^3$	2.60 ± 0.03	With surfactant in EDTA syringe
$9.7 \pm 0.8 \times 10^3$	2.8 ± 0.1	With surfactant in La syringe
$10 \pm 1 \times 10^3$	3.30 ± 0.08	With surfactant in both syringe

Indicator concentration dependence

Though the linear plots of k_{obs} vs. [EDTA] establish the essential validity of the kinetic interpretation, it is also important to demonstrate that AAIII is not a participant in the ligand exchange process. The dependence of the reaction rate on lanthanum and AAIII concentrations has been determined; experiments were run with various concentrations of La^{3+} at constant pH and lactate concentration. At pH = 3.6, experiments were run at $[La^{3+}] = [AAIII] = 1 \times 10^{-4}$ M and $[La] = [AAIII] = 2 \times 10^{-4}$ M. In this range of concentrations, La and AAIII concentrations have no influence on the kinetics of La-EDTA complexation. For concentration 1×10^{-4} M, k_{form} was $9.2 (\pm 0.1) \times 10^3$ M⁻¹s⁻¹ while k_{diss} was $2.0 (\pm 0.1)$ s⁻¹. At 2×10^{-4} M, the corresponding values were $k_{form} = 8840 (\pm 190)$ M⁻¹s⁻¹ and $k_{diss} = 2.6 (\pm 0.2)$ s⁻¹. These results are interpreted to indicate that AAIII is not involved in the rate determining step of the reaction and further that the reaction rate in independent on the lanthanide cation concentration (thus there are no polynuclear or metal bridged intermediate species involved).

Lanthanide series trends

Differences in the rate constants have been determined in a progression across the lanthanide series (with the exception of promethium). This study can provide information on the interactions between lanthanide ion and ligand with respect to the changing cation radius and hydration energy of the aquo ions. Experiments have been completed in the range [EDTA] from

0.2 - 1.2 mM; [Ln] = [AAIII] = 10^{-4} M; 0.3M Na/Lactate buffer at pH 3.6 and 25°C. As observed in Figure 9, the rate constants vary across the series in an unexpected manner. The apparent anomalies in the complex dissociation rates of Sm-Tb and the distinct formation rate constants of Gd and Tb are noteworthy. The rate constant for complex dissociation is small and steady for Dy to Lu. This pattern is not observed in an inspection of the stability constants for the Ln-EDTA complex. The stability constants, Figure 9, show a 10^4 increase across the series. This magnitude of change is not observed in k_f/k_d.

	k_f/k_d	log β
La	1400	15.36
Ce	1400	15.93
Pr	1980	16.3
Nd	2200	16.51
Sm	1300	17.06
Eu	1300	17.25
Gd	3700	17.35
Tb	3500	17.87
Dy	18000	18.3
Ho	48000	18.56
Er	21000	18.89
Tm	9600	19.32
Yb	8000	19.49
Lu	15000	19.74
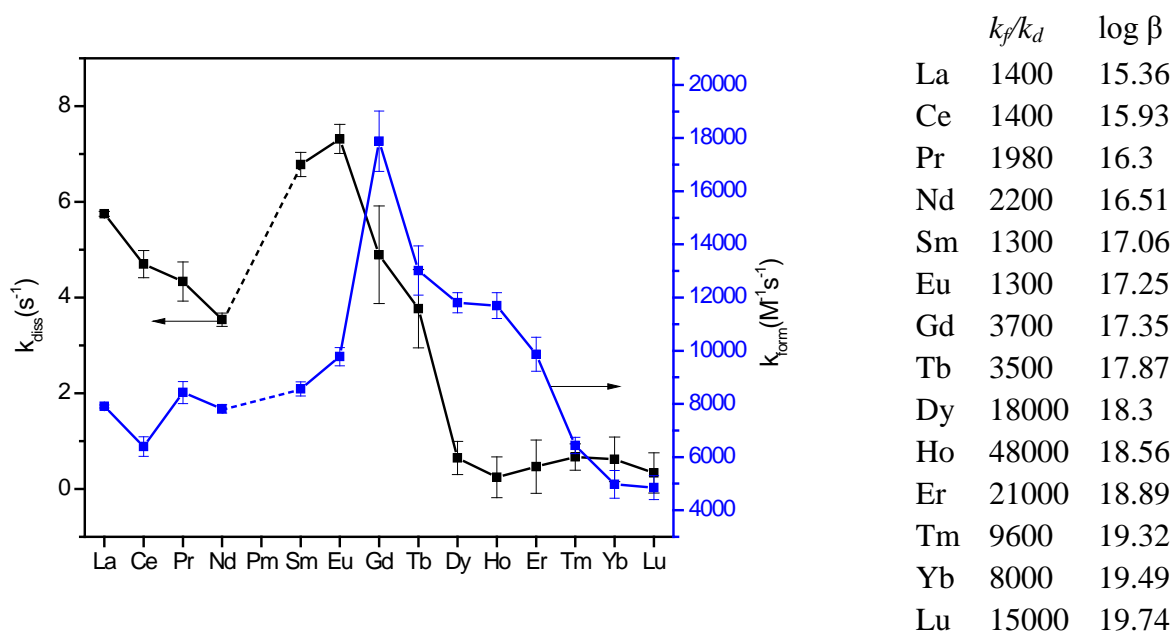
Figure 9: Rate constants for complex formation and dissociation reactions of lanthanides with EDTA at pH 3.5, 25 °C and $[Lac]_{tot}$ = 0.3 M. Stability constants for Ln-EDTA complexes and k_f/k_d values.

Discussion

It has been shown in earlier studies of lanthanide phase transfer reactions relevant to the TALSPEAK solvent extraction system that the lactate ion (present at significant concentrations) greatly facilitates the rate of the phase transfer reaction.[13,14] A principle objective of this investigation is to help establish the role of lactate ion in the rate and mechanism of the complex

association and dissociation reaction of lanthanide ions in concentrated lactate media for the present lanthanide-aminopolycarboxylic acid system. It also has been demonstrated previously that the ligand displacement approach utilized in this investigation typically yields information on the rate and mechanism of the reaction of interest generally without direct involvement of the colorimetric indicator in the kinetics of the process.[11,15] The experiments conducted as a function of the concentration of the lanthanide Arsenazo III complex described above confirm that in the present system Arsenazo III is not an active participant in the kinetics of lanthanide - EDTA complexation.

Given that H_2EDTA is the dominant free ligand species, the reaction should proceed as follows.

$$\text{La-AAIII} \longrightarrow \text{La}^{3+} + \text{AAIII} \qquad \text{(fast)} \qquad \qquad (4)$$

$$\text{La}^{3+} + \text{H}_2(\text{EDTA})^{2-} \underset{k_{diss}}{\overset{k_{form}}{\rightleftharpoons}} \text{La-EDTA}^- + 2\text{H}^+ \qquad \qquad (5)$$

In this standard reversible reaction the observed rate constant will be a sum of the forward and reverse reactions.

<u>Lactate dependence</u>

Previous studies of the kinetics the Ln complexation/dissociation with EDTA have been conducted in systems either un-buffered or using acetate buffer.[2,16-19] In this work, the influence of lactic acid concentration has been studied in the range of 0.1 - 0.3 M. Lactic acid has proven to behave as more than just a buffer in systems where it is present. The concentration of lactate has negligible effects in the rate of complex formation where $k_{form} = 6.6 \, (\pm \, 0.3) \times 10^3 \, \text{M}^{-1}\text{s}^{-1}$, 6.7 $(\pm \, 0.8) \times 10^3 \, \text{M}^{-1}\text{s}^{-1}$ and $7.0 \, (\pm \, 0.2) \times 10^3 \, \text{M}^{-1}\text{s}^{-1}$ for 0.1, 0.2 and 0.3 M total lactate respectively (Figure 7). The rate of complex dissociation; however, demonstrates an inverse relationship to changes in the lactate concentration, shown in Figure 7 with $k_{diss} = 6.9 \, (\pm \, 0.2) \, \text{s}^{-1}$, 3.8 $(\pm \, 0.6) \, \text{s}^{-1}$

70

and 2.0 ($\pm$ 0.2) s^{-1} for 0.1, 0.2 and 0.3 M total lactate respectively. A plot of k_{diss} vs. [Lactate]$_{total}$ (Figure 10) provides a lactic acid independent rate constant for the complex dissociation of 9 $\pm$ 1 s^{-1} and a lactic acid dependent rate constant for the complex formation of -24 $\pm$ 5 M^{-1}s^{-1}.
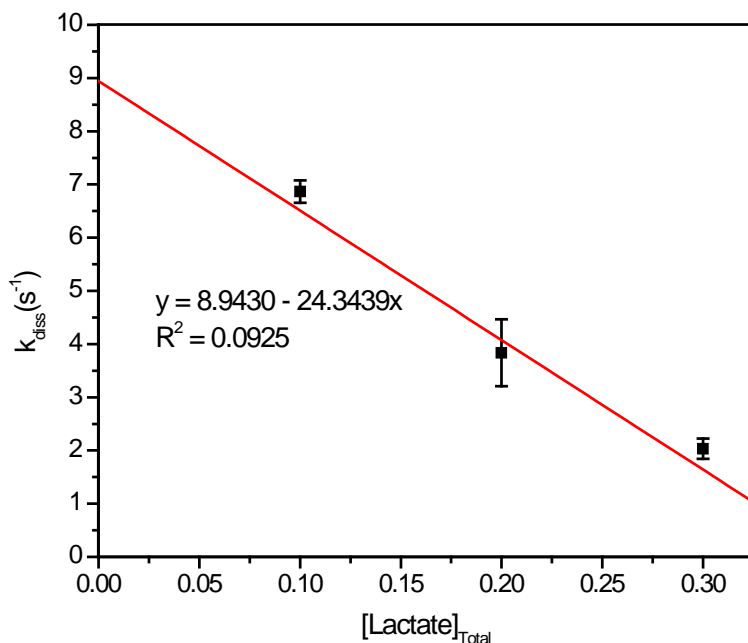
Figure 10: Plot of k_{diss} vs. [Lactate]$_{total}$ providing a [Lactate] independent rate constant for complex dissociation.

<u>Acid dependence</u>

The variation of the pseudo-first order rate constants for the dissociation of La^{3+} with [EDTA] and with pH (Figure 6) indicates the expected linear plots with finite positive intercepts. The constant intercept value (k_{diss}) indicates that the complex dissociation reaction is apparently independent of pH under these conditions, a somewhat surprising result based on earlier studies in acetate buffer media. In contrast, the complex formation rate increases with increasing [H$^+$], but in a nonlinear fashion. An increasing rate of complex formation with increasing [H$^+$] is contrary to what should be expected, as the thermodynamic driving force for the reaction of La^{3+} with H$_n$EDTA increases with decreasing [H$^+$]. It is postulated that this behavior is an indirect

result of the increase in [H$^+$]. If the change in pH ([H$^+$]) is related to the free lactate concentration by Equation 7 and k_{form} is plotted as a function of [Lac]$_{free}$, the relationship between changes in pH and k_{form} can be determined.

$$[Lac]_{free} = [Lac]_{total} / (1 + K_a*[H^+]) \qquad (7)$$

In Figure 11, the plot of k_{form} vs. [Lac]$_{free}$ shows that k_{form} decreases with an increase in the [Lac]$_{free}$ in the system. The [Lac]$_{free}$ will increase as the pH is increased. Therefore, the change in pH affects k_{form} only in that it changes the quantity of free lactate in the system.
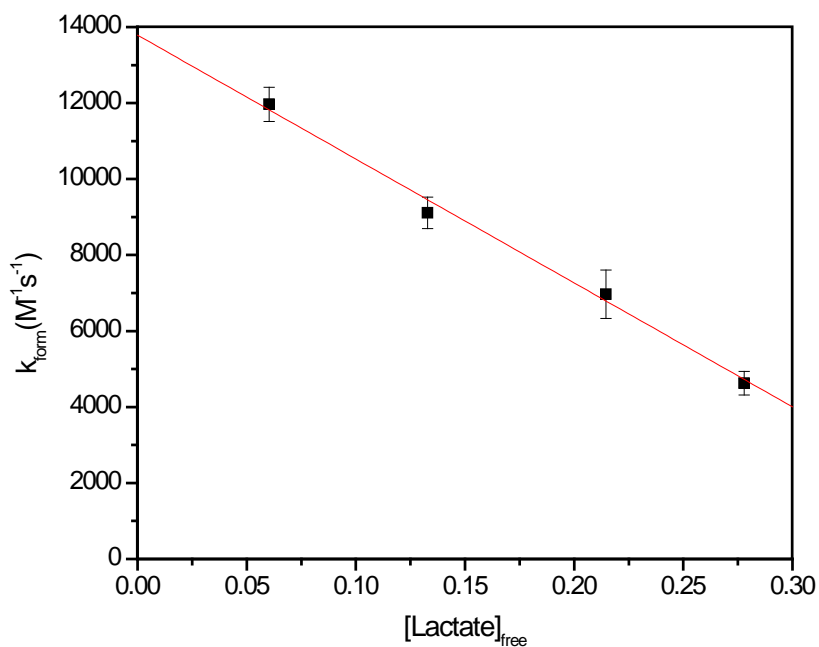
Figure 11: Plot of k_{form} vs. [Lactate]$_{free}$. The [Lactate]$_{free}$ has been calculated from Equation 7. A lactate independent rate constant has been determined from this data to be 1.38 ($\pm$ 0.04) x 10^4 M^{-1}s^{-1} with a lactate dependent rate constant of -3.3 ($\pm$ 0.2) x 10^4 s^{-1}. In the pH range of this investigation, the predominant protonated form of EDTA remains H$_2$EDTA^{2-} throughout. This ligand species should exist on average with both amine nitrogens protonated and all four carboxylates ionized.

Activation parameters

Determination of the activation parameters of the Ln/EDTA complexation helps in defining the mechanism of the reaction. To determine activation parameters, reactions were studied as a function of temperature, generally in the range of 5^oC to 35^oC. The activation parameters are calculated using the transition state theory equation (TST - Equation 8), using the variable temperature results.

$$k = \kappa (k_b T / h) \exp(\Delta S^* / R) \exp(\Delta H^* / RT) \qquad (8)$$

In this equation, k_b is Boltzmann's constant; h, is Planck's constant; κ, transmission factor (usually $\kappa = 1$); and R, the gas constant. The rate constants for complex formation k_{form} and dissociation k_{diss} determined previously were adjusted using the linearized form of Equation 8, shown as Equation 9.

$$\ln(k/T) = \ln(k_b/h) + \Delta S^* / R - \Delta H^* / RT \qquad (9)$$

A plot of $\ln(k/T)$ vs. $1/T$ produces a straight line from which the enthalpy (ΔH^*) is determined from the slope and the entropy (ΔS^*) from the intercept (Figure 11). Using the Eyring relation, the enthalpy, entropy and free energy of activation are calculated, for both reverse and forward reaction of the acid catalyzed dissociation process. In the following equations, k_B and h are the Boltzmann and Planck constants respectively, T is the absolute temperature and R is the gas constant. The transition state theory also provides the Gibbs free energy through Equation 10.

$$\Delta G^* = \Delta H^* - T\Delta S^* \qquad (10)$$

Figure 12: TST plot for complex formation in M-EDTA system (M = La and Tb) (I = 0.3 M). Errors are shown at 3σ.

Activation parameters have been determined for the Ln-EDTA system using La^{3+}, Tb^{3+} and Lu^{3+}. The parameters presented in Table 2 have been determined at pH 3 and 3.5 at temperatures of 5, 15, 20, 25 and 35°C for the La-EDTA system and 5, 15, 25 and 35°C for the Tb/Lu-EDTA. To calculate ΔG*, the reference temperature of 25 °C (298 K) was chosen. Comparison of the La^{3+}, Tb^{3+} and Lu^{3+} parameters provides insight into behavior of lanthanides throughout the series (Table 2). The activation entropy for the formation of Ln-EDTA is negative but very close to zero for La^{3+} whereas activation entropy for the dissociation of Ln-EDTA is largely negative with values of -20 ± 9 J/(mole*K) and -120 ± 24 J/(mole*K) respectively. At Tb^{3+}, ΔS* has become more negative for both complex formation, -126 ± 1 J/(mole*K) and complex dissociation, -241 ± 32 J/(mole*K) as compared to La^{3+}. By Lu, the activation entropy for both complex formation and dissociation has become effectively equal with values of -165 ± 16 J/(mole*K) and -154 ± 8 J/(mole*K) correspondingly. The unfavorable activation entropies are compensated by reduced activation enthalpy barriers (Table 2).

The negative ΔS^* implies that there is not a substantial dehydration of the Ln^{3+} prior to interaction with the EDTA. The incoming EDTA first interacts with the metal as an outer sphere complex (per the Eigen mechanism). Water will get pushed out of the coordination sphere as the EDTA carboxylate oxygen atoms begin to interact with the Ln^{3+}. This bonding is not surprising being that the lanthanides behave as hard-acid cations that prefer hard bases such as oxygen. A significant interaction with the softer nitrogen occurs when complexants such as EDTA sterically force the interaction.[7] The formation of the metal/nitrogen bond has generally been considered to be the slow step in the reaction.

Table 2: Activation parameters for complex formation and dissociation reactions of Ln with EDTA. T = 25 °C, $[Lac]_{tot}$ = 0.3 M and I = 0.3M

EDTA	k_{form}			k_{diss}		
	ΔH^* (kJ/mol)	ΔS^* (J/mol.K)	ΔG^* (kJ/mol)	ΔH^* (kJ/mol)	ΔS^* (J/mol.K)	ΔG^* (kJ/mol)
La (pH 3)	64 ± 3	-10 ± 8	67 ± 6	45 ± 3	-139 ± 39	87 ± 14
La (pH 3.5)	62 ± 3	-20 ± 9	68 ± 5	50 ± 3	-120 ± 24	86 ± 10
La w/X-114 (pH 3.5)	51 ± 4	-54 ± 1	67 ± 5	53 ± 3	-111 ± 9	86 ± 6
Tb (pH 3.5)	28 ± 2	-126 ± 1	65 ± 2	15 ± 1	-241 ± 32	86 ± 19
Lu (pH 3.5)	19 ± 1	-165 ± 16	68 ± 6	46 ± 1	-154 ± 8	92 ± 3

Effects of a surfactant

A surfactant is expected to alter the properties of hydration and solvation, both major factors in kinetics of complexation, modifying the rates for both complex formation and dissociation reactions. Surfactants lower the surface tension of a liquid and the interfacial tension between two liquids. They are usually amphipathic organic compounds, meaning they contain both hydrophobic groups ("tails") and hydrophilic groups ("heads"). They are; therefore,

typically sparingly soluble in both organic solvents and water. Triton X-114, a nonionic surfactant, was chosen as the surfactant in this set of experiments. Many surfactants can also assemble in the bulk solution into aggregates that are known as micelles. The concentration at which surfactants begin to form micelles is known as the critical micelle concentration or CMC. When micelles form in water, their tails form a core that is like an oil droplet, and their heads form an outer shell, or corona, that maintains favorable contact with water. For Triton X-114, the CMC in distilled water is 0.2 mM at 20 - 25 °C according to Sigma Aldrich. To determine the effect of adding a surfactant on the activation parameters, the experiment was run at the CMC for La-EDTA as a function of temperature.

Activation parameters for complex formation and dissociation reactions in the presence of surfactant were determined using the Arrhenius and Eyring relations. The conditions were set such that surfactant was present in both metal indicator or EDTA syringes individually and with the surfactant in both syringes at the same time. The critical micelle concentration (CMC) is reached, resulting in the formation of non ionic micelles in solution. Presumably, with non ionic Triton X-114, the lanthanide cation is neither attracted nor repulsed by micelles, a tris $Ln(Lac)_3$ complex with H_2EDTA^{-2} might interact more strongly with the micelle. As a result, the concentrations and thus complex formation rates in both micelles and bulk solution might not be significantly affected by surfactant presence. However, the complex dissociation rate constant is increased slightly by the presence of a micelle. We believe that the increase in rates results from an increase in concentration of each reactant in the surface region of the micelle as compared with the bulk solution. The most profound effect on activation parameters is for ΔS^*. This difference can be explained by the change of chemical activity in solution provoked by addition

76

of surfactant. The increase in viscosity that occurs with adding surfactant in solution could also have affected the change in entropy within the system.

Rate Law

Summation of the results and observations provide the overall rate law shown in Equation 13 below.

$$\text{Rate} = k_{form}[\text{Ln}][\text{EDTA}]/(1+ k'[\text{Lac}]_{free})$$

$$- k_{diss}[\text{Ln-EDTA}]/(1+ k''[\text{Lac}]_{tot}) \qquad (13)$$

The $[\text{H}^+]$ dependence was determined through an evaluation of the free lactate in the system. The TALSPEAK process requires a tight control on pH which is corroborated by this work that shows an increase in pH increased free lactate lowering rate of formation. The k_{diss} was shown to be inversely dependent on the total lactate concentration (k_{diss} decreases as $[\text{Lactate}]_{total}$ increases). In the context of TALSPEAK separations this result is contrary to the presumed role of lactate in speeding up phase transfer. A steady increase occurs in the thermodynamic complex stability as a function of atomic number. In this case, this increased stability cannot be attributed directly to the rate of dissociation which shows a non steady decrease with increasing atomic number with a spike occurring at Eu^{3+}, i.e. stability does not show the same trend as k_{diss}. The spike observed in the plot of k_{form} and k_{diss} (Figure 9) most closely matches the change in hydration number that occurs in the lanthanides near Eu^{3+} or Gd^{3+}. These observations are important to TALSPEAK since the DTPA used is a holdback reagent for Am^{3+} and Cm^{3+}. With EDTA a lower [Lactate] would increase dissociation of Ln-EDTA complexes (or by extension Ln-DTPA) thereby increasing extraction of the lanthanide into the organic phase. Decreases are observed in k_{form} and k_{diss} after Gd^{3+} which would be a problem in TALSPEAK, excepting that the heavier lanthanides are not present in used fuel.

Conclusion

The rates of complexation of lanthanides by EDTA have been investigated by stopped-flow spectrophotometry using the ligand displacement technique. The reaction proceeds as a first-order approach to equilibrium under all conditions. The results of this study provide addition evidence that solvation and geometric constraints are major factors in the kinetics of lanthanide complexation by polyaminocarboxylate ligand. The complex formation rate has been shown to be proportional to hydrogen ion concentration. The predominant pathway for lanthanide EDTA dissociation is inversely proportional to lactic acid concentration. Negative values for ΔS^* have been interpreted as an indication of an associative mechanism for both complex formation and dissociation of the Ln/EDTA complex though ΔS^* for lanthanum k_{form} differs from the other lanthanides showing that it could be more of an associative interchange mechanism. The addition of surfactant did not affect the rate of complex formation and only had a small effect on the rate of complex dissociation.

Acknowledgements

References

1) Weaver, B.; Kapplemann, F. A. *TALSPEAK: A New Method of Separating Americium and Curium from the Lanthanides by Extraction from an Aqueous Solution of an Aminopolyacetic Acid Complex with a Monoacidic Organophosphate or Phosphonate.* Oak Ridge National Laboratory Report– 3559: Oak Ridge, TN, 1964.

2) Ryhl, T. The dissociation of Pr, Nd, Eu and Er EDTA complexes. Acta Chemica Scandinavica. **1973**, *27*, 303-314.

3) Glentworth, P.; Wiseall, B.; Wright, C. L.; Mahmood, A. J. A Kinetic Study of Isotopic Exchange Reactions Between Lanthanide Ions and Lanthanide Polyaminopolycarboxylic Acid Complex Ions. I. Isotopic Exchange Reactions of Ce(III) with Ce(HEDTA), Ce(EDTA)$^-$, Ce(DCTA)$^-$, and Ce(DTPA)$^{2-}$. *J. Inorg. Nucl. Chem.* **1968**, *30(4)*, 967-986.

4) Martell, A. E.; Smith, R. M.: NIST Standard Reference Database 46 version 8.0, 2004.

5) Moeller, T.; Martin, D. F.; Thompson, L. C.; Ferrus, R.; Fiestel, G. R.; Randall, W. J. The coordination chemistry of yttrium and the rare earth metal ions. *Chem. Rev*. **1965**, *65(1)*, 1-50.

6) Lincoln, S. F. Solvation, Solvent Exchange, and Ligand Substitution Reactions of the Trivalent Lanthanide Ions. *Adv. Inorg. Bioinorg. Mech.* **1986**, *4*, 217-287.

7) Nash, K. L; Sullivan, J. C. Kinetics of Complexation and Redox Reactions of the Lanthanides in Aqueous Solutions. In *Handbook on the Physics and Chemistry of Rare Earths*, Gscheidner, K. A., Eyring, L. Eds.; Elsevier Science Publishers B.V.: San Diego, CA, 1991, Vol. 15, pp 341-391.

8) Hoard, J. L.; Lee, B.; Lind, M. D. Structure-dependent behavior of ethylenediamine tetraaceto complexes of the rare earth Ln^{3+} ions. *J. Am. Chem. Soc*. **1965**, *87(6)*, 1611.

9) Breen, Patrick J.; Horrocks, William D., Jr.; Johnson, Kenneth A. Stopped-flow Study of Ligand-exchange Kinetics Between Terbium(III) Ion and Calcium(II) ethylenediaminetetraacetate(4-). *Inorg. Chem.***1986**, *25(12)*, 1968-1971.

10) Brucher, E.; Banyai, I.; Krusper, L. Aminopolycarboxylates of rare earths, XI. Kinetics of metal ion-exchange and ligand exchange reactions of the (ethylene glycol)bis(2-aminoethylether)tetraacetate complex of cerium(III). *Acta Chim. Hung.,* **1984**, *116(1)*, 39-50.

11) Nash, K. L.; Sullivan, J. C. Kinetics of Actinde Complexation Reactions. *J. Alloys Compd.* **1998**, *271-273*, 712-718.

12) Rowatt, E.; Williams, J.P. The Interaction of Cations with the Dye Arsenazo III. *Biochem.J.* **1999**, *259*, 295-298.

13) Kolařík, Z.; Koch, G.; Kuhn, W. The Rate of Ln(III) Extraction by HDEHP From Complexing Media. *J. Inorg. Nucl. Chem.* **1974**, *36*, 905-909.

14) Nilsson, M; Nash, K. L. Trans-lanthanide extraction studies in the TALSPEAK system; investigating the effect of acidity and temperature. *Solvent Extr. Ion Exch.* **2009**, *27(3)*, 354-377.

15) Fugate, G.; Feil-Jenkins, J. F.; Sullivan, J. C.; Nash, K. L. Actinide Complexation Kinetics: Rate and Mechanism of Dioxoneptunium(V) Reaction with Chlorophosphonazo III. *Radiochim. Acta*, **1996**, *73(2)*, 67-72.

16) Laurenczy, G.; Brucher, E. Aminopolycarboxylates of Rare Earths. 12. Determination of Formation Rate Constants of Lanthanide(III)-Ethylenediaminetetraacetate Complexes Via a Kinetic Study of the Metal-Exchange Reactions. *Inorg. Chim. Acta.* **1984**, *95(1)*, 5-9.

17) Brücher, E.; Laurenczy, G. Kinetic study of exchange reactions between Eu^{3+} ions and lanthanide III DTPA complexes. *J. Inorg. Nucl. Chem.* **1981**, *43*, 2089-2096.

18) Ryhl, T. The dissociation of Yb, La and Cu EDTA complexes. Acta Chemica Scandinavica. **1972**, *26*, 3955-3968.

19) Nilsson, M; Nash, K. L. A review of the development and operational characteristics of the TALSPEAK process. *Solvent Extr. Ion Exch.* **2007**, *25*, 665-701.

Chapter 4

Redox-based Separation of Americium from Lanthanides in Sulfate Media

Preface

  Chapters two and three of this dissertation covered the kinetics of EDTA and DTPA complexation with lanthanides in lactic acid media. This work is directly related to the TALSPEAK process which separates trivalent actinides from trivalent actinides. The intention of Chapter 4 is to look at alternative methods to separate these elements in a reprocessing scheme. The separation that was developed in this chapter was extremely fortuitous. Persulfate was anticipated to oxidize americium to its hexavalent state with the lanthanides being precipitated by carbonate. As it turned out, persulfate served a dual role as the oxidizing and precipitating agent. Separation factors of 11 have been achieved for U, Np, Pu and Am from europium.

  This paper has been submitted to *Separation Science and Technology* and has had the general formatting done to submit the work to *Separation Science and Technology*. WSU requires that the entire document be double spaced, numbered sequentially and one inch margins. These parameters will be met initially. All other formatting will be performed under the guidelines of *Separation Science and Technology*. Guidelines for this journal can be found in the appendix.

Redox-based Separation of Americium from Lanthanides in Sulfate Media

Thomas Shehee[1], Leigh R. Martin[2], Peter J. Zalupski[2], Kenneth L. Nash*, [1]

[1]Chemistry Department, Washington State University, PO Box 644630, Pullman, WA 99164-4630

[2]Idaho National Laboratory, P.O. Box 1625, Idaho Falls, ID, 83415-2208

* Author for correspondence

Abstract

Dissolved used nuclear fuel mixtures contain U, Np, Pu, trivalent transplutonium actinides and lanthanides and other fission products representing a total of about 1/3 of the periodic table. Americium, being a long-lived α-emitter (and increasing in concentration during storage due to decay of ^{241}Pu) is the greatest contributor to the radiotoxicity of used fuel in the 300 - 70,000 year time frame after removal from the reactor. On this basis, Am is an attractive target for transmutation. Unfortunately, the lanthanides, representing about 40% of the mass of fission products, are neutron poisons that will compete with Am for neutrons in any advanced transmutation process. Thus the mutual separation of Am from chemically similar lanthanides remains one of the largest obstacles to the implementation of advanced closed-loop nuclear fuel cycles that include Am transmutation. The focus of the work described herein is on the utilization of the upper oxidation states of Am(V, VI) to facilitate a more efficient separation of Am from fission product lanthanides. The separation of americium from the lanthanides and curium has been achieved in the laboratory through oxidation of trivalent Am to the hexavalent state by the use of $Na_2S_2O_8$. Oxidized Am species remain predominantly in the supernatant phase while the lanthanides and curium are precipitated as sodium lanthanide/curium sulfate double

82

salts. A variety of chemical and physical characterization techniques have been applied to profile the performance of the system.

Introduction

The separation of americium from the lanthanides has typically proven challenging. Most approaches to accomplishing this separation have relied on the slightly greater strength of interaction of trivalent actinides with ligand donor atoms softer than oxygen. The TALSPEAK process, based on the application of diethylenetriamine-N,N,N',N",N"-pentaacetic acid (DTPA) and developed during the 1960s at Oak Ridge National Laboratory[1] is currently considered the best option for the transmutation-enabling separation of trivalent Am and Cm from fission product lanthanides in the U.S. research effort. Advanced separations processes and specialized polyaza complexants are at the core of lanthanide/trivalent actinide separation by advanced nuclear fuel processing in the European research program. [2] Thiophosphinic acids have also been advanced as possible reagents for separating trivalent actinides from fission product lanthanides. [3-5] Average Am/Ln separation factors of 10 - 100 have been reported in laboratory research. Unfortunately, each approach has been plagued by ligand instability and/or extraction/complexation kinetics complications.

A separation method based on oxidized Am species would accrue the added advantage of allowing Cm to remain with the lanthanide fraction. It is widely noted that in a given oxidation state, actinides and lanthanides behave similarly, hence in a process that maintains trivalent Cm while Am is oxidized, it should be expected that Cm will accompany the lanthanides. A Cm/Ln waste stream would only require a few hundred years of decay before the greatest threat to radiotoxicity was abated. In addition, the main curium isotope in used fuel (^{244}Cm) with its high specific activity would make the creation of Am transmutation targets more difficult. With Cm

present the targets would have to be made within a hot cell; without the Cm, the targets could probably be produced in a glove box.

A disadvantage associated with the oxidation of Am to promote separation comes from the strongly oxidizing nature of these species in acidic aqueous media; hence their application in solvent extraction processes could be problematic. Among others, Belova and coworkers [6] report that the radiolysis products of TBP would reduce the oxidized americium as well as consume the HNO_3 present within the system. For such a solvent extraction-based process to be viable, reagents capable of maintaining oxidized Am species (a holding oxidant) that does not simultaneously destroy the phase transfer ability of the extractant phase would be required. Mincher et al. [7] have reported preliminary results investigating the application potential of $NaBiO_3$ for such applications. Given the apparent limitations of separating oxidized Am species from lanthanides and Cm by solvent extraction and the evident advantages of isolating Am from Cm, developing separations based on oxidized Am still has significant appeal.

Though it was ultimately replaced by the far cleaner (and more efficient) option of solvent extraction, the first isolation of actinides either at the laboratory or industrial scale was accomplished using solid-liquid partitioning schemes. The $BiPO_4$ process [9] was scaled up from the microgram to the kilogram scale (a factor of 10^9) in the Manhattan Project to enable the creation of kilogram quantities of plutonium. Lanthanide fluoride co-precipitation processes were (and remain today) important analytical procedures supporting the isolation of the first samples of transuranium elements in the laboratory. [8] Though separation processes based on solid-liquid separation have a number of limitations, in the case of Am partitioning from Cm and lanthanides, accomplishing this task by other means has proven a formidable task.

There are a number of known approaches to lanthanide/actinide partitioning that involve (at an analytical scale) solid-liquid separations. Most are based on the observation that oxidized actinides stay in solutions while lanthanides (or reduced actinides) can be precipitated. A fractional precipitation of americium and lanthanum oxalates has been shown to provide a highly enriched americium precipitate and about 50% of the lanthanum being rejected at each stage. [10] Separation of americium and curium by oxidizing americium to the hexavalent state with peroxydisulfate followed by a precipitation of CmF_3 has been reported. [11] Separation of Am (VI) from large quantities of the lanthanides has also been shown through precipitation of the lanthanide trifluorides. [12] These fluoride precipitations do achieve > 90% separation; both employ 3 - 4 M HF as the precipitating agent. Use of HF for commercial reprocessing would be challenging due to its corrosive nature and general difficulty in handling HF solutions.

The approach chosen for demonstration in this work to separate Am from fission product lanthanides and curium begins with selective adjustment of the oxidation state of Am to the accessible upper oxidation states, of which the tetra-, penta- and hexavalent oxidation states are known. Such oxidation state adjustments are not accessible for Cm or the lanthanides, which remain predominantly trivalent. In the following, the results of an investigation of the oxidation of Am (III) by persulfate ($S_2O_8^=$) and the concomitant precipitation of lanthanide and curium ions will be demonstrated.

Experimental

Reagents

The oxidizing agents Oxone - $2KHSO_5 \cdot KHSO_4 \cdot K_2SO_4$ (Sigma Aldrich) or $Na_2S_2O_8$ 98+% (Acros) were used as received. Europium used in these experiments was diluted to 0.1M from a 0.488M $Eu(ClO_4)_3$ stock solution that was prepared from 99.999% Eu_2O_3 from Arris

International Corp. and standardized using ICP-OES. A 0.5 M silver solution was made from ACS grade 99.0% AnNO$_3$ from EM Science.

Radioisotopes

Progress of the partitioning reaction was monitored radiometrically using $^{152/154}$Eu (as a representative fission product lanthanides) and actinide (^{233}U, ^{237}Np, ^{238}Pu, and ^{241}Am) radiotracers. The use of a radioactive tracer allowed for accurate tracking of the lanthanide and actinide during the multi-step precipitation separation process. The isotope $^{152/154}$Eu has been made through by neutron irradiation of 99.999% Eu$_2$O$_3$ from Arris International Corp. at the Washington State University Nuclear Radiation Center's 1 MW TRIGA reactor. Actinide radiotracers were obtained from standardized stocks of the WSU and INL inventories.

Procedures

Both single and dual label experiments have been performed during this work depending on the location at which the work was performed. Single label experiments composed the majority of all experiments performed during this study. Work at the radiotracer level performed at the Harold Dodgen Research Center at Washington State University utilized single label experiments. All samples containing ^{241}Am and $^{152/154}$Eu were analyzed using a Packard Cobra II Auto-gamma counter with a three inch NaI(Tl) crystal. Single label experiments were also performed at this location using ^{233}U, ^{237}Np and ^{238}Pu radiotracers and a Beckman LS 6500 Multi-Purpose Scintillation Counter using National Diagnostics "Ecoscint" scintillation fluid. Studies performed at the Idaho National Lab were either single or dual label for ^{244}Cm or ^{243}Am and ^{154}Eu respectively. The use of curium with its 5.81MeV α decay required the employment of a liquid scintillation counter. All curium samples produced at the INL were placed in a 20mL glass scintillation vial with 20mL of Ultima Gold LLT scintillation fluid and counted on a Tri-

Carb 3170TR/SL liquid scintillation counter. All americium samples produced at the INL were counted using an ORTEC Digital Gamma Ray Spectrometer, DSPEC Jr. 2.0. The counter has been optimized for 1 mL of solution in a 20 mL scintillation vial. Each sample was diluted to 1 mL to match this optimized geometry.

In single label experiments, 5 µL of the desired radiotracer was added to 250 µL of a 0.1 M $Eu(ClO_4)_3$ solution. To this homogeneous aqueous solution, 300 µL of 0.5 M $Na_2S_2O_8$ or 0.4 M Oxone and 25 µL of 0.5 M $AgNO_3$ were added to a 12 x 75 mm capped polypropylene tube. The tubes were then heated to above 90 ºC in a water bath for 15 minutes with periodic shaking to help facilitate the oxidation of the Am tracer. [13] A solid precipitate appeared during this equilibration period. After the fifteen minute heating period, the tubes were removed from the water bath, capped and centrifuged for 5 minutes to firmly pack the solid in the base of the round bottom tube. Separation was achieved by decanting the supernatant into a second gamma tube. In the americium and europium studies, a 300 µL aliquot of the supernatant was removed and counted with the Cobra system to determine the percent of the tracer retained in the solution. During the heating period it has been assumed that a 10% loss in solution volume is occurring during the course of the experiment. Taking into account the 10% loss, the initial reaction volume and aliquot size, the percent radiotracer can be determined through a comparison with an average of counts from a 5 µL spike from the respective radiotracer. Studies using [233]U, [237]Np and [239]Pu were performed in the same manner as the americium and europium studies with the only change coming in the sample prep for counting purposes. In these experiments, a 200 µL aliquot was removed from the supernatant and placed in a 7 mL glass scintillation vial in 7 mL scintillation fluid.

Evaluation of the effect of added silver on the precipitation of the lanthanides or oxidation of the americium followed the same as described in the single label experiment above. In these experiments, the solid precipitate was used for γ-counting after decanting the supernatant. The solids were left in the original 12 x 75 mm tube and analyzed using the Packard Cobra II Auto-gamma counter. Since the total solid was used for counting, the total counts obtained from the detector were used to determine the percent radiotracer found in the solid phase.

Macro americium studies were performed at the Idaho National Laboratory. All work was performed in accordance to necessary Radiological Work Permit (RWP) and Lab Instructions (LI). Conformation to these procedures required slight modifications to the previously described procedure. Changes included use of 1.5 mL screw cap micro-centrifuge tubes instead of the 12 x 75 mm gamma tubes, dual labels for experiments looking at the separation of americium from a europium containing solution and a high purity germanium detector. In dual label experiments, 5 µL of both ^{243}Am and ^{154}Eu was added to 250 µL of a 0.1 M Eu(ClO$_4$)$_3$ solution. To this homogeneous aqueous solution, 300 µL of 0.5 M Na$_2$S$_2$O$_8$ or 0.4 M Oxone and 25 µL of 0.5 M AgNO$_3$ were added to the screw cap micro-centrifuge tube. These experiments were also performed without added silver. A ^{244}Cm single label experiment had 5 µL of the radiotracer added to 250 µL of a 0.1 M Eu(ClO$_4$)$_3$ solution with the experiment proceeding same as with the dual label. After the 15 minutes in the water bath and centrifugation, a 350 µL aliquot of the supernatant was removed and placed in a 20 mL glass scintillation vial. The sample was diluted to 1 mL to match the geometry the detector had been optimized. The data was evaluated in the same manner as described previously.

Spectroscopic analysis was performed with a Cary 50 spectrophotometer using a Cary 50 fiber optic coupler allowing the cell holder and samples to remain in the fume hood. The progress of the americium oxidation using sodium persulfate ($Na_2S_2O_8$) was monitored through the Am (III) characteristic peaks at 503 and 811 nm and the Am (VI) characteristic peaks at 666 and 996 nm. A 100 µL aliquot of the 1mM americium working stock was placed in a Hellma Quartz Suprasil Type# 105.253 – QS 1 cm cell along with 50 µL of 1 M $Na_2S_2O_8$ and the spectra recorded. This solution was allowed to sit for 1 hour without heating with the spectrum being recorded again after 1 hour. The americium solution was removed from the cell, placed in a 1.5 mL screw cap micro-centrifuge tube then placed in a 98°C water bath for 5 minutes. The solution was returned to the cell to record the spectrum. The sample was then returned to the water bath to heat for another 5 minutes. The heat and spectrum recording repeated at 5 minute intervals to provide spectra of the solution from 0 - 25 minutes. After final heating the solution was allowed to cool for 1 hour and a final spectrum was recorded.

X-ray powder diffraction was performed on a sample of the dried solid precipitate. The powder was held in place on a 2" square glass plate using petroleum jelly spread in an oval shape ~ 1 x 1.5". X-ray powder diffraction was performed using a Siemens Kristalloflex D500 diffractometer with the following parameters: Copper source (Kα; 1.540Å); 35 keV, 30 mA, Kβ filter: Ni; scintillation counter detector; Continuous mode: 0.02 d/min; 2θ range: 5-55. The diffractograms were produced using supporting MDI Data Scan 4 and Jade 8 software packages. The raw pattern was compared to powder patterns in the ICSD (International Crystal Structure Database) to identify the material in the solid phase. Radiometric analysis of the supernatant was also completed to determine the amount of each isotope remaining in the supernatant phase.

Results

<u>Tracer Studies</u>

The separation was monitored using lanthanide ($^{152/154}$Eu) and actinide (^{233}U, ^{237}Np, ^{238}Pu, and ^{241}Am) radiotracers. The ^{233}U, ^{237}Np and ^{239}Pu have been used as analogues of americium for comparative purposes. Uranium being most stable in its hexavalent oxidation state is the best analogue for americium in this system, as it provides a clear picture of the extent of the precipitation and retention of the oxidized americium without need of first oxidizing the actinide. The initial oxidation states of the radiotracer neptunium and plutonium were the V and IV states, respectively. In contact with $S_2O_8^=$, each is expected to have been relatively quickly oxidized to the VI state. These studies were designed to confirm the general performance of hexavalent actinides in this system. To evaluate directly the separation of americium from the lanthanides, ^{241}Am was utilized at the radiotracer level. Europium radiotracer, $^{152/154}$Eu, was used exclusively as a representative of the trivalent lanthanides. The results of these radiotracer experiments are shown in Table 1.

The $^{152/154}$Eu radiotracer results demonstrated that about 8% of the lanthanide will remain in solution after the precipitation has occurred. Neither longer times in the water bath nor higher concentrations of $S_2O_8^=$ increased the completeness of the precipitation of the trivalent europium. On average, 93% of ^{233}U remained in the solution phase after precipitation occurred. As $S_2O_8^=$ cannot oxidize U(VI), it is expected that this value represents the essential separation capacity of the system. As no solubility limiting species for U(VI) are known, the 7% defect is attributed to entrained ^{233}U radiotracer in the solid phase. Similar results were obtained for Np (86%) and Pu. (94%); the slightly lower solubility of Np is statistically significant and might indicate the presence of some residual Np(V).

Table 1: The results of the separation in terms of the percent actinide (An) radiotracer remaining in the solution after precipitation when using 25µL 0.5 M $AgNO_3$ + 300µL 0.5 M $Na_2S_2O_8$ (upper section). The results of macro americium experiments with an [Am] = 2 x 10^{-5} M both with silver present (middle section) and without silver present (lower section). All errors presented in this table are at the 1σ level.

Radiotracer experiment using silver catalyst			
	Conditions	% Radiotracer (aq)	$SF_{An/Eu}(aq)$
$^{152/154}$Eu		8.2 ± 0.8	
^{233}U	25 µL 0.5 M	93 ± 1	11 ± 1
^{237}Np	$AgNO_3$ + 300	86 ± 2	10 ± 1
^{238}Pu	µL $Na_2S_2O_8$	94 ± 2	11 ± 1
^{241}Am (2 x 10^{-8} M)		93.6 ± 0.3	11 ± 1

Macro Am experiment using silver catalyst				
	Conditions	% Radiotracer (aq)	$SF_{Am/Eu}(aq)$	$SF_{Am/Cm}(aq)$
^{243}Am (2 x 10^{-5} M)	$Na_2S_2O_8$	95 ± 7	4 ± 1	10 ± 3
	Oxone	18.9 ± 0.8	0.9 ± 0.3	1.2 ± 0.1
^{154}Eu (aq)	$Na_2S_2O_8$	23 ± 6		
	Oxone	20 ± 6		
^{244}Cm (aq)	$Na_2S_2O_8$	10 ± 3		
	Oxone	16 ± 1		

Macro Am experiment without silver catalyst			
	Conditions	% Radiotracer (aq)	$SF_{Am/Eu}(aq)$
^{243}Am (2 x 10^{-5} M)	$Na_2S_2O_8$	100 ± 5	3.7 ± 0.2
	Oxone	20 ± 6	1.5 ± 0.8
^{154}Eu (aq)	$Na_2S_2O_8$	27 ± 1	
	Oxone	13 ± 5	

The percent americium that was retained in the supernatant phase is more consistent with the U and Pu results than those for Np, implying (based on the argument above regarding Np) that Am is predominantly hexavalent under these conditions. The average actinide/europium separation factor $SF_{An/Eu}$ (SF = %Am_{aq}/%Eu_{aq}) is about 11. As noted above, an average of 6% of the actinide is lost to the solid phase in a single contact. After some initial tests, it was

determined that washing of the solid with various fluids led to unacceptable levels of redissolution of the $NaEu(SO_4)_2$ (s).

Through radiotracer studies, the effect of silver nitrate concentration has also been evaluated over a silver concentration range of 0.004 - 0.04 M (Figure 1). Lower [AgNO₃] yields the lowest percent of Eu in the solid phase, providing the worst overall separation efficiency. At 0.02 M [AgNO₃], the percent Eu in the precipitate has achieved a maximum that does not change with further addition of silver to the system over the range of silver concentrations studied in this work. The concentration of silver present in the system had at best only negligible effects on the oxidation of americium and therefore on the percent of americium being found in the precipitate. At ±1σ error the percent americium in the precipitate is equivalent across the silver concentration range shown.
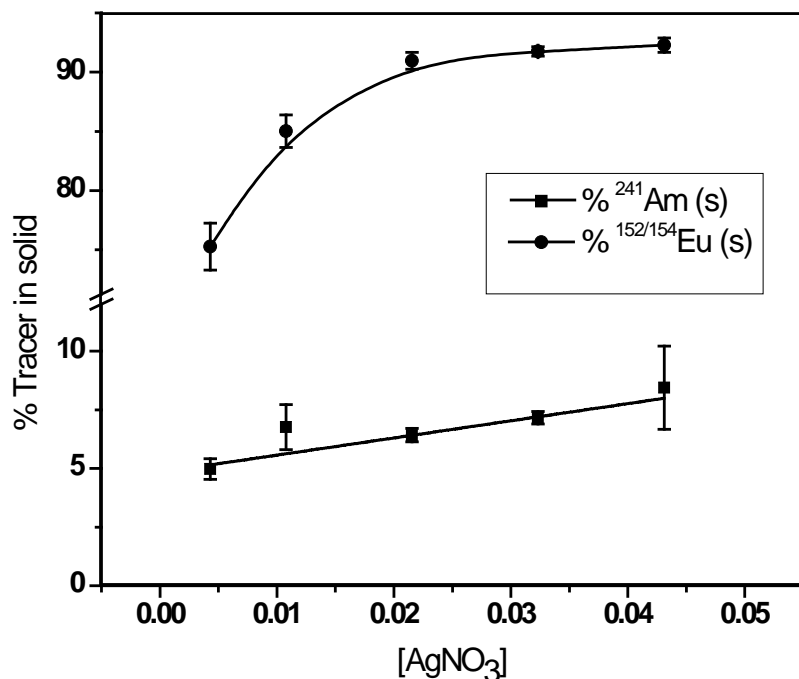
Figure 1: The effects of changing the overall concentration of Ag^+ from 0.004 to 0.04 M while holding the Eu^{3+} and $S_2O_8^=$ constant. Uncertainties are presented at the ±1σ level.

Identification of predominant solid species

Powder XRD has been used to identify solids formed in both the Oxone and $Na_2S_2O_8$ oxidation/precipitation separations. The precipitation was performed on a cold (sample containing no radiotracer) sample of $Eu(ClO_4)_3$ following the same procedure as before. The pattern gave a best match for the double sulfate salt of the lanthanide, $Gd_2(SO_4)_3 \cdot Na_2SO_4 \cdot 2H_2O$. [14] The double sulfates of sodium and the lanthanides have been reported for the complete series of the lanthanides. [15] Solids formed with Oxone or $Na_2S_2O_8$, providing K^+ or Na^+ respectively for the co-precipitation, both matched the XRD pattern for the Gd analogue closely. The double sulfates of the lanthanides are isostructural and show a steady decrease in the cell volume across the lanthanide series as would be expected with the lanthanide contraction. [16] These solids are reported to be insoluble in alcohol, ether, and acetone, sparingly soluble in water, and readily soluble in dilute hydrochloric and nitric acids. [15] These solids are stable to ~350°C at which temperature the loss of water from the crystal is observed. At ~ 747°C, the anhydrous salt has been observed to dissociate into its component parts $Ln_2(SO_4)_3$ and M_2SO_4. Upon heating to 1100°C, XRD of the resulting solid shows only the structure of lanthanum oxide sulfate. [17]

Macro studies

In experiments performed at the Idaho National Laboratory the overall concentration of americium in solution was increased from 2×10^{-8} (in the radiotracer experiments) to 2×10^{-5} M. This study was performed both with and without silver present. Parallel radiotracer studies were also completed at this time to profile the partitioning of ^{244}Cm.

Dual label experiments using ^{243}Am and ^{154}Eu, evaluated the differences in oxidation ability of Oxone and $Na_2S_2O_8$. When $Na_2S_2O_8$ was used to oxidize americium, 95% of americium and 23% of the europium remained in the supernatant after separation. Oxidation with

Oxone provided only 19% of americium and 20% of the europium in the supernatant phase. These experiments were then repeated without the addition of silver. In both oxidation by $Na_2S_2O_8$ and Oxone, the results without the silver are within $\pm 1\sigma$ error of the results with the silver included.

As this procedure is designed to separate americium from curium <u>and</u> the lanthanides, the $Na_2S_2O_8$ separation was tested using [244]Cm in a single label experiment. The $Na_2S_2O_8$ system was chosen exclusively as it provides the best separation over that of Oxone. Ten percent of the curium tracer remained in the supernatant phase after treatment of the sample following the same procedure as followed with both americium and europium (i.e., $NaEu(SO_4)_2$ formed the bulk of the solid phase). This result is in good agreement with the percent europium that remains in the solution phase during the separation in the absence of [244]Cm. All associated errors are at the $\pm 1\sigma$ level. The results clearly establish the viability of the separation of Am from both Cm and lanthanides by this method. Results of these experiments can be seen in Table 1.

<u>Spectrophotometric studies of oxidation of Am by $S_2O_8^=$</u>

The oxidation of americium by $Na_2S_2O_8$ has been followed spectrophotometrically by monitoring the disappearance americium (III) characteristic peaks at 503 and 811 nm, simultaneously monitoring the appearance of the characteristic peaks of Am(VI) at 666 and 996 nm. No spectrophotometric evidence is seen for any intermediate species. Am (1 mM) was oxidized in a persulfate solution with the spectra being taken at intervals from 0 - 25 minutes. The characteristic Am(III) peak was observed in the solution even after 5 minutes in contact with 0.5 M $S_2O_8^=$ at room temperature. The reaction vessel was placed in a boiling water bath for 5 minutes before the spectrum was taken a second time. At this point the Am(III) peak at 503 nm was greatly diminished and the peak at 811 nm had completely disappeared. The heating was

repeated at 5 minute intervals up to 25 minutes. The final solution was left in the cuvette at room temperature for 1 hour with no change in the absorbance of the Am(VI) and no reappearance of the Am(III) or peaks characteristic of Am(V).
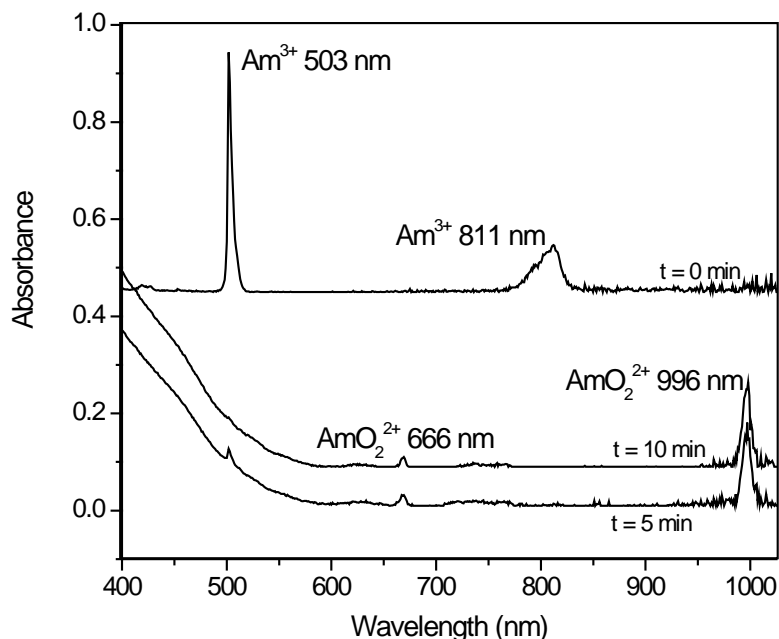
Figure 2: Spectra of 1 mM americium in 0.1 M H_2SO_4. The spectra shown include T = 0 (no time in the water bath), T = 5 min and T = 10 min for the upper, lower and middle spectra respectively. In the T = 0 sample, $Na_2S_2O_8$ has been added without heating the solution. T = 5 and 10 minutes are after heating the solution. Note - The spectra have been offset to improve clarity.

Discussion

The separation of americium from curium and the lanthanides as described here requires the oxidation of Am to its pentavalent or hexavalent oxidation state. Standard reduction potentials for the Am (VI/V), (V/IV) and (IV/III) couples are 1.60, 0.83 and 2.60 V respectively. [18] Despite the large IV/III couple, quantitative oxidation of americium to the hexavalent oxidation state has been achieved through the use of ozone [19] and $S_2O_8^=$ [13]. Persulfate has been

chosen in this work due to its ability to completely oxidize americium, for its stability in acid solution and as the primary source for the sulfate that precipitates the lanthanides.

A study of the speciation of the hexavalent and pentavalent actinides vs. the trivalent lanthanides gives an indication of the thermodynamic basis for the separation by $S_2O_8^=$ oxidation and sulfate precipitation. The hexavalent actinide and trivalent species have been represented here by UO_2^{2+} and Eu^{3+} respectively. The speciation of Eu^{3+} in sulfate is taken as representative of the probable speciation for trivalent lanthanide ions and curium. The parameters chosen for calculation have the concentrations of the metal at 0.025 M and the ligand ($SO_4^=$) at 0.5 M. These concentrations correspond to the total concentration of lanthanide and sulfate present in the experimental procedure. The log β values selected for these calculations are at an ionic strength of 1, approximating the experimental conditions (I = 1.5 M). The stability constants used are shown in Table 2. Under the conditions of the calculation and at experimental pH = 1; the 1:3 uranyl sulfate species is the dominant species yet the 1:2 and 1:1 make up respectively 17.6 and 11.6 percent of the total uranium in solution The uncharged UO_2SO_4 complex is known to be present in solution, but is thought to become increasingly important at higher temperatures. [20] Secoy found that the solubility of this species continued to increase up to 180ºC. [21] In the presence of excess sulfate ion, as in this system, it is likely that the anionic complexes $AnO_2(SO_4)_2^=$ and $AnO_2(SO_4)_3^{4-}$ will dominate the actinide speciation over the entire range of temperatures employed. The major species present below pH 9 in the europium simulation is the $NaEu(SO_4)_2$ (s) double salt; at higher pH, the thermodynamic data predicts conversion to $Eu(OH)_{3\ (S)}$.
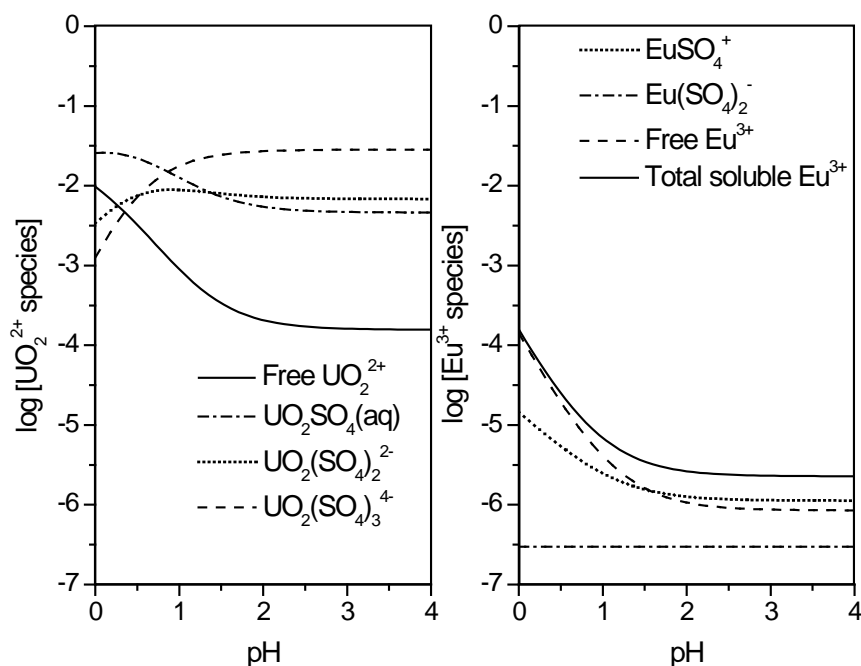
Figure 3: Comparison of speciation diagrams for Eu^{3+} and UO_2^{2+} ions in sulfate containing solution. Concentrations are set at 0.025M metal ion in both to match the [Ln] and 0.5M $SO_4^=$ under the experimental conditions. The pH throughout the separation is 1. At a reaction pH of ~1, three uranyl sulfate species are important, UO_2SO_4, $UO_2(SO_4)_2^{2-}$ and $UO_2(SO_4)_3^{4-}$. At the same reaction pH the dominate sulfate species is $NaEu(SO_4)_2$ is in the form of a solid precipitate. The europium species remaining in solution are shown in the figure. Stability constants used are found in Table 2.

Americium oxidation by persulfate

The results shown in Figure 2 demonstrate the successful oxidation of americium by $S_2O_8^=$ at temperatures above 90°C. The americium (III) characteristic peaks at 503 and 811 nm disappear while peaks characteristic of Am(VI) at 666 and 996 nm simultaneously appear. The initial americium solution (upper spectrum) included $Na_2S_2O_8$, but had not been heated in the water bath. The spectrum remained unchanged; showing only Am(III) peaks remaining while monitoring for one hour. Upon heating for only five minutes, the characteristic Am(III) peak at 503 nm was observed to disappear almost completely with the peak at 811 nm completely disappearing, demonstrating the oxidizing power of $S_2O_8^=$ at elevated temperatures.

97

Table 2: The stability constants used for calculation of speciation diagrams of uranyl and europium in sulfate containing media.

	$\log \beta$		$\log \beta$
$UO_2(OH)^+$	-6.2	$EuSO_4^+$	0.47
$UO_2(OH)_2$ (aq)	-11.3	$Eu(SO_4)_2^-$	0.24
$(UO_2)_2(OH)_2^{2+}$	-6.604	$NaEu(SO_4)_2$ (s)	-5.8
UO_2SO_4 (aq)	1.85	$EuOH^{2+}$	-8.07
$UO_2(SO_4)_2^{2-}$	2.4	$Eu_2(OH)_2^{4+}$	-14.34
$UO_2(SO_4)_3^{4-}$	3.4	$Eu(OH)_3$ (s)	-16.81
$H(SO_4)^-$	1.08	$H(SO_4)^-$	1.08

1) All values $\mu = 1$ and $t = 25°C$ except $NaEu(SO_4)_2$ (s)
2) $NaEu(SO_4)_2$ (s) - value extrapolated from literature data [22,23] - μ = unknown and $t = 20°C$
3) Stability constants for UO_2^{2+} are found in Chemical Thermodynamics of Uranium [24]
4) Stability constants for Eu^{3+} are found in the Martell and Smith Database [25]
5) Eu hydrolysis products – $xM^{3+} + yH_2O \equiv M_x(OH)_y^{3x-y} + yH^+$
6) UO_2^{2+} hydrolysis products – $xM^{2+} + yH_2O \equiv M_x(OH)_y^{2x-y} + yH^+$
7) Eu sulfate products - $xM^{3+} + ySO_4^{2-} \equiv M_x(SO_4)_y^{3x-2y}$
8) UO_2^{2+} sulfate products – $xM^{2+} + ySO_4^{2-} \equiv M_x(SO_4)_y^{2x-2y}$
9) Solubility product $NaEu(SO_4)_{2\,(s)}$: $NaEu(SO_4)_2$ (s) $\equiv Na^+ + Eu^{3+} + 2\,SO_4^{=}$

Further heating (to 10 minutes) resulted in the complete disappearance of the Am(III) at 503 nm as observed in the middle spectrum in Figure 2. The final solution remained in the cuvette at room temperature for 1 hour with no change in the absorbance of the Am(VI) and no reappearance of the Am(III). The resulting solution takes on an amber-orange coloration.

Of note in the spectra from 5 and 10 minutes of heating is the broad feature in the 400 - 600 nm range. This feature only appears upon heating, during which time americium is being oxidized; this feature may be associated with the formation of an americium (VI) sulfate species in solution. After 10 minutes of heating, the absorptivity is more intense at 400 nm than is seen at 5 minutes, coincident with the disappearance of the final traces of Am(III) at 503 nm. To test whether this absorption band might be replicated in uranyl-sulfate solutions, a spectrum was taken of uranyl sulfate; no change in the spectrum was seen upon heating the system. Upon

adding ethanol to reduce americium, the feature from 400 - 600 nm began to disappear as characteristic peaks for Am(V) appeared. The precise origin of this change in color is not clear at this stage, though it is clearly associated with the presence of Am(VI).

The oxidation of americium is thought to occur through two possible reaction paths. The first proposed path involves the Ag^+ being oxidized by $S_2O_8^=$, which then splits the $S_2O_8^=$ into two sulfate radicals. The radical is thought to be responsible for the oxidation of the Am(III) to Am(VI). Following oxidation of the americium, the sulfate binds with the lanthanide thus precipitating the sodium lanthanide salt. The second proposed path involves the oxidation of Ag^+ to Ag^{2+}. Americium present as Am (III) is then oxidized by the divalent silver. It is known from the prior literature that $S_2O_8^=$ oxidations (absent a catalyst) often proceed after a substantial induction period. The standard reduction potentials of Ag^{2+} and $S_2O_8^=$ are:
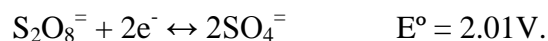
$$Ag^{2+} + e^- \leftrightarrow Ag^+ \qquad\qquad E^o = 1.989V$$

$$S_2O_8^= + 2e^- \leftrightarrow 2SO_4^= \qquad\qquad E^o = 2.01V.$$

Both the Ag^{2+} and $S_2O_8^=$ are sufficiently strong oxidants to oxidize the Am (III) to the hexavalent oxidation state. It is probable that both Ag^{2+} and $SO_4^-\cdot$ contribute to Am oxidation when silver is present. A possible complication arises in the decomposition of $S_2O_8^=$ under acidic conditions. At acid concentrations ≥ 0.5 M, the peroxydisulfate is decomposed by a first order, acid-catalyzed path giving peroxy-mono-sulfuric acid which forms hydrogen peroxide[26], which is known to reduce Am (VI). This should not be a concern within this system, as the $S_2O_8^=$ should be stable under these conditions toward this possibly detrimental decomposition path. Silver nitrate has been used in all of the tracer studies given that the majority of the literature has used it in the oxidation of Am. [13, 27] Penneman has been suggested that the use of silver nitrate as a catalyst is not necessary. [28]

The stability of $S_2O_8^=$ under the conditions of these experiments must be examined to probe the chemical and radiological robustness of this separations process. Persulfate in solutions will decompose by three different reaction pathways dependent on the conditions of the system. In the dilute acid solutions utilized in this separation, the decomposition proceeds through the acid catalyzed first order reaction. [26]

$$S_2O_8^= + H_2O \rightarrow 2HSO_4^- + \tfrac{1}{2} O_2$$
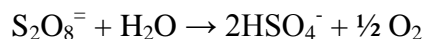
Also, there is considerable evidence that sulfate free radicals ($SO_4 \cdot$) are created by the thermal decomposition of $S_2O_8^=$ in neutral and alkaline solutions. [29] The mechanisms proposed for the thermal decomposition of $S_2O_8^=$ in aqueous solutions are shown below.

A: Un-catalyzed reaction $S_2O_8^= \rightarrow 2\ SO_4^- \cdot$

$2\ SO_4^- \cdot + 2H_2O \rightarrow 2HSO_4^- + 2HO\cdot$

$2HO\cdot \rightarrow H_2O + \tfrac{1}{2} O_2$
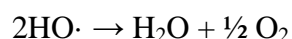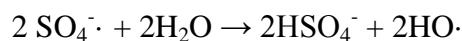
B: Hydrogen-ion catalyzed reaction $S_2O_8^= + H^+ \rightarrow HS_2O_8^- \rightarrow SO_4 + HSO_4^-$

$SO_4 \rightarrow SO_3 + \tfrac{1}{2} O_2$

These reactions are independent and occur simultaneously in aqueous solutions. The studies that proposed the above mechanisms, noted that in dilute acid solutions ozone was present as detected by the odor of the gas and by action of the gas on starch iodide paper. [26] Notice also the production of the hydroxyl radical in the un-catalyzed reaction. The formation of this radical could also contribute to the oxidation of americium in this system. The hydroxyl radical is a strong oxidizing agent with a standard potential of ~2.7V. [30,31] From this information, the decomposition rates of $S_2O_8^=$ and the reaction completion rate observed in this study it can be concluded that during the time scale of this separation the decomposition of the $S_2O_8^=$ will not be a detriment to the process.

Tracer study

With >90% U, Pu, Am and 86% Np remaining in the solution phase after the precipitation, it is clear that oxidized actinides can be partitioned away from Cm and Ln(III) by this means in acidic sulfate systems. The americium is being oxidized to its hexavalent state as demonstrated in Figure 3 and is truly soluble in a sulfate containing solution as was demonstrated with uranyl in the speciation calculations. Silver was added in these experiment as a catalyst as per previous literature, however as observed in Figure 1 the addition of silver provided little advantage in the oxidation of americium. Over the silver concentration range studied, the percent americium found in the solid appears to increase slightly over the concentration range studied; however upon inspection of the $\pm 1\sigma$ errors at each concentration, the effect has been determined to not be statistically significant. The addition of silver does produce a statistically significant increase in the percent europium found in the precipitate. This increase could result from the formation of a silver lanthanide salt that has been reported. [32] The increased partitioning of Eu to the solid phase suggests that $AgEu(SO_4)_2$ may be either less soluble than $NaEu(SO_4)_{2\,(S)}$ or that Eu^{3+} is more efficiently incorporated into the resulting solid.

Macro study

At macro americium concentrations, the percentages of the americium and europium in solution are in very good agreement with results observed in radiotracer studies. The results of both sets are found in Table 1. The similarity in these percentages indicates that americium species are indeed soluble in a sulfate containing solution. This study was repeated without silver present. This experiment indicated that Ag^+ was not needed to achieve separation of Am from the Ln and Cm at macro concentrations of Am. The spectrum of americium was recorded to directly observe the oxidation state of americium in this system. The results of the analysis of

101

these spectra clearly establish that Am(VI) is (as expected) the terminal oxidized americium species under these conditions, that Ag^+ need not be present for the oxidation to occur, and that Am(VI) persists at least for some time in this medium. The spectra indicate that Am(VI) was stable towards reduction to Am(V) for at least 1 hour which should provide adequate time to complete the separation of the solid and supernatant phases. It is likely that this condition would persist for an extended period of time as long as excess $S_2O_8^=$ remained in the solution. To implement an industrial-scale procedure based on these results, it is clear that an excess of $S_2O_8^=$ and elevated temperatures would be necessary.

Conclusion

A successful separation of oxidized americium from europium and curium has been demonstrated. The optimized method has resulted in the retention of 86, 90 and 94% of the actinide in the solution for ^{237}Np, ^{241}Am and ^{238}Pu respectively. The analog studies are consistent with the presence of oxidized Am species in these experiments. Addition of more $Na_2S_2O_8$ (up to 500 µL) does not appreciably increase the percent actinide found in solution giving results that were within ±1σ of the above results for ^{241}Am studies. As was expected, curium precipitated along with the europium during this separation. These retention percentages give an Am-Eu/Cm separation factor of ~11 in a single contact. About 7% of the Am is lost to the solid phase.

In the context of advanced fuel cycle processing schemes, a solid-liquid separation based on acidic $S_2O_8^=$ media could be envisioned to follow the application of a TRUEX (or DIAMEX or TODGA) process for the separation of lanthanides and actinides from fission products. The dilute acid conditions of a TRUEX strip would appear to be ideally suited to the application of $S_2O_8^=$ oxidation and precipitation of Ln/Cm double sulfate salts. Subsequent manipulation of the

supernatant phase to again reduce the Am to the trivalent oxidation state would enable transmutation target fabrication.

References

1. Weaver, B.; Kapplemann, F.A. <u>TALSPEAK: A New Method of Separating Americium and Curium from the Lanthanides by Extraction from an Aqueous Solution of an Aminopolyacetic Acid Complex with a Monoacidic Organophosphate or Phosphonate</u> Oak Ridge National Laboratory Report – 3559, 1964, 61pages.

2. Christiansen, B.; Apostolidis, C.; Carlos, R.; Courson, O.; Glatz, J.-P.; Malmbeck, R.; Pagliosa, G.; Roemer, K.; Serrano-Purroy, D. Advanced aqueous reprocessing in P&T strategies: Process demonstrations on genuine fuels and targets. Radiochimica Acta. **2004**, 92(8), 475.

3. Modolo, G.; Nabet, S. Thermodynamic Study on the Synergistic Mixture of Bis(chlorophenyl)dithiophosphinic Acid and Tris(2-ethylhexyl)phosphate for Separation of Actinides(III) from Lanthanides(III) Solvent Extraction and Ion Exchange **2005**, 23(3), 359.

4. Law, J.D.; Peterman, D.R.; Todd, T.A.; Tillotson, R.D. Separation of trivalent actinides from lanthanides in an acetate buffer solution using Cyanex 301. Radiochimica Acta. **2006**, 94(5), 261.

5. Liu, J.; Wang, B.; Liang, J. Study on extraction behavior of Pu (III) in bis (2,4,4-trimethylpentyl) dithiophosphinic acid (kerosene)-HNO3 system. Yuanzineng Kexue Jishu. **2007**, 41(1), 41.

6. Belova, E. V.; Egorov, G. F.; Nazin, E. R. Thermochemical oxidation of components of extraction solutions and the boundary conditions of thermal explosion: 2. effect of radiolysis and hydrolysis products of TBP on the kinetics of gas evolution in thermal oxidation of TBP with nitric acid. Radiochemistry (Moscow) (Translation of Radiokhimiya). **2000**, 42(3), 257.

7. Mincher, B.J.; Martin, L.R.; Schmitt, N.C.   Tributylphosphate Extraction Behavior of Bismuthate-Oxidized Americium. Inorg. Chem. **2008**, 47(15), 6984.

8. Seaborg, G.T.; Wahl, A.C. The chemical properties of elements 94 and 93. J. Am. Chem. Soc. **1948**, 70, 1128.

9. Thompson, S.G.; Seaborg, G.T. *Bismuth phosphate process for the separation of plutonium from aqueous solutions.* US 2785951 19570319. 1957.

10. Hermann, J.A. *United States Atomic Energy Commission Unclassified and Declassified Reports* (Atomic Energy Commission and Its Contractors) 1956.

11. Stephanou, S.E.; Penneman, R.A. Curium valence states; a rapid separation of americium and curium. J. Am. Chem. Soc. **1952**, 74, 3701.

12. Proctor, S.G.; Conner, W.V. Separation of cerium from americium. J. of Inorg. And Nuc. Chem. **1970**, 32(11), 3699.

13. Ward, M.; Welch, G.A. The oxidation of americium to the sexavalent state. J. Chem. Soc. **1954**, 4038.

14. Storozhenko, D.; Molodkin, A.K.; Shevchuk, V.G.; Akimov, V.M.; Grigor'ev, Y.A. Double sulfates of alkali elements and ammonium with gadolinium of composition $M_2SO_4.Gd_2(SO_4)_3.nH_2O$. Russ. J. Inorg. Chem. (English translation). **1983**. 28. 65.

15. Zaitseva, L.L.; Konarev, M.I.; Kruglov, A.A.; Chebotarev, N.T. Doubled sodium sulfates of rare earth elements. Russian J. of Inorg. Chem. **1964**, 9(11), 1380.

16. Iyer, P.N.; Natarajan, P.R. Double sulfates of plutonium (III) and lanthanides with sodium. J. Less. Com. Met. **1989**. 146. 161.

17. Zaitseva, L.L.; Konarev, M.I.; Kruglov, A.A.; Cherstvenkova, E.P.; Yaroshinskii, V.I. Thermal properties of double sulfates of some rare earth elements of the cerium subgroup. Russian J. of Inorg. Chem. **1965**, 10(6), 783.

18. Newton, T.W.; Sullivan, J.C. *Handbook on the Physics and Chemistry of the Actinides* Vol. 3. Elsevier Science Ltd 1985. pp 387-406.

19. Coleman, J.S.; Keenan, T.K.; Jones, L.H.; Carnall, W.T.; Penneman, R.A. Preparation and properties of americium(VI) in aqueous carbonate solutions. Inorg. Chem. **1963**, 2(1), 58.

20. Neuefeind, J.; Skanthakumar, S.; Soderholm, L. Structure of the UO_2^{2+} - SO_4^{2-} Ion Pair in Aqueous Solution. Inorg. Chem. **2004**, 43, 2422.

21. Secoy, C.H. The system uranyl sulfate-water. I. Temperature-concentration relationships below 300°. J. Am. Chem. Soc. **1948**, 70, 3450.

22. Lokshin, E.P.; Tareeva, O.A.; Ivlev, K.G.; Kashulina, T.G. Solubility of Double Alkali Metal (Na, K) Rare-Earth (La, Ce) Sulfates in Sulfuric-Phosphoric Acid Solutions at 20°C. Russian J. of App. Chem. **2005**, 78(7), 1058.

23. Lokshin, E.P.; Tareeva, O.A.; Kashulina, T.G. A study of the solubility of yttrium, praseodymium, neodymium, and gadolinium sulfates in the presence of sodium and potassium in sulfuric-phosphoric acid solutions at 20° C. Russian J. of App. Chem. **2007**, 80(8), 1275.

24. Chemical Thermodynamics, Vol. 1. *Chemical Thermodynamics of Uranium*. North-Holland: New York. 1992.

25. Martell, A.E.; Smith, R.M. NIST Standard Reference Database 46 version 8.0, 2004

26. Kolthoff, I.M. and Miller, I.K. The Chemistry of Persulfate. I. The Kinetics and Mechanism of the Decomposition of the Persulfate Ion in Aqueous Medium. J. Am. Chem. Soc. **1951**, 73(7), 3055.

27. Asprey, L. B.; Stephanou, S. E.; Penneman, R. A. A new valence state of americium, Am(VI). J. of the Am. Chem. Soc. **1951**, 73, 5715.

28. Penneman, R.A. and Keenan, T.K. *The Radiochemistry of Americium and Curium* (Subcommittee on Radiochemistry – National Academy of Sciences – National Research Council), 1960.

29. Bartlett, P.D. and Cotman, J.D., Jr. The kinetics of the decomposition of potassium persulfate in aqueous solutions of methanol. J. of the Am. Chem. Soc. **1949**, 71, 1419.

30. Boucher, H.; Sargeson, A.M; Sangster, D.F.; Sullivan, J.C. Oxidation of azidopentaamminecobalt(III) by hydroxyl radicals. Inorg. Chem. **1981**, 20, 3719.

31. Wood, P.M. The potential diagram for oxygen at pH 7. Biochem. J. **1988**, 254, 287.

32. Jordanovska, V. and Shiftar, J. Synthesis and dehydration of double sulfates of some rare earths (lanthanons) with silver. Thermochimica Acta. **1992**, 209, 259.

Chapter 5

Kinetic Features of Lanthanide Complexation Reactions with EDTA

and DTPA in Alkaline Solutions

Preface

The kinetic features of lanthanide complexation with both EDTA and DTPA have been investigated using many different methods including metal and ligand exchange. Typically these reactions have been studied in acidic media. Chapters Two and Three of this dissertation also address issues of similar reaction kinetics in lactic acid media that allows for a direct relation to the TALSPEAK process. The intention of this chapter is to examine this kinetic process as it occurs in alkaline media. Little or no work has been performed under these conditions to date. As a portion of the work presented here is a separation method devised and performed under alkaline carbonate conditions, an extension of the previous kinetic data into the alkaline realm seemed logical.

It is intended that this data be submitted as a paper to an inorganic chemistry journal most likely *Inorganic Chemistry*. WSU formatting, which requires that the entire document be double spaced, numbered sequentially and one inch margins will be met initially. All other formatting will be performed under the American Chemical Society guidelines. Figures have been placed throughout the text near the location of referencing.

Kinetic Features of lanthanide complexation reactions with EDTA and DTPA in alkaline solutions

Thomas C. Shehee[1] and Kenneth L. Nash[1,*]

[1]Chemistry Department, Washington State University, PO Box 644630, Pullman, WA 99164-4630

* Author to whom correspondence should be addressed

Keywords: kinetics, alkaline, aminopolycarboxylic acid, lanthanide complexation, EBT

Abstract

The present work examines the kinetic features of formation of lanthanide complexes with DTPA and EDTA under alkaline conditions. A select number of these reactions are observed to occur with a half life convenient to the application of stopped flow spectrometry. A ligand competition method used in earlier investigations is applied in this system. Eriochrome Black T is used as an indicator in the borax buffered system. With the exception of the complexation of La^{3+}, the reactions occur in a time regime suitable for study by conventional spectrophotometry. Nearly a 1000 fold range in k_{obs} is observed in the progression across the lanthanide series with both EDTA and DTPA. For all systems the reactions were seen to conform to the general features of a Michaelis-Menten model, which allows for the determination of k_2 and K_m. Activation parameters associated with k_2 have also been calculated from the observed rate constants from a set of temperature dependent studies for a selected set of lanthanides.

Introduction

Ligand and solvent exchange rates for the lanthanides are generally rapid with the rates of ligand exchange sometimes being accessible through rapid-kinetic techniques like stopped-flow spectrophotometry. This technique is advantageous for the study of fast reactions because mixing can be completed within milliseconds, allowing the observation of absorptivity changes to begin

almost instantaneously. F-element complexation with polydentate ligands generally occurs rapidly with the fast kinetics reflecting the strong ionic nature of f-element bonding.[1] Both DTPA (diethylenetriamine-N,N,N',N",N"-pentaacetic acid, Figure 1A) and EDTA (ethylenediamine-N,N,N',N'-tetraacetic acid, Figure 1B) effectively complex actinides above pH 2 with the actinide complexes being soluble; however, the complexants demonstrate relatively limited solubility in acid solutions.[2]
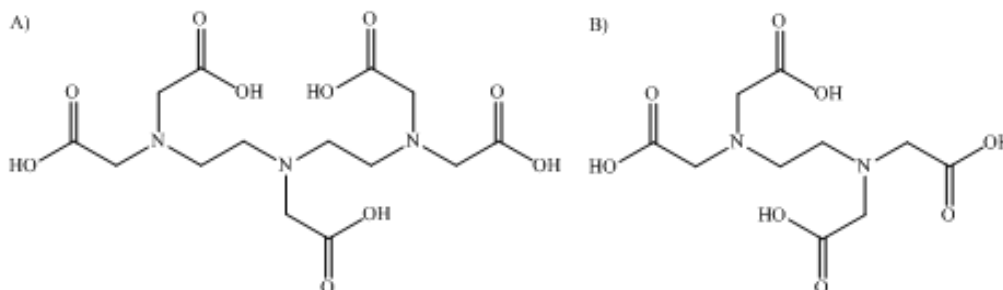
Figure 1: Structures of DTPA - Diethylenetriaminepentaacetic acid (A) and EDTA - Ethylenediaminetatraacetic acid (B)

Rates of lanthanide complexation and dissociation reactions have been investigated experimentally typically by either metal ion or ligand exchange reaction and using mainly spectroscopic methods.[3] These earlier investigations have been performed in the pH region wherein $H_2(EDTA)^{2-}$ and $H_3(DTPA)^{2-}$ are the predominant species. Laurency and Brücher derived the rate constants for the formation of Nd^{3+}, Gd^{3+}, Er^{3+} and Y^{3+} with $H(EDTA)^{3-}$ and $H_2(EDTA)^{2-}$ by exchange with $Ce(EDTA)^-$.[4] That work was performed in an un-buffered system whereas much work has been performed in acetate buffered systems. Ryhl has used an acetate buffer in an investigation of the dissociation rates of Yb^{3+}, La^{3+} and Cu^{2+} as well as Pr^{3+}, Nd^{3+}, Eu^{3+} and Er^{3+}.[5,6] It was found in the study that acetate ions cause a small increase in the dissociation of the EDTA complex. The acetate was presumed to be bound directly to the metal ion in a mixed lanthanide complex.[6] For this reason, Breen and coworkers chose to use the alternative buffers 3, 5-dichloropyrazole, hexamethylenetetramine and piperazine in later work

evaluating the exchange of Tb^{3+} and $CaH(EDTA)^-$.[7] They report a strong dependence of the observed rate on pH and a rate-reducing effect on increasing $[Tb^{3+}]$ with the latter becoming less pronounced upon increase in pH. This was interpreted as evidence for two competing pathways; a fast attack by Tb^{3+} forming a bridged intermediate followed by a slow dissociation of Ca^{2+}, vs. a fast H^+-catalyzed dissociation of the $Ca(EDTA)^{2-}$ followed by a fast binding of free Tb^{3+} to EDTA.[7]

A study of the kinetics of lanthanide complexation with DTPA in a lactate buffer, pH = 3.6, provides valuable information applicable to the trivalent actinide/lanthanide separation process, TALSPEAK.[8] Information on the rate of formation or dissociation of lanthanides with DTPA was derived in earlier work with lactic acid (HLac) by studying the rate of extraction of the radioactive isotopes of the lanthanides.[9] The authors presented rate constants for the forward and back extraction of the metal in a system containing DTPA and HLac, noting that it seemed that HLac played an important role in the overall reaction. From the rates of extraction, the authors concluded that the formation or dissociation of the Ln(III) DTPA complexes formed in the aqueous phase could be considered the rate determining step in the extraction.[9] A different approach has been used in previous work performed in this lab. These reactions make use of a competition study where a metal and indicator complex is rapidly mixed with either EDTA or DTPA in a stopped flow spectrophotometer.[10,11] In this work it was found that there was inverse dependence of the dissociation rate constant on the lactate concentration.

Although much work on lanthanide complexation dynamics has been performed in acidic media, little work has been performed under basic conditions. In large measure, this absence of information is a result of the limited solubility of lanthanide hydroxides under alkaline conditions. In the current investigation, the results of a study of the kinetics and mechanism of

lanthanide amino polycarboxylate complexation in alkaline solutions are reported. Experiments have been conducted as a function of pH, ligand concentration and temperature. Progress of the reaction is monitored using the distinctive visible spectral changes attendant to lanthanide complexation by the colorimetric indicator ligand Eriochrome Black T (Figure 2).
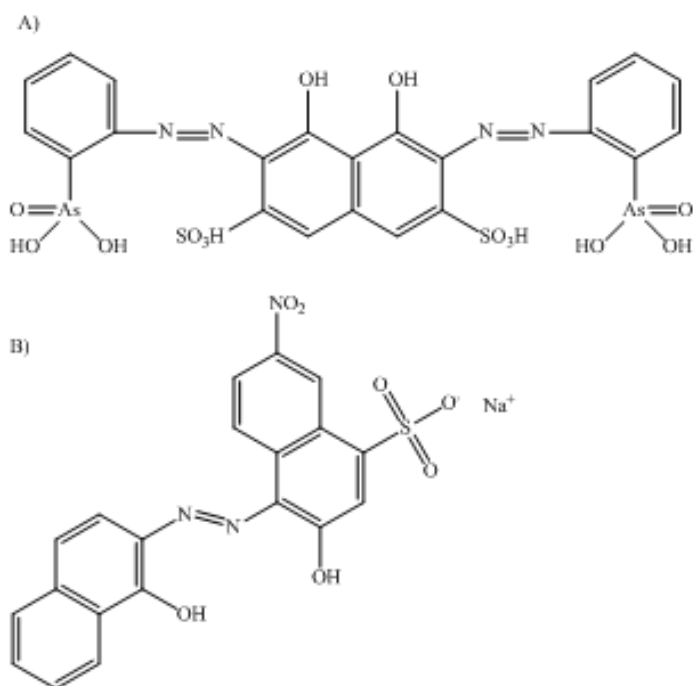
Figure 2: Structures of Arsenazo III (A) and Eriochrome Black T (B)

Experimental

<u>Reagents</u>

All reagents were used as received unless otherwise specified. Lanthanide perchlorate stock solutions were prepared from 99.999% Ln_2O_3 (Arris International Corp. now Michigan Metals & Manufacturing, Inc. of West Bloomfield, MI) through dissolution of the solid in $HClO_4$ (Fisher Reagent Grade). The cation concentration was determined using a Perkin Elmer Optima 3200RL ICP-OES. These lab stocks were used to prepare each lanthanide sample in the series. A stock solution of the colorimetric indicator ligand Eriochrome Black T (3-Hydroxy-4[(1-hydroxy-2-naphthalenyl)azo]-7-nitro-1-naphthalenesulfonic acid monosodium salt, EBT, Figure

112

2) was prepared by weight using indicator grade material obtained from Sigma Aldrich. The EBT solution was protected from light to prevent photodegradation of the ligand. Solutions of variable EDTA concentration were prepared volumetrically using a standardized EDTA solution made from 99.9% Na$_2$EDTA (Fluka Chemical Corporation). Solutions of variable DTPA concentration were prepared volumetrically using a standardized DTPA solution made from 99.9% Na$_2$DPTA (Fluka Chemical Corporation). Both EDTA and DTPA were standardized by potentiometric titrations using a Mettler Toledo T50 Autotitrator. A borax buffer was prepared by mixing 50 mL of 2.5 mM borax and 19.5 mL of 0.1 M NaOH and diluting to 100 mL with H$_2$O.[12] This provided a pH 10.1 buffer that gave pH ~ 9.5 for all working stocks. A Thermo Orion Model 720A pH meter in association with a VWR Ag/AgCl pH electrode was used to measure the pH. The electrode was calibrated in millivolts using standard pH 4.01, 7.00 and 10.01 buffers. Ionic strength was maintained at 0.4 M using Na(ClO$_4$)$_3$ obtained from Fisher Scientific and purified by recrystallization. Adjustment of pH was accomplished by the addition of standardized NaOH or HCl. All solutions were prepared in deionized water polished to 18 MΩ with a Labconco water polisher.

Procedure

The optimum wavelength to observe monitor the kinetics was determined with an OLIS Cary-14 Spectrophotometer. The spectra of both the Ln(III)-EBT complex and free EBT at pH = 9.5 were measured and are shown in Figure 3; the respective lanthanide complexes with EDTA or DTPA are transparent in the wavelength region and at the lanthanide concentrations tested. The spectrum of the Ln(III)-EBT indicator complex reached a maximum absorbance at 522 nm. The observed λ_{max} for the free indicator was at 608 nm, after being displaced by DTPA or EDTA. The progress of the reaction was monitored at this wavelength. The spectrum of the free

EBT ligand was not altered upon addition of either DTPA or EDTA, indicating that there is no interaction between competing chelating agents.
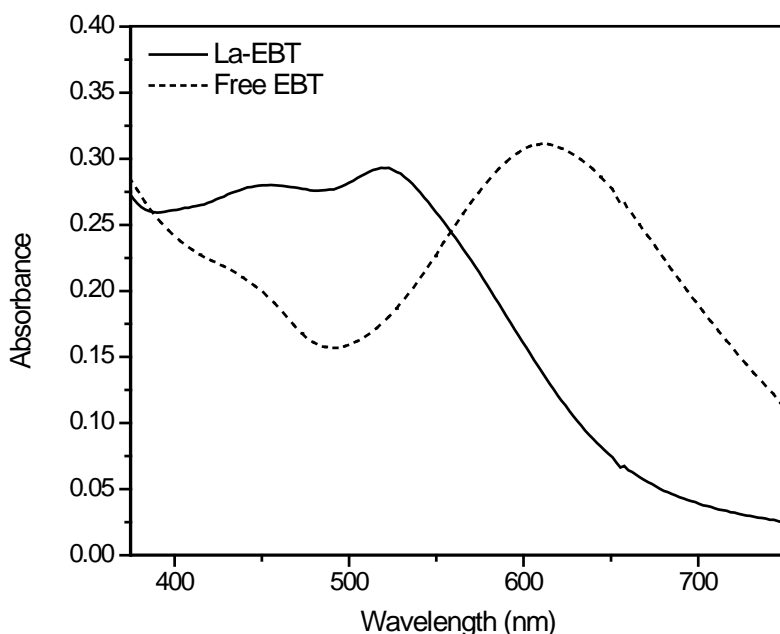
Figure 3: Absorbance of Eriochrome Black T (EBT) and La-EBT complex; 0.5 mL of [EBT] or [Ln-EBT] = 1 x 10^{-4} M mixed with 0.5 mL of [DTPA] = 4.6 mM; pH = 9.5; T = 25 °C.

The OLIS Cary 14 Spectrophotometer was also used to measure absorbance change vs. time data that was used to calculate k_{obs} for the lanthanide series. This set of experiments was performed under the following conditions: [Ln-EBT] = 1 x 10^{-4} M, [EDTA] = [DTPA] = 4.6 mM, 25 °C and buffer at pH = 9.5 with a borax buffer. A stopped flow attachment was used for the faster reactions, primarily La^{3+} + EDTA and La^{3+} + DTPA, and for most of the lanthanide series with EDTA, though the reactions were seen to occur with lifetimes suitable for conventional spectrophotometry. A 1 cm cell was used to determine k_{obs} for Ce^{3+} - Lu^{3+} + DTPA which were very slow reactions. For determinations using the stopped flow attachment, the drive syringes were filled and allowed to thermally equilibrate at 25 °C for 5 minutes before making the first injection. The first three injections were rejected and the fourth and subsequent

injections being recorded for kinetic analysis. For determinations using the 1 cm cell, 0.5 mL of each reactant solution was placed in the cell. The mixture was allowed to thermally equilibrate for 2 minutes which was determined previously to be long enough to bring fresh reactants in the cell to the desired temperature. The 1 cm cell was generally used when reactions times were 10 minutes or longer. Enough absorbance change data was collected after the 2 minute equilibration to not affect the calculated rate constant.

After performing experiments at a fixed set of conditions for the lanthanide series, an OLIS RSM-1000 stopped-flow spectrophotometer was used for data acquisition in the kinetics experiments to determine higher order rate constants and temperature variation to enable calculation of activation parameters for selected lanthanides. In these experiments, La^{3+} was measured using the 1000 scan/sec acquisition mode. After La(III), the reaction of Ln(III) with EDTA could be performed using the stopped flow attachment and RSM, yet the average mode had to be changed from 1000 scans/sec to 62 scans/sec. This allowed for a study of reactions that were complete in as long as 55 seconds, as was the case with Sm(III) + EDTA. After the middle of the lanthanide series, the rates slowed enough to require a change from the RSM and stopped flow to a single wavelength and a 1 cm cuvette holder. For Lu^{3+}, these reactions were complete in 20 minutes at 25 °C. Lanthanide (III) complexation with DTPA was slower still than what had been observed with EDTA. Like La(III)/EDTA, the La(III)/DTPA study was fast enough to be studied with the RSM on a second timescale. By Lu(III), these reactions took over 30 minutes to complete.

Under reaction conditions that provided a completion of the reaction in less than one minute, the rapid scanning monochromator (RSM) was used at a center wavelength of 605 nm. The OLIS RSM Robust Global Fitting software package was used to determine k_{obs}. La^{3+}, Pr^{3+},

Nd^{3+} and Sm^{3+} + EDTA and La^{3+} + EDTA have been determined by this method. With reactions that reached completion in more than one minute, kinetic traces were obtained at a single wavelength 605 nm using the same instrument with a 1 cm cell holder and single wavelength monochromator installed. For the lanthanides exhibiting slower kinetics, non-linear regression analysis protocols in Origin 8.0 was used to determine k_{obs}.[13]

La^{3+}, Pr^{3+}, Nd^{3+}, Sm^{3+}, Ho^{3+} and Lu^{3+} have been selected to determine higher order rate constants with Pr^{3+}, Sm^{3+} and Lu^{3+} being chosen to determine the activation parameters for complexation with EDTA. Reactions were considerably slower for DTPA experiments; therefore, only La^{3+}, Sm^{3+} and Lu^{3+} were selected for investigation. In the experiments, the Ln-EBT complex concentration in the syringe was 2×10^{-4} M with an EDTA/DTPA concentration in the range of 5 - 15 mM. A dilution of 50% occurs upon mixing. Ln(III)-EBT and EDTA/DTPA solutions were prepared using the borax buffer solution which maintained the solutions at a pH = 9.5. The temperature range of 15°C to 40°C has been chosen to allow calculation of the activation parameters. Solutions were allowed to thermally equilibrate at each temperature for five minutes before the first injection. The first three injections were not used in calculations. Determinations of the observed rate constants were made in at least triplicate under each set of conditions and averaged for data analysis. Additional reactions were performed with changes in the indicator concentration from 1.5 - 0.4 mM EBT to determine whether this limiting species had an effect on the rate of complexation. Ionic strength was held constant at 0.4 M $NaClO_4$ unless otherwise noted.

Results

Experiments have been performed to establish the reaction order with respect to EDTA and DTPA at pH 9.5 in a borax buffer. The significant difference between these experiments and

most of the previous data on these and similar solutions is that previous studies were performed under conditions of low to moderate acidity. With the exception of La^{3+}, the reactions in this work do not occur in a time regime suitable for study by stopped-flow spectrophotometry as has been performed in the previously mentioned experiments. Under all conditions the kinetic traces are adequately adjusted using the rate law appropriate for a single exponential decay.

Using the following experimental conditions, [Ln-EBT] = 1 x 10^{-4}, [EDTA] = [DTPA] = 4.6 mM, 25 °C and buffered at pH = 9.5 with a borax buffer, the variation in the observed pseudo-first order rate constants across the lanthanide series have been evaluated (Figure 4). It is seen that the lanthanide-EDTA complex formation rate decreases steadily from La^{3+} through about Dy^{3+}, then levels off; for the corresponding lanthanide-DTPA series the rates continue to decline through to the end of the series. After observing the trend in the lanthanide series under a fixed set of conditions, the experimental setup was changed so the higher order rate constants for Ln(III) with both the EDTA and DTPA could be determined. More detailed mechanistic studies were conducted with the lanthanides La^{3+}, Pr^{3+}, Nd^{3+}, Sm^{3+}, Eu^{3+}, Ho^{3+} and Lu^{3+} in the EDTA system and in the significantly slower DTPA system La^{3+}, Sm^{3+} and Lu^{3+} were used. The experimental conditions used set the concentrations of reactants at [Ln-EBT] = 2 x 10^{-4}, [EDTA] = [DTPA] = 5 - 15 mM and pH = 9.5 buffered with a borax buffer. The temperature was varied typically from 15 - 25 - 35 - 40°C. Table 1 shows the impact of a changing EDTA concentration on k_{obs} for La and Eu at 25 ℃. The rise in rate at low concentration and leveling off at higher concentrations is consistent with the postulation of a precursor equilibrium that is kinetically important.
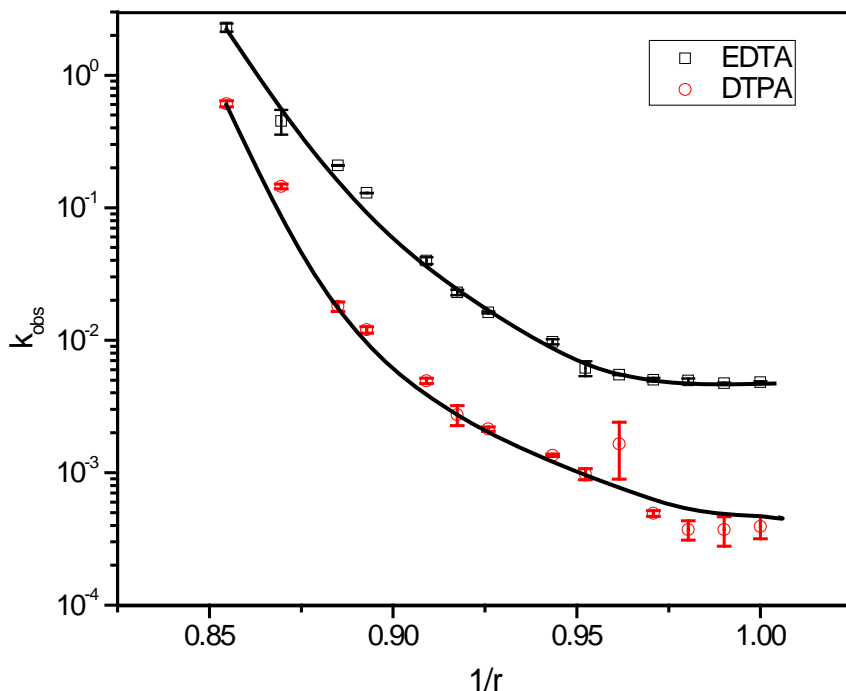
Figure 4: Plot of $\log(k_{obs})$ vs. $1/r$ showing changes in k_{obs} across the lanthanide series; [Ln-EBT] = 1 x 10^{-4} M, [EDTA] = 4.6 mM (upper); [DTPA] = 4.6 mM (lower); pH = 9.5; T = 25 °C.

Table 1: Observed rate constants for T = 25 °C, pH = 9.5 and $[M^{3+}]$ = [EBT] = 2 x 10^{-4} M.

	Lanthanum			Europium		
[EDTA]	k_{obs}	±	1σ	k_{obs}	±	1σ
0.005	4.9	±	0.2	0.05	±	0.01
0.007	6.4	±	0.3	0.065	±	0.001
0.009	7.4	±	0.3	0.070	±	0.003
0.012	9.6	±	0.5	0.081	±	0.006
0.015	12	±	1	0.094	±	0.002
0.02	14.0	±	0.7	0.102	±	0.005
0.03	17.1	±	0.9	0.120	±	0.003
0.035	18	±	2	0.121	±	0.003
0.04	16	±	1	0.11	±	0.02

Experiments to determine the dependence of the reaction rate on changes in indicator concentration have been performed by varying the concentration of EBT. Concentrations of EBT

118

used are 1.5, 2, 3 and 4 x 10^{-4} M with the [Ln] = 2 x 10^{-4} M, [EDTA] = 5 - 15 mM, pH = 9.5 and T = 25°C. Care had to be taken to not lower the EBT concentration below the point where precipitation of the lanthanide would occur. A precipitate was not observed with the 1.5 x 10^{-4} M EBT and was not expected at the higher concentrations as the lanthanum EBT complex is soluble and would not allow the precipitation of a hydroxide. The average observed rate constants for all EBT concentrations are 5.2 ± 0.3, 6.5 ± 0.3, 7.2 ± 0.4, 9.3 ± 0.9 and 11 ± 1 for [EDTA] = 5, 7, 9, 12 and 15 mM, respectively $\pm 1\sigma$ uncertainties. Results of these experiments compare favorably with work by Martin et.al[10,11] in that a change in [EBT] shows the rate of reaction is independent of indicator concentration, implying the rate of dissociation of Ln-EBT is not kinetically important.

Determination of System Parameters

Experiments performed at varying temperature also provided data that has been used to calculate activation parameters for the complexation reaction of the Ln-EDTA system. The concentration of the Ln-EBT complex in the syringe was 2 x 10^{-4} M with an EDTA/DTPA concentration in the range of 5 - 15 mM. Both solutions were prepared with a borax buffer solution which maintained the solutions at a pH = 9.5. The temperature range of 15°C to 40°C has been chosen to allow calculation of the activation parameters. From the variable temperature results, activation parameters can be calculated using Equation 1, the Arrhenius equation.

$$k = A\mathrm{e}^{-\mathrm{Ea/RT}} \tag{1}$$

The activation energy (E_a) and frequency factor (A) were fit using the linear form of Equation 1 as shown in Equation 2.

$$\ln k = \ln A - E_a/RT \tag{2}$$

The ln(k_{obs}) has been plotted for selected lanthanides vs. 1/T. This plot provides a straight line with slope equal to the activation energy and the intercept equaling the natural log of the frequency factor. The activation enthalpy and entropy are calculated from E_a and A using the Eyring formalism, Equations 3 and 4 respectively.

$$\Delta H^* = E_a - RT \tag{3}$$

$$\Delta S^* = R\ln A - R\ln(kT/h) - R \tag{4}$$

In Equation 4, k and h are Boltzmann and Planck constants respectively, T is the absolute temperature and R is the is the gas constant. The activation parameters related to k_2 for Pr^{3+}, Sm^{3+} and Lu^{3+} have been calculated and are listed in Table 2. All uncertainties are at the $\pm$ 1σ level unless otherwise noted.

Table 2: Activation parameters related to k_2 for selected lanthanides in the Ln-EDTA system at T = 25°C, pH = 9.5 and I = 0.4 M.

	ΔH* (kJ/mol)			ΔS* (J/mol·K)			ΔG* (kJ/mol)		
Pr	104	±	14	32	±	3	94	±	14
Sm	137	±	38	48	±	6	122	±	38
Lu	21	±	10	-50	±	2	36	±	10

Discussion

In experiments determining k_2, K_m and activation parameters, the EDTA/DTPA was present in sufficient excess over Ln(III) to maintain pseudo-first order conditions. For individual experiments, the absorbance vs. time data were adequately adjusted using a single exponential expression. The kinetics of lanthanide reactions with the chelating agents EDTA and DTPA in alkaline borate media have not been previously investigated by stopped-flow spectrophotometry. While stopped-flow spectrophotometry enables the measurement of rates of reactions that are complete within milliseconds, in this study it was found that the rate of the reaction varied greatly for reactions reaching completion in seconds for the lighter lanthanides and minutes for

the heavier lanthanides when forming complexes with EDTA or DTPA. In the work by Martin et.al, the complexation rates occurred in a timescale fast enough to require the stopped-flow technique throughout.

Since lanthanide aqueous ions are not strongly colored, application of spectrophotometric techniques to their complexation kinetics must rely on the use of a strongly colorimetric chelating agent, either as the subject ligands or as indicators of the free metal ion in the reaction of interest. Derivatives of chromotropic acid have proven to be quite useful in kinetic investigations of this type. Previous studies examined the rates of complex formation of a variety of lanthanide cations with Arsenazo – III (2, 2'- (1,8-dihydroxy - 3, 6 - disulfonaphthylene - 2, 7 - bisazo)bis(benzenearsonic acid).[2,10,11] Structures of Arsenazo III and EBT are shown in Figure 2A and 2B respectively for comparison.

While Arsenazo III is a good indicator for acidic conditions, it is not suitable for alkaline studies since no color change would occur. In acidic solutions, AAIII is blue when bound to the metal and changes to a pink after displacement and protonation. Under basic conditions, AAIII would be blue whether complexed or not. EBT is an azo dye complexometric indicator and was chosen to follow the reaction in this work owing to its good color change between complexed EBT and free EBT. The extinction coefficients of the bands at the λ_{max} = 608 nm are greater than 10^4 $M^{-1}cm^{-1}$, allowing the spectrophotometric monitoring of lanthanide concentration at 10^{-4} M. The observed λ_{max} for the free indicator, after being displaced by DTPA, is in good agreement but shifted slightly from the 616 nm at pH 9.0 and 10.1 reported by Ensafi and Selzer respectively.[14,15] Bound EBT ranges from 520 - 555 nm putting the observed λ_{max} for the La-EBT in reasonable agreement with literature values.[15-17] The best agreement came in the Selzer paper which presented a spectrum of the Mg-EBT complex with a λ_{max} of 520 nm at a pH = 10.

[15] The significant change in the visible spectrum upon changing from the Ln-EBT complex spectrum to the spectrum for free EBT is adequate to use in the determination of the kinetics for this system under these conditions. The observed rate constant was determined experimentally at both of these wavelengths for La^{3+}. The rates were the same within the accuracy of the measurements. The free EBT absorbance was chosen to monitor completion of the reaction showing the complete dissociation of the Ln(III)-EBT complex, thus indicating completion of Ln(III)-DTPA/EDTA complex formation.

In Figure 4, a plot of $log(k_{obs})$ vs. 1/radius for the complexation of lanthanides (except promethium) with both EDTA and DTPA (at fixed conditions) shows the decrease in k_{obs} with decrease in atomic radius. The rates of the reactions for La^{3+} + EDTA/DTPA are considerably faster than the rest of the series. The rate constants vary over a nearly 1000 fold range in values between La^{3+} and Lu^{3+}. Also shown is the divergence of the EDTA and DTPA upon moving across the series. It is interesting that the rate of reaction should decrease with increase z^2/r, as the electrostatic driving force for complexation should instead increase. This could imply that the stability of the Ln-EBT complex or the Michaelis-Menten bridged intermediate is increasing faster than that of the Ln-EDTA/DTPA product. Alternatively, this result might indicate that the hydration/dehydration rate of the cation or the intermediate is important. It is expected that the free energy of hydration of the lanthanide cations should increase across the series. Trends observed in this work showed a steady decrease in k_{obs} across the series with a large change between La and Ce. The work by Martin et al. did not display this behavior. In that work, all k_{obs} values were of the same order of magnitude with a maximum observed at gadolinium.[11]

In the previous lanthanide complexation kinetics study performed in this lab under TALSPEAK conditions,[10,11] a plot of k_{obs} vs. [EDTA/DTPA] gave a straight line with a slope

equal to k_{form} and a y-intercept equal to k_{diss}. If the data from this work is plotted as k_{obs} vs. [L], the pseudo-first-order rate constant (k_{obs}) shows a saturation effect as $[EDTA]_t$ and $[DTPA]_t$ increases (Figure 5).
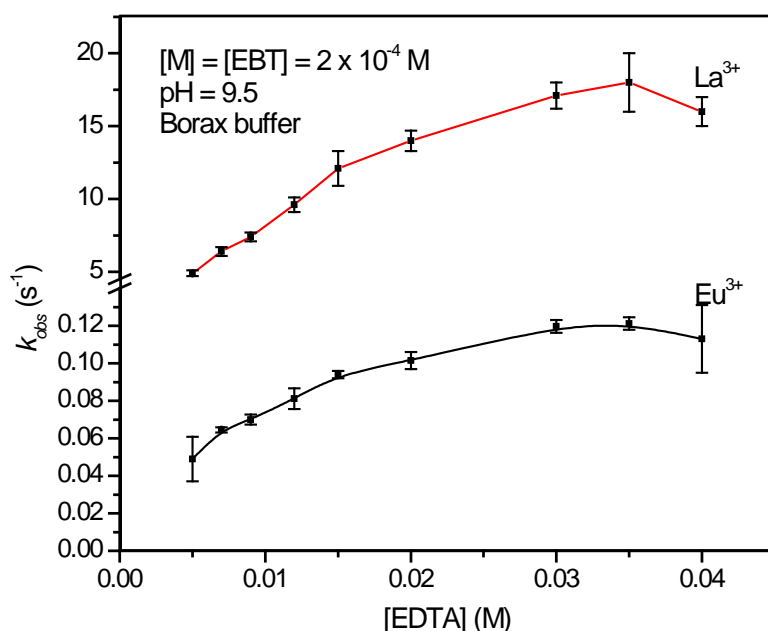
Figure 5: Plot of k_{obs} vs. [EDTA] for 2 x 10^{-4} M Ln/EBT solution (Ln = La or Eu) at 25°C and pH 9.5 using a borax buffer.

The apparent "saturation effect" is consistent with the interpretation of the formation of a stable precursor complex. A standard approach used to fit rate data that exhibits reactant dependence is the Michaelis-Menten reaction mechanism for enzyme kinetics.[18] This model describes the formation and dissociation of an intermediate complex via a steady-state approximation or a rapid pre-equilibrium. The steady-state approximation assumes that a reactive intermediate forms but will disappear as quickly as it forms whereas in the rapid pre-equilibrium the reactive intermediate has a finite lifetime. The steady-state approximation has been chosen here to be the best description of the system since a reactive intermediate was not observed

during the experiments. Under this formalism, the observed rate constant relates to the concentration of the EDTA or DTPA as follows:

$$k_{obs} = k_2[\text{L}]/(Km + [\text{L}]) \tag{5}$$

$$Km = (k_{-1} + k_2)/k_1 \tag{6}$$

From these equations it can be seen that a plot of $1/k_{obs}$ vs. $1/[\text{L}]$ will provide a straight line with a slope of K_m/k_2 and a y-intercept of $1/k_2$. Such a plot is shown in Figure 6 for La^{3+} and Eu^{3+} at pH = 9.5, μ = 0.4 M and T = 25 °C.

The steady state approximation has been chosen to describe the mechanism of lanthanide complexation with EDTA and DTPA at pH 9.5. This mechanism invokes an unstable intermediate of some defined structure. The steady state approximation assumes that this intermediate will disappear as quickly as it is formed. The reaction mechanism shown in Equation 7 is suggested for the present study.

$$\tag{7}$$

The first half of the reaction defines the formation of a ternary complex between the Ln-EBT complex and free ligand (L = EDTA or DTPA). The second half of the reaction shows the dissociation of this intermediate and the formation of free EBT and a 1:1 Ln-ligand complex. Due to the large excess of ligand relative to the indicator, the reverse of the second half of the reactions has been assumed to be negligible.

The reaction rate for the proposed mechanism can then be defined in Equation 8.

$$d[\text{Ln-L}]/dt = -d[\text{Ln-EBT}]/dt = k_2[(\text{Ln-EBT})\text{-L}] \tag{8}$$

The steady state approximation can now be applied to describe the formation and dissociation of the intermediate complex (Ln-EBT)-L as defined in Equation 9.

$$d[(Ln\text{-}EBT)\text{-}L] = k_1[Ln\text{-}EBT][L] - (k_{-1} + k_2)[(Ln\text{-}EBT)\text{-}L] = 0 \qquad (9)$$

which yields:

$$[(Ln\text{-}EBT)\text{-}L] = k_1[Ln\text{-}EBT][L] / (k_{-1} + k_2) \qquad (10)$$

The mass balance for the limiting reactant (Ln-EBT) is $[Ln\text{-}EBT]_t = [(Ln\text{-}EBT)\text{-}L] + [Ln\text{-}EBT]$ which can be combined with Equation 10, eliminating [Ln-EBT], to yield Equation 11.

$$[(Ln\text{-}EBT)\text{-}L] = k_1[Ln\text{-}EBT]_t[L]/(k_{-1} + k_2 + k_1[L]) \qquad (11)$$

Substituting Eq.11 into the rate law, Eq.8 and simplifying the resulting expression gives Equation 12.

$$-d[Ln\text{-}EBT]/dt = k_2[Ln\text{-}EBT]_t[L]/((k_{-1} + k_2)/k_1 +[L]) \qquad (12)$$

From which, the experimental rate constant, k_{obs}, is as follows.

$$k_{obs} = k_2[L]/((k_{-1} + k_2)/k_1) +[L]) \qquad (13)$$

The data, shown in Figure 6 for La^{3+} and Eu^{3+}, has been plotted in the form of $1/k_{obs}$ vs. $1/[L]$ which provides a straight line proving that evaluation of the data by the Michaelis-Menten reaction mechanism is valid under the experimental conditions. From the plot of $1/k_{obs}$ vs. $1/[L]$ the resolved rate constant (k_2) is determined from the y-intercept which equals $1/k_2$. The Michaelis-Menten composite rate constant $K_m = (k_{-1} + k_2)/k_1)$ can be determined from the slope, $m = K_m/k_2$. The values for k_{-1} and k_1 cannot be resolved from experimental information available. The resolved rate constants for k_2 and K_m (Michaelis constant) are provided in Table 2.
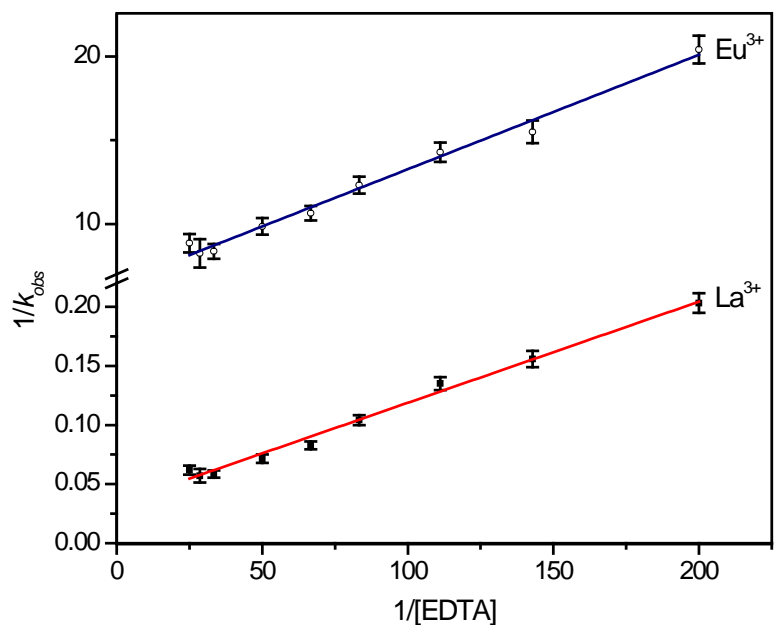
Figure 6: Michaelis-Menten plot of $1/k_{obs}$ vs. 1/[EDTA] for 2 x 10^{-4} M Ln/EBT solution (Ln = La or Eu) at 25°C and pH 9.5.

Table 3: Calculated values for k_2 and K_m, I = 0.4 M, pH = 9.5, T = 25 °C

Metal	ligand	k_2 (s^{-1})			K_m		
La	EDTA	19.8	±	0.7	.0145	±	.0007
Sm	EDTA	0.21	±	0.05	0.024	±	0.006
Eu	EDTA	0.16	±	0.01	0.011	±	0.001
Ho	EDTA	0.008	±	0.001	0.008	±	0.003
Lu	EDTA	0.0052	±	0.0002	0.0044	±	0.0005
La	DTPA	11	±	8	0.08	±	0.06
Sm	DTPA	0.014	±	0.006	0.03	±	0.01
Lu	DTPA	0.0018	±	0.0001	0.0030	±	0.0002

Activation parameters related to k_2 for Pr^{3+}, Sm^{3+}, and Lu^{3+} complexation with EDTA have been calculated. The Ln-EBT complex concentration in the syringe was 2 x 10^{-4} M with an EDTA/DTPA concentration ranging from 5 - 15 mM. A borax buffer solution maintained the solutions at a pH = 9.5. The temperature range of 5°C to 40°C has been chosen to allow calculation of the activation parameters. The parameters related to k_2 for these lanthanides at pH

= 9.5 are presented in Table 1. To calculate free energy of activation, the reference temperature of 25 °C (298 K) was chosen for each. Comparison of Pr^{3+}, Sm^{3+} and Lu^{3+} parameters provides insight into behavior of lanthanides throughout the series. The free energy of activation is the same for Pr^{3+} and Sm^{3+} lanthanides within a ±1 σ error and lower but still positive for Lu^{3+}. Typically ΔH* is less informative than ΔS* in these types of reactions. Relatively small values occur for ΔS* which result from small changes in the structure. Initially, the metal is bound by EBT acting as a tridentate ligand through the O, N and O shown in Figure 7. The incoming EDTA or DTPA binds through a similar O, N and O manner preserving the tridentate chelation. Changes in ΔS* of ~30 J/(mole·K) between metals can be explained by differences in hydration for the metal. This change is equivalent to one water molecule. The rate determining step in this reaction is the entrance of EDTA/DTPA followed by leaving of the EBT during which time a symmetrical EBT-M^{3+}-L intermediate is formed (Figure 7). The wrapping of the incoming ligand around the metal tips the balance resulting in the displacement of the EBT. The closing of the EDTA or DTPA around the metal probably comes after the rate determining step. A significant interaction with the softer nitrogen occurs when complexants such as EDTA or DTPA sterically forces the interaction.[3] The formation of the metal/nitrogen bond will be the slow step in the reaction.
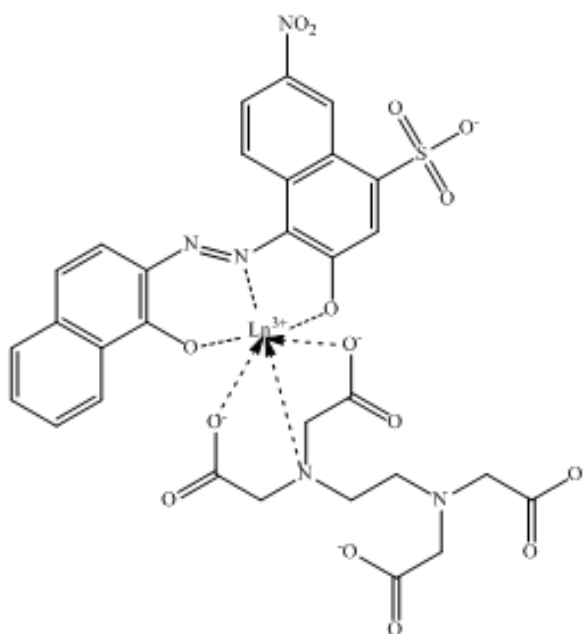
Figure 7: Proposed unstable intermediate/mechanism of EDTA/DTPA binding. EDTA is shown as an incoming group providing the O, N and O to replace EBT's O, N and O interaction with the Ln^{3+}.

As a comparison, activation parameters determined for the Ln-EDTA/DTPA system in lactate using La^{3+}, Tb^{3+} and Lu^3 show the entropy of formation as negative but very close to zero for La^{3+} (-20 ± 9 J/mol*K) and increasingly more negative upon moving across the series (Tb^{3+} = -126 ± 1 and Lu^{3+} = -165 ±16 J/mol*K).[10] The activation entropy associated with complex dissociation is largely negative for all three, -120 ± 24, -241 ± 32 and -154 ± 8 J/mol*K for La^{3+}, Tb^{3+} and Lu^{3+} respectively. The negative ΔS* had been interpreted to imply that there was not a substantial dehydration of the Ln^{3+} prior to interaction with the EDTA. The incoming EDTA first interacts with the metal as an outer sphere complex. Water will get pushed out of the coordination sphere as the EDTA carboxylate oxygen atoms begin to bond to the Ln^{3+}. This bonding would not be surprising being that the lanthanides behave as hard-acid cations that prefer hard bases such as oxygen. A significant interaction with the softer nitrogen occurs when complexants such as EDTA sterically forces the interaction.[3] On a whole; the reactions in lactic

128

acid have been mainly described by an associative reaction mechanism across the series. In the borate system, water may still be present in the intermediate complex however; it is of secondary concern in the kinetics of this system.

Conclusion

The rate of complexation of Ln(III) by EDTA and DTPA in basic media has been investigated by stopped-flow spectrophotometry and UV-visible spectrophotometry using the ligand displacement technique. A comparison of the results of this investigation with the prior work performed in moderately concentrated lactic acid media shows a considerable slowing of the reaction rate from acidic to basic conditions. This slowing became more pronounced across the lanthanide series with the rate of Lu(III) + DTPA being the slowest reaction of all performed. The saturation behavior observed in this system, i.e. appearance of Michaelis-Menten type kinetic behavior, was an unexpected observation. The postulation provided by Friese and coworkers most likely applies to this work as well. They suggest that the reaction pathway observed in their study may be common in ligand displacement reactions of the M-M type when the metal affinities of the competing ligands are of comparable strength.[19] The formation of a reactive intermediate even short lived one is probably necessary in the pH region studied. At pH 9.5, the $Ln(OH)_3$ would precipitate if nothing was available to compete against hydrolysis. The lack of precipitation helps confirm the Michaelis-Menten kinetics. The ligand exchange occurs without the release of free metal cations.

Acknowledgements

References

1) Choppin, G. R. Complexation Kinetics of F-elements and Polydentate Ligands. *J. of Alloys and Compounds* **1995**, *225*, 242-245.

2) Nash, K. L. and Rickert, P. G. Thermally Unstable Complexants: Stability of Lanthanide/Actinide Complexes, Thermal Instability of the Ligands, and Applications in Actinide Separations. *Sep. Sci. Tech.* **1993**, *28(1-3)*, 25-41.

3) Nash, K. L; Sullivan, J. C. Kinetics of Complexation and Redox Reactions of the Lanthanides in Aqueous Solutions. In *Handbook on the Physics and Chemistry of Rare Earths*; Gscheidner, K. A.; Eyring, L. Eds.; Elsevier Science Publishers B.V., 1991; Vol. 15, pp 341-391.

4) Laurenczy, G.; Brucher, E. Aminopolycarboxylates of Rare Earths. 12. Determination of Formation Rate Constants of Lanthanide(III)-Ethylenediaminetetraacetate Complexes via a Kinetic Study of the Metal-Exchange Reactions. *Inorg. Chim. Acta.* **1984**, *95(1)*, 5-9.

5) Ryhl, T. The Dissociation Rates of Yb, La and Cu EDTA Complexes. *Acta Chem. Scand*. **1972**, *26*, 3955-3968.

6) Ryhl, T. The Dissociation Rates of Pr, Nd, Eu and Er EDTA Complexes. *Acta Chem. Scand.* **1973**, *27*, 303-314.

7) Breen, P. J.; Horrocks, W. D., Jr.; Johnson, K. A. Stopped-flow Study of Ligand-exchange Kinetics Between Terbium(III) Ion and Calcium(II) ethylenediaminetetraacetate(4-). *Inorg. Chem.* **1986**, *25(12)*, 1968-1971.

8) Weaver, B.; Kapplemann, F. A. *TALSPEAK: A New Method of Separating Americium and Curium from the Lanthanides by Extraction from an Aqueous Solution of an Aminopolyacetic Acid Complex with a Monoacidic Organophosphate or Phosphonate* Oak Ridge National Laboratory Report No. 3559, 1964, 61pages.

9) Kolařík, Z.; Koch, G.; Kuhn, W. The Rate of Ln(III) Extraction by HDEHP from Complexing Media. *J. Inorg. Nucl. Chem.* **1974**, *36*, 905-909.

10) Martin, A.; Shehee, T. C.; Sullivan, J. C.; Nash, K. L. Kinetics of Lanthanide Complexation with Polyaminocarboxylates in Lactic Acid Media, I, EDTA. *Dalton Trans.* **2010**, Manuscript in preparation.

11) Martin, A.; Shehee, T. C.; Sullivan, J. C.; Nash, K. L. Kinetics of Lanthanide Complexation with Polyaminocarboxylates in Lactic Acid Media, II, DTPA. *Inorg. Chim. Acta.* **2010**, Manuscript in preparation.

12) *CRC Handbook of Chemistry and Physics*, 61st ed.; Weast, R. C., Astle, M. J., Eds.; CRC Press, Inc.: BocaRaton, FL, 1981, p D-148.

13) Origin Pro 8.0 (student version) Copyright 1991-2009 OriginLab Corporation.

14) Ensafi, A. A.; Hemmateenejad, B.; Barzegar, S. Non-extraction Flow Injection Determination of Cationic Surfactants Using Eriochrome Black –T. *Spectrochim. Acta, Part A* **2009**, *73(5)*, 794-798.

15) Selzer, G. and Ariel, M. Spectrophotometric Determination of Magnesium in Aluminum Alloys. *Anal. Chim. Acta* **1958**, *19*, 496-502.

16) Mushran, S. P.; Prakash, O.; Kushwaha, R. L.; Verma, C.K. Investigations on La(III) and Y(III) Chelates with Mordant Black Dyes. *J. Indian Chem. Soc.* **1978**, *LV*, 548-551.

17) Sulkowska, J.; Budych, A.; Staroscik, R. Extraction – Spectrophotometric Determination of Erythromycin in the Form of an Ion Pair with EBT. *Chemia Analityczna* **1985**, *30(3)*, 387-393.

18) Jordan, R. B. *Reaction Mechanisms of Inorganic and Organometallic Systems*, 2nd ed.; Oxford U. Press: New York, 1998, pg 263-264.

19) Friese, J. I.; Nash, K. L.; Jensen, M. P. and Sullivan, J. C. Interactions of Np(V) and U(VI) with Dipicolinic Acid *Radiochim. Acta.* **2001**, *89*, 35-41.

Chapter 6

Redox-based Separation of Americium from Lanthanides in Carbonate Media

Preface

Chapters Two and Three of this dissertation covered the kinetics of EDTA and DTPA complexation with lanthanides in lactic acid media. This work is directly related to the TALSPEAK process which separates trivalent actinides from trivalent actinides. The intention of this chapter is look at alternative methods to separate these elements in a reprocessing scheme. The separation that was developed in this chapter takes advantage of oxidized americium species to facilitate a separation. Ozone was used to oxidize americium to its hexavalent state with the lanthanides being precipitated by carbonate. The separation was studied in both sodium carbonate and bicarbonate solutions at a 1 M concentration. An initial precipitation of the trivalent hydroxide species was performed prior to oxidation in a carbonate solution. The separation was much more complete in the bicarbonate than in carbonate solution.

This paper will be submitted to *Radiochimica Acta* and has had the general formatting done to submit the work to this journal. WSU basic formatting requirements have been used which sets the entire document at double space one inch margins. All other formatting will be performed under the guidelines of *Radiochimica Acta*. Guidelines for this journal can be found in the appendix.

Redox-based Separation of Americium from Lanthanides in Carbonate Media

Thomas C. Shehee[1], Leigh R. Martin[2], Peter J. Zalupski[2], Kenneth L. Nash*[, 1]

[1]Chemistry Department, Washington State University, PO Box 644630, Pullman, WA 99164-4630

[2]Idaho National Laboratory, P.O. Box 1625, Idaho Falls, ID, 83415-2208

* Author for correspondence

Abstract

Dissolved used nuclear fuel mixtures contain U, Np, Pu, trivalent transplutonium actinides and lanthanides and other fission products representing a total of about 1/3 of the periodic table. Americium, being a long-lived α-emitter (and growing in concentration with storage due to decay of [241]Pu) is the greatest contributor to the radiotoxicity of the waste in the 300 - 70,000 year time frame after removal from the reactor. On this basis, Am is an attractive target for transmutation. Unfortunately, the lanthanides, representing about 40% of the mass of fission products, are neutron poisons that will compete with Am for neutrons in any advanced transmutation process. Thus the difficult mutual separation of Am from chemically similar lanthanides remains one of the largest obstacles to the implementation of advanced closed-loop nuclear fuel cycles that include Am transmutation. Early research utilized a solid-liquid separation in the first isolation and identification of plutonium. The upper oxidation states of Am (V, VI) are unstable but obtainable whereas the V/VI states are not accessible for Cm and the lanthanides. Furthermore, Am (VI) carbonate is soluble whereas the carbonates of Ln and Cm are insoluble. Higher order carbonate complexes of dioxo actinides have shown unusual stability,

as demonstrated by stability constants (log β_3 = 17.7, 22.1 and 21.6 for Pu, Np and U respectively), and solubility in basic media. Stability constants for Np and Pu are found in the Chemical Thermodynamics of Neptunium and Plutonium. Stability constants for U are found in the Chemical Thermodynamics of Uranium. If Am can be oxidized in, a separation is possible in carbonate containing solutions. Ozone with a standard potential of 2.075 V is a very strong oxidizing agent which makes it an adequate oxidant for americium. Ozone use is also advantageous in that only O_2 would remain after the redox adjustment is performed. The best separation results have been obtained in 1 M $NaHCO_3$ solution with < 2% Eu in the Am (VI) product and 4% Am being lost to the solid. At [Am] = 10^{-5} M the separation continues to work, with best separation results obtained in 1 M $NaHCO_3$ solution with < 1% Eu in the Am (VI) product and 4% Am being lost to the solid.

Introduction

Reprocessing of used nuclear fuel will be required in closing the nuclear fuel cycle. Several advantages can be had by reprocessing used fuel including the better utilization of uranium resources and reduction of both repository space required and the long-term hazards associated with high level waste. Current uranium resources are not adequate for the US to continue a once-through cycle that is based entirely on ^{235}U enriched fuel. Effective separation of Am from the lanthanides and Cm would allow for a more compact waste disposal plan; regardless if the goal is long-term storage or transmutation of transuranic elements. Removal of the lanthanides during the reprocessing of used nuclear fuel provides two main benefits. First, the lanthanides are neutron poisons that would interfere with the transmutation of transuranics in reactors or accelerators. Second, the lanthanides require a significant amount of volume in a long-lived storage facility. Destruction of the transuranics Pu, Np and Am would drastically

reduce the long-term radiotoxicity and heat load of any waste product [1]. After actinide recycle and transmutation, a repository must remain intact for only several hundred years rather than 10's of thousands or more years.

The separation of americium from the lanthanides has proven a challenge in acidic solution. Most approaches to accomplishing this separation have relied on the slightly greater strength of interaction of trivalent actinides with ligand donor atoms softer than oxygen. The TALSPEAK process [2], which was developed during the 1960s at Oak Ridge National Laboratory is, at present, considered the best option for the transmutation-enabling separation of trivalent Am and Cm from fission product lanthanides. TALSPEAK does not support separation of Am from Cm. TALSPEAK relies on diethylenetriaminepentaacetic acid (DTPA) to selectively retain Am and Cm in the aqueous phase while the lanthanides are extracted by bis(2-ethylhexyl)phosphoric acid (HDEHP) into the organic phase. Overall, it is a challenging process to control owing to the need for pH control in a narrow range, the enigmatic contribution from the buffer (lactic acid) and considerable strength of HDEHP balanced against DTPA. It could also be more challenging in UREX+1a process because of the presence of Np and Pu with Am and Cm. In the UREX+1a, which is the current baseline process shown in Figure 1, all TRUs remain together and all fission products are separated with the lanthanides being removed using TALSPEAK (Trivalent Actinide/Lanthanide Separation by Phosphorus reagent Extraction from Aqueous Komplexes. This reduces the short-term heat load and volume of waste disposal [1].
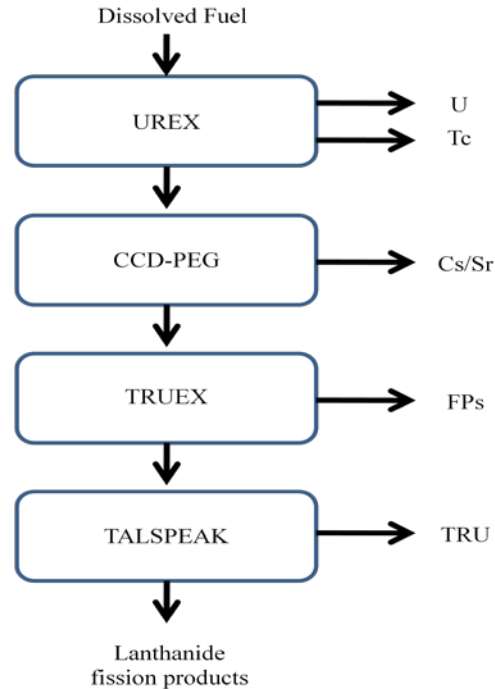
Figure 1: UREX flow sheet: UREX uses TBP (tri-butyl phosphate) as the extractant with acetohydroxamic acid added to reduce plutonium to its inextractable Pu(III) state; CCD/PEG – chlorinated cobalt dicarbolide/ polyethylene glycol; TRUEX – recovers transuranic actinides along with fission product lanthanides from remaining fission products; TALSPEAK.

An alternative approach to the previously mentioned processes might be to selectively separate Am from Cm and fission product lanthanides by selectively adjusting the oxidation state of Am to the penta- and/or hexavalent oxidation states followed by the precipitation of curium and the lanthanides. A separation method based on oxidized Am species would include the added advantage of allowing Cm to remain with the lanthanide fraction. It is widely noted that in a given oxidation state, actinides and lanthanides behave similarly, hence in a process that maintains trivalent Cm while Am is oxidized, it should be expected that Cm will accompany the lanthanides. A Cm/Ln waste stream would only require a few hundred years of decay before the greatest threat to radiotoxicity was abated.

The main curium isotope in used fuel (^{244}Cm) with its high specific activity would make the creation of Am/Cm transmutation targets more difficult. With Cm present the targets would have to be made within a hot cell; without the Cm, the targets could probably be produced in a

glove box. A disadvantage associated with the oxidation of Am to promote separation comes from the strongly oxidizing nature of Am (IV,V,VI) in acidic aqueous media; hence their application in solvent extraction processes could be problematic. Among others, Belova and coworkers [3] report that the radiolysis products of TBP would reduce the oxidized americium and consume the HNO_3 present within the system. For such a solvent extraction-based process to be viable, reagents capable of maintaining oxidized Am species (a holding oxidant) that does not simultaneously destroy the phase transfer ability of the extractant phase would be required. Mincher et al. [4] have reported preliminary results investigating the application potential of $NaBiO_3$ for such applications. Given the apparent limitations of separating oxidized Am species from lanthanides and Cm by solvent extraction and the evident advantages of isolating Am from Cm, developing separations based on oxidized Am still has significant appeal.

Though it was ultimately replaced by the far cleaner (and more efficient) option of solvent extraction, the first isolation of actinides either at the laboratory or industrial scale was accomplished using solid-liquid partitioning schemes. The $BiPO_4$ process [5] was scaled up from the microgram to the kilogram scale (a factor of 10^9) in the Manhattan Project to enable the creation of kilogram quantities of plutonium. Lanthanide fluoride co-precipitation processes were (and remain today) important analytical procedures supporting the isolation of the first samples of transuranium elements in the laboratory [6]. Though separation processes based on solid-liquid separation have a number of limitations, in the case of Am partitioning from Cm and lanthanides, accomplishing this task by other means has proven a formidable task.

There are a number of known approaches to lanthanide/actinide partitioning that involve (at an analytical scale) solid-liquid separations. Most are based on the observation that oxidized actinides stay in solutions while lanthanides (or reduced actinides) can be precipitated. A

fractional precipitation of americium and lanthanum oxalates has been shown to provide a highly enriched americium precipitate and about 50% of the lanthanum being rejected at each stage [7]. Separation of americium and curium by oxidizing americium to the hexavalent state with peroxydisulfate followed by a precipitation of CmF_3 has been reported [8]. Separation of Am (VI) from large quantities of the lanthanides has also been shown through precipitation of the lanthanide trifluorides [9]. These fluoride precipitations do achieve >90% separation; both employ 3 - 4 M HF as the precipitating agent. Use of HF for commercial reprocessing would be challenging due to its corrosive nature and general difficulty in handling HF solutions.

Americium oxidation has been accomplished using persulfate, ozone and electrochemical techniques which can be applied directly and indirectly in the oxidation of Am(III) to Am(VI). Current literature claims that Am (V) and Am (VI) have been prepared through the use of ozone in carbonate containing solution [10].Temperature, flow rate and contact time are all significant parameters to be considered when optimizing this system. Without a consideration of the possible complexes that can be formed with americium, the oxidation of Am(III) could be described by the following equations [11].

$$Am(III) + O_3 + 2OH^- \rightarrow AmO_2^+ + O_2 + H_2O \qquad (2)$$
$$AmO_2^+ + O_3 \rightarrow AmO_2^{2+} + O_3^- \bullet \qquad (3)$$
$$Am(III) + O_3^- \bullet \rightarrow Am(IV) + O_2 \qquad (4)$$
$$Am(IV) + O_3 + 2OH\text{-} \rightarrow AmO_2^{2+} + O_2 + H_2O \qquad (5)$$
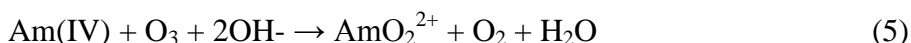
Experiments with 5 M K_2CO_3 verified the reaction mechanism seen in Equation 2 where the oxidation with ozone is accompanied by a replacement of the water molecule in the coordination sphere of the Am(III), however this experiment also demonstrated that an increased concentration of carbonate can sterically hinder the insertion of ozone resulting in an outer sphere process to form Am(IV) [11].

It has been reported that carbonate complexation may significantly increase the solubility of An(VI) [11]. It is well known that basic carbonate solutions form strong complexes with hexavalent actinide ions. The terminal complex, $AnO_2(CO_3)_3^{4-}$ ion, has been observed in U, Pu and Np and becomes the dominant species at relatively low carbonate concentrations between pH ≈ 7-11 [12,13]. The stability of uranyl triscarbonato ion $UO_2(CO_3)_3^{4-}$ allows its application to in situ leaching with carbonate as an effective mining and decontamination tool [14,15]. To add to the complexity of this system, a soluble tetra-hydroxide species has been identified as the dominant species at pH 12-14 [16-18]. It has been shown that the limiting species for Am(VI) in carbonate containing solution is $AmO_2(CO_3)_3^{4-}$ [19,20].

The separation of Am from Cm^{3+} and Ln^{3+} in this work will take advantage of the accessible pentavalent and hexavalent states as well as the ability of carbonate to stabilize these upper oxidation states of americium. The approach to obtaining oxidized americium, in this work, will be through ozonolysis. The chief benefit of ozone use for oxidation is that the by-products of ozonation will leave no residue.

Experimental

Reagents

Europium used in these experiments was diluted to 0.1M from a 0.488M $Eu(ClO_4)_3$ stock solution that was prepared from 99.999% Eu_2O_3 from Arris International Corp. and standardized using ICP-OES. Sodium carbonate and sodium bicarbonate were A.C.S. reagent grade from Fisher and J.T. Baker, respectively, and used as received.

Radioisotopes

Progress of the partitioning reaction was monitored radiometrically using [152/154]Eu (as a representative fission product lanthanide) and actinide ([233]U, [237]Np, [238]Pu, and [241]Am)

radiotracers. The use of a radioactive tracer allowed for accurate tracking of the lanthanide and actinide during the multi-step precipitation separation process. The isotope $^{152/154}$Eu has been made through by neutron irradiation of 99.999% Eu_2O_3 from Arris International Corp. at the Washington State University Nuclear Radiation Center's 1 MW TRIGA reactor. Actinide radiotracers were obtained from standardized stocks of the WSU and INL inventories.

Procedures

Both single and dual label experiments have been performed during this work depending on the location at which the work was performed. Single label experiments composed the majority of all experiments performed during this study. Work at the radiotracer level performed at the Harold Dodgen Research Center at Washington State University utilized single label experiments. All samples containing ^{241}Am and $^{152/154}$Eu were analyzed using a Packard Cobra II Auto-gamma counter with a three inch NaI(Tl) crystal. Single label experiments were also performed at this location using ^{233}U, ^{237}Np and ^{238}Pu radiotracers and a Beckman LS 6500 Multi-Purpose Scintillation Counter using National Diagnostics "Ecoscint" scintillation fluid. Studies performed at the Idaho National Lab were either single or dual label for ^{244}Cm or ^{243}Am and ^{154}Eu respectively. The use of curium with its 5.81MeV α decay required the employment of a liquid scintillation counter. All curium samples produced at the INL were placed in a 20mL glass scintillation vial with 20mL of Ultima Gold LLT scintillation fluid and counted on a Tri-Carb 3170TR/SL liquid scintillation counter. All americium samples produced at the INL were counted using an ORTEC Digital Gamma Ray Spectrometer, DSPEC Jr. 2.0. The counter has been optimized for 1 mL of solution in a 20 mL scintillation vial. Each sample was diluted to 1 mL to match this optimized geometry.

In single label experiments, 5 µL of the desired radiotracer was added to 250 µL of a 0.1 M Eu(ClO$_4$)$_3$ solution. To this homogeneous aqueous solution, 250 µL of 1 M NaOH was added to a 12 x 75 mm capped polypropylene tube to precipitate the trivalent hydroxide. Total concentration of americium in these experiments was 2 x 10^{-8} M. The tubes were centrifuged for 2 minutes to compact the solid precipitate followed by decanting the supernate. The hydroxide precipitate was slurried in 500 µL of either 1 M Na$_2$CO$_3$ or NaHCO$_3$. Ozone was then bubbled through the solution at a rate of 40mL/min. Ozone was produced by an AZCO Industries Limited laboratory ozone generator model CDO-8000S capable of producing up to 8 grams of ozone per hour. A 1 mL disposable pipette tip was used to deliver the ozone to the reaction vessel. After the ozone was bubbled through the solution for the desired time period of 2 hours, the sample was centrifuged for 10 minutes followed by decanting the supernate and sampling. The solid was washed once using the 1 M carbonate followed by a final centrifugation/separation step. All samples were analyzed by a Cobra II Auto Gamma counter with a three inch NaI(Tl) crystal.

Macro americium studies were performed at the Idaho National Laboratory. All work was performed in accordance to necessary Radiological Work Permit (RWP) and Lab Instructions (LI). Conformation to these procedures required slight modifications to the previously described procedure. Changes included use of 1.5 mL screw cap micro-centrifuge tubes instead of the 12 x 75 mm gamma tubes, dual labels for experiments looking at the separation of americium from a europium containing solution and a high purity germanium detector. In dual label experiments, 5 µL of both ^{243}Am and ^{154}Eu was added to 250 µL of a 0.1 M Eu(ClO$_4$)$_3$ solution. To this homogeneous aqueous solution, 250 µL of 1.0 M NaOH was added to a 1.5 mL screw cap micro-centrifuge tube. The tube was centrifuged for 2 minutes then a 350 µL aliquot was removed from the supernatant. The remaining solution and solid

hydroxide precipitate was slurried with 750 µL of either 1 M Na_2CO_3 or $NaHCO_3$. Ozone was then bubbled through the solution at a rate of 40 mL/min for two hours. Ozone was produced by an Ozone Solutions TS-10 ozone generator capable of producing 10 grams of ozone per hour. A 1mL pipette tip was used to deliver the ozone to the reaction vessel. After the ozone was bubbled through the solution for the desired time period, the sample was centrifuged for 10 minutes followed by removal of a 350 µL aliquot from the supernate. The use of curium with its 5.81MeV α decay required the employment of a liquid scintillation counter. All samples were placed in a 20 mL glass scintillation vial with 20 mL of Ultima Gold LLT scintillation fluid and counted on a Tri-Carb 3170TR/SL liquid scintillation counter. All americium samples were counted using an ORTEC Digital Gamma Ray Spectrometer, DSPEC Jr. 2.0. The counter has been optimized for 1 mL of solution in a 20 mL scintillation vial. Each sample was diluted to 1 mL to match this optimized geometry.

Identification of predominant solid species

X-ray powder diffraction was performed on a sample of the dried solid precipitate. The powder was held in place on a 2" square glass plate using petroleum jelly spread in an oval shape ~ 1 x 1.5". X-ray powder diffraction was performed using a Siemens Kristalloflex D500 diffractometer with the following parameters: Copper source (Kα; 1.5406Å); 35 keV, 3 0 mA, Kβ filter: Ni; scintillation counter detector; Continuous mode: 0.02 d/min; 2θ range: 5-55. The diffractograms were produced using supporting MDI Data Scan 4 and Jade 8 software packages. The raw pattern was compared to powder patterns in the ICSD (International Crystal Structure Database) to identify the material in the solid phase. Radiometric analysis of the supernatant was also completed to determine the amount of each isotope remaining in the supernatant phase.

The longer half-life of Am-243 allowed for utilization of macro concentrations (1 mM) of Am in UV-Vis investigations. Spectrophotometric analysis was performed with a Cary 50 spectrophotometer using a Cary 50 fiber optic coupler allowing the cell holder and samples to remain in the fume hood. The progress of the americium oxidation using ozone was monitored through the Am (III) characteristic peaks at 503 and 811 nm and the Am (VI) characteristic peaks at 666 and 996 nm. The americium was prepared by adding 0.5 mL of 1 M Na_2CO_3 to a dried sample of americium-243 in a 100 mm glass test tube. A 100 µL aliquot of the 1mM americium working solution was placed in a Hellma Quartz Suprasil Type# 105.253 – QS 1 cm cell and the spectra recorded. This aliquot was then returned to the test tube and ozone bubbled was bubbled through the solution until a color change occurred. A 100 µL aliquot of the 1mM americium working solution was then returned to the quartz cell and the spectrum recorded.

Results

Tracer Studies

To evaluate directly the separation of americium from the lanthanides, [241]Am was utilized at the radiotracer level. The europium radiotracer, [152/154]Eu, was used exclusively as a representative of the trivalent lanthanides. The results of these radiotracer experiments are shown in Table 1. The [152/154]Eu radiotracer results demonstrated that about 1.6% of the lanthanide will remain in solution after the ozonolysis when performed in 1M $NaHCO_3$ as compared to 12% in 1 M Na_2CO_3. The percent americium that was retained in the supernatant phase is consistent with the Am being predominantly hexavalent under these conditions. The average americium/europium separation factor $SF_{Am/Eu}$ (SF = %Am $_{aq}$/%Eu $_{aq}$) is about 47 and 1.6 for the bicarbonate and

carbonate systems respectively. The solid was washed with the results of the initial supernate and the wash supernate being combined to give a total radiotracer in the solution phase.

Table 1: Results of radiotracer [241]Am and macro [243]Am evaluation of the aqueous phase.

	Conditions	% Radiotracer	$SF_{Am/Eu}$ (aq)	$SF_{Am/Cm}$ (aq)
[241]Am (2×10^{-8} M)	$NaHCO_3$	95 ± 4	47 ± 2	
	Na_2CO_3	19 ± 2	1.5 ± 0.09	
[152/154]Eu (aq)	$NaHCO_3$	2.02 ± 0.04		
	Na_2CO_3	12 ± 5		
	Conditions	% Radiotracer	$SF_{Am/Eu}$ (aq)	$SF_{Am/Cm}$ (aq)
[243]Am (2×10^{-5} M)	$NaHCO_3$	96 ± 8	160 ± 13	96 ± 8
	Na_2CO_3	84 ± 7	1.5 ± 0.3	93 ± 13
[154]Eu (aq)	$NaHCO_3$	0.6 ± 0.3		
	Na_2CO_3	57 ± 16		
[244]Cm (aq)	$NaHCO_3$	1 ± 2		
	Na_2CO_3	0.9 ± 1.2		

Identification of predominant solid species

The pattern which gave a best match for the powder XRD has been used to identify solids formed in ozone oxidation/precipitation separations. The precipitation was performed on a cold (sample containing no radiotracer) sample of $Eu(ClO_4)_3$ following the same procedure as before. The powder XRD of experimental sample shown in Figure 2 is a $Nd_2(CO_3)_3 \cdot xH_2O$. Shown in the inset table are the 2 theta values for the tetra- and octa-hydrate used in the determination of the experimental sample. The 2:3 complex was observed in the speciation diagram as one of the major products in the pH 9 region. In this area, the expected dominate species present are the 2:3 and lanthanide hydroxy carbonate species. These two species would be responsible for precipitating trivalent species in this system.

Experimental sample	ICSD Database 8 hydrate	ICSD Database 4 hydrate
10.6	10.517	10.586
21.02	21.075	21.085
31.68	31.08	31.797
42.48	42.845	42.76
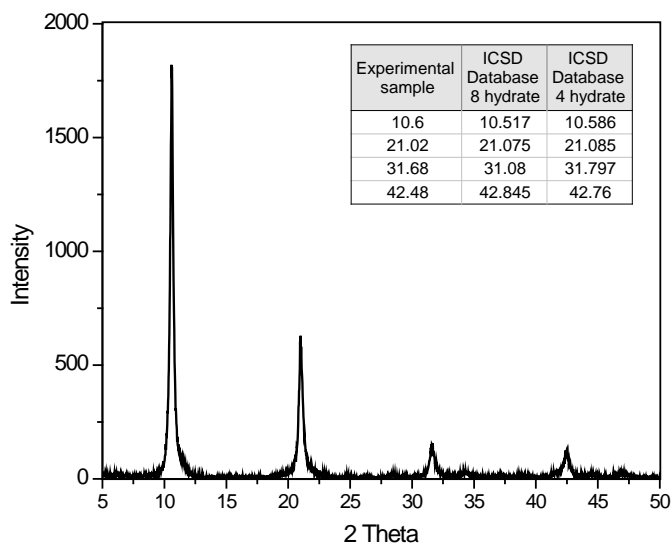
Figure 2: Powder XRD of experimental sample $Nd_2(CO_3)_3 \cdot xH_2O$ with 2 theta values for the tetra- and octa-hydrate.

<u>Macro studies</u>

In experiments performed at the Idaho National Laboratory the overall concentration of americium in solution was increased from 2 x 10^{-8} (in the radiotracer experiments) to 2 x 10^{-5} M. Parallel radiotracer studies were also completed at this time to profile the partitioning of ^{244}Cm. Dual label experiments using ^{243}Am and ^{154}Eu, evaluated the oxidation ability of ozone. When $NaHCO_3$ was used to slurry the hydroxide precipitate prior to oxidizing americium, 96% of americium and 1% of the europium remained in the supernatant after separation. Oxidation in Na_2CO_3 provided only 84% of americium and 57% of the europium in the supernatant phase.

As this procedure is designed to separate americium from curium <u>and</u> the lanthanides, the ozone/carbonate separation was tested using ^{244}Cm in a single label experiment. One percent of the curium tracer remained in the supernatant phase after treatment of the sample following the same procedure as followed with both americium and europium in Na_2CO_3 and $NaHCO_3$. This result is in good agreement with the percent europium that remains in the solution phase during

145

the separation in the absence of [244]Cm when NaHCO₃ is used. All associated errors are at the ± 1σ level. The results clearly establish the viability of the separation of Am from both Cm and lanthanides by this method. Results of these experiments can be seen in Table 1.

<u>Spectrophotometric studies of oxidation of Am by ozone</u>

The oxidation of americium by ozone has been followed spectrophotometrically by monitoring the disappearance americium (III) characteristic peaks at 503 and 811 nm, simultaneously monitoring the appearance of the characteristic peaks of Am(VI) at 666 and 996 nm. The initial spectrum of the reconstituted americium in carbonate solution displayed the characteristic peaks of trivalent americium at both 503 and 811 nm. After bubbling ozone through the solution for only a short time, the solution turned a brick red color which has been reported as the characteristic color of Am(VI) in a carbonate containing solution [21]. The spectrum of this solution has two small features at 689 and 757 nm and a very broad feature with a large molar absorptivity at ~ 600 nm as observed in Figure 3.
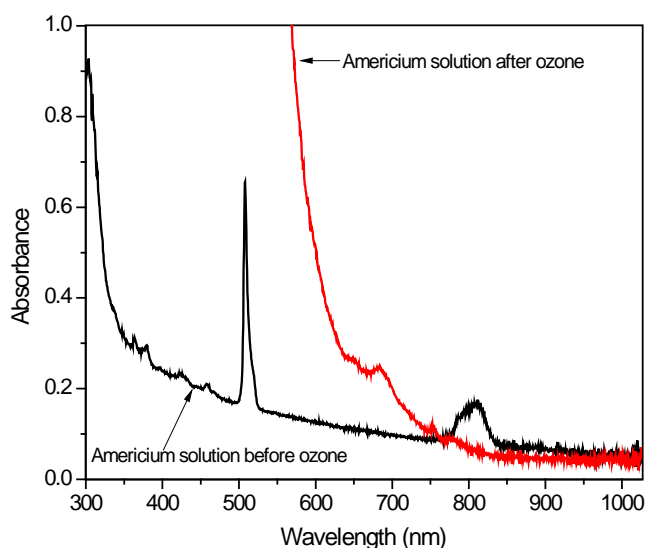
Figure 3: Spectra of 1.6 mM americium in 1 M NaHCO₃ before and after ozone.

Discussion

The separation of americium from curium and the lanthanides as described here requires the oxidation of Am to its pentavalent or hexavalent oxidation state. Actinides exist in four main oxidation states - lanthanides are primarily trivalent. For Am the higher oxidation states are still accessible, but the upper oxidation states are strong oxidants, i.e., easily reduced. The redox chemistry of americium changes considerably upon changing from perchlorate to carbonate media as demonstrated by the reduction potentials tabulated by Newton and Sullivan and reproduced partially here in Table 2 [22].

Table 2: Americium Reduction Potentials. Volts vs. S.H.E. at 25°C

Couple	1 M CO_3^{2-}	1 M $HClO_4$	Difference
Am(VI)/(V)	0.964	1.600	0.636
Am(V)/(IV)	1.1	0.83	-0.27
Am(IV)/(III)	0.92	2.60	1.68

In carbonate solutions, Am(VI) can oxidize Am(III) by means of the following equilibrium.

$$Am(III) + Am(VI) \leftrightarrow Am(IV) + Am(V) \tag{6}$$

This allows four valence forms to be present in aqueous carbonate solutions at any given time. Only the aquo ions Am^{3+} and AmO_2^{2+} are stable in dilute acid solutions, Am(IV) will disproportionate to Am(V) and Am(III) while Am(VI) will oxidize Am(V) to Am(VI) leaving only Am(III) and Am(VI) present in the solution.

Curium has a barely accessible tetravalent oxidation state as can be seen upon inspection of its standard potential of 3.1V [23], but does not appear in the penta- or hexavalent oxidation states in aqueous solutions. Likewise the only lanthanides that can be oxidized to the tetravalent oxidation state are Ce, Pr and Tb. All Ln(IV) are strong oxidants.

A study of the speciation of the hexavalent and pentavalent actinides vs. the trivalent lanthanides gives an indication of the thermodynamic basis for the separation by ozone oxidation and carbonate precipitation. The hexavalent actinide and trivalent species have been represented here by UO_2^{2+} and Eu^{3+} respectively. The speciation of Eu^{3+} in carbonate is taken as representative of the probable speciation for trivalent lanthanide ions and curium. The parameters chosen for calculation have the concentrations of the metal at 0.025 M and the ligand $(CO_3^=)$ at 0.5 M. These concentrations correspond to the total concentration of lanthanide and carbonate present in the experimental procedure. The log β values selected for these calculations are as close to or equal to an ionic strength of 1, approximating the experimental conditions (I = 1.5 M) with the exception of the solids produced. The stability constants used are shown in Table 3. The log β for the majority of Eu species used in these calculations came from the Martell and Smith database [24]. The exception to this is the β_{103} and β_{104} determined from log K_3 [25] and log K_4 [26] respectively. Stability constants for uranium were found in <u>Chemical Thermodynamics of Uranium</u> [27] and are set at infinite dilution to take advantage of the more complete and up to date constants present in this reference. Figure 4 presents log plots of UO_2^{2+} and Eu^{3+} species present in a 0.5 M CO_3^{2-} solution over the range pH 8-12. As can be observed in the speciation plots, the species present in solution at any point is pH dependent. During the separation scheme presented, the pH changes as follows:

1. 0.1M Eu(ClO$_4$)$_3$ pH = 3.4
2. After NaOH precipitation   pH = 12.0
3. Slurry with   NaHCO$_3$ pH = 9.2 / Na$_2$CO$_3$ pH = 11.7
4. After 2 hours under ozone   NaHCO$_3$ pH = 9.5 / Na$_2$CO$_3$ pH = 10.3

These pH changes become important to the quality of the separation when using sodium carbonate or bicarbonate. The dominant species observed calculations for the Eu(III) was the

hydrolysis product $Eu(OH)CO_3$ with concentrations remaining near that of the total metal, 0.025 M. $Eu(CO_3)_4^{5-}$ is the dominant species remaining in solution reaching its highest concentration at pH 10. This species would only make up ~ 0.3% of the total europium in the separation system. The insoluble europium species $Eu_2(CO_3)_3$, $Eu(OH)CO_3$ or $Eu(OH)_3$ dominate the speciation under the experimental pH range of 8-12.

Table 3: Stability constants for speciation plots

	log β		log β
$UO_2(OH)^+$	-5.2	$Eu(OH)_{3\ (s)}$	-16.8
$UO_2(OH)_{2\ (aq)}$	-10.3	$Eu(OH)_4^-$	-37.8
$UO_2(OH)_3^-$	-19.2	$EuOH^{2+}$	-8.07
$(UO_2)_2(OH)_2^{2+}$	-5.62	$Eu_2(OH)_2^{4+}\ \mu = 2$	-14.34
$UO_2CO_{3\ (aq)}$	9.68	$EuCO_3^+$	5.88
$UO_2(CO_3)_2^{2-}$	16.94	$Eu_2(CO_3)_{3\ (s)}\ \mu = 0.1$	31.8
$UO_2(CO_3)_3^{4-}$	21.6	$Eu(OH)CO_{3\ (s)}\ \mu = 0.1$	6.43
HCO_3^-	10.33	$Eu(CO_3)_2^-$	10.4
H_2CO_3	6.35	$Eu(CO_3)_3^{3-}$	13.1
		$Eu(CO_3)_4^{5-}$	14.95
		HCO_3^-	9.57
		H_2CO_3	6.03

1) Values for UO_2^{2+} - $\mu = 1$ and $t = 25°C$
2) All values for Eu speciation - $\mu = 1$ and $t = 25°C$ unless otherwise noted
3) Stability constants for UO_2^{2+} are found in Chemical Thermodynamics of Uranium [24]
4) Stability constants for Eu^{3+} are found in the Martell and Smith Database [25]
5) Eu hydrolysis products – $xM^{3+} + yH_2O \leftrightarrow M_x(OH)_y^{3x-y} + yH^+$
6) UO_2^{2+} hydrolysis products – $xM^{2+} + yH_2O \leftrightarrow M_x(OH)_y^{2x-y} + yH^+$
7) Eu carbonate products - $xM^{3+} + yCO_3^{2-} \leftrightarrow M_x(CO_3)_y^{3x-2y}$
8) UO_2^{2+} carbonate products – $xM^{2+} + yCO_3^{2-} \leftrightarrow M_x(CO_3)_y^{2x-2y}$

In the uranyl system, the predominant species held in solution were carbonate species. This is most likely due to the excess carbonate concentration that was used in the experiment.

The solubility limiting species $UO_2(CO_3)_3{}^{4-}$ is dominant for the pH of interest in this system, pH 8-12. This shows that the solubility limit of $UO_2{}^{2+}$ is ~ 10^{-2} M from pH 8 - 12 due to the triscarbonato complex. The species $UO_2(CO_3)_2{}^{2-}$ is a minor product from pH 8 – 12, yet it's concentration decreases from pH 8 – 11 at which the concentration begins to level. The 1:3 hydroxide species is a minor product that starts increasing at pH 11 yet does not have an appreciable affect over the desired pH range. The triscarbonato species would be the species responsible for achieving a separation of Am from Cm and the Ln's in this system. For comparison, the limiting species of a hexavalent americium solution is the triscarbonato, $AmO_2(CO_3)_3{}^{4-}$ [19,20].
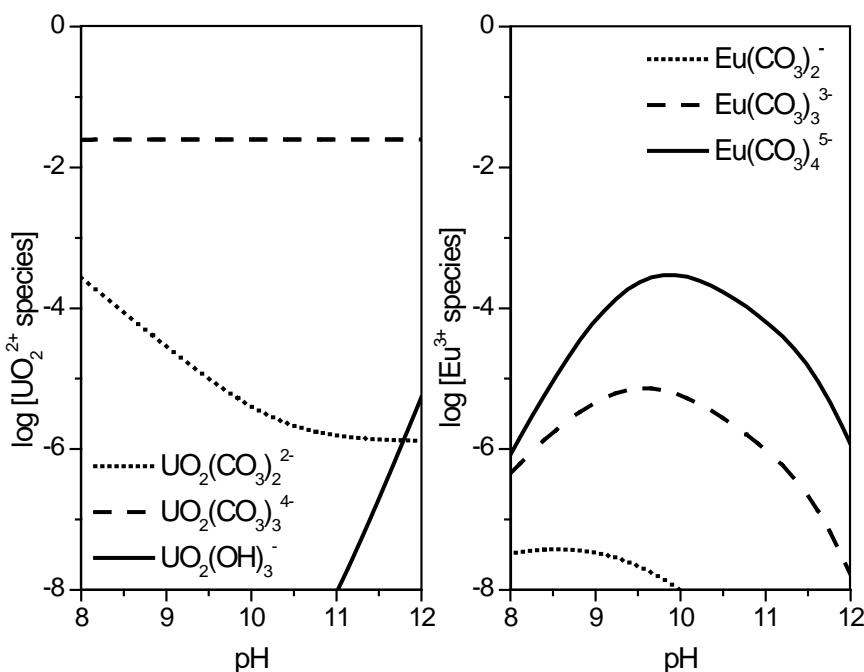
Figure 4: Log plot of $UO_2{}^{2+}$ and Eu^{3+} species present in a 1 M carbonate solution. The total metal in the calculation is set to 0.025 M.

Despite the presence of species favorable towards an Am/Ln separation over the pH range 8 - 12, it was determined that the best separation can be achieved at a pH ~ 9. This pH can

be achieved through the use of a 1 M $NaHCO_3$ solution to slurry the solid prior to oxidation with ozone. This separation has been studied with an $[Am]_{tot}$ of 2 x 10^{-8} and 2 x 10^{-5} with a dual label experiment being utilized with the higher concentration work performed at INL. The results of both can be found in Table 1.

Upon comparison of the results from radiotracer studies and this work, data from the oxidation of americium in a 1 M $NaHCO_3$ solution are in good agreement when taking into account the errors which are presented at $\pm$ 1σ. The percent Am remaining in solution after treatment with ozone is ~ 96%. This quantity of americium in the solution phase is interpreted to represent the completeness of americium oxidation under this set of conditions in the presented separation procedure. As predicted by the speciation calculations, the percent Eu remaining in the solution phase is low. Europium remaining in the solution phase after treatment was ~ 1 and 2% for work performed at INL and WSU respectively. Evaluation of this procedure with Cm afforded more insight into the capability of this procedure. As would be expected, the curium that remained in the solution phase was in perfect agreement with the percent Eu (1%) remaining in solution after treatment with ozone in the bicarbonate system.

Results from the oxidation of americium in 1M Na_2CO_3 do not agree between work performed at 10^{-5} and 10^{-8} M total [Am]. Percent americium in solution was considerably lower in this system at 19% with [Am] = 2 x 10^{-8} and was close to expected at 84% with [Am] = 2 x 10^{-5}. Drastic differences also occurred in the europium remaining in the solution phase. A higher concentration of Eu remains in the solution when Na_2CO_3 is chosen over $NaHCO_3$ at 12% Eu in solution after treatment. In the dual label experiment this increased to 57%. This increase was not observed when Cm tracer was evaluated under these conditions. The 1% curium remaining in the solution phase matches predicted values in the Eu speciation shown in Figure 4. Clearly there

are issues present in the oxidation in 1M Na_2CO_3 carbonate, whether pH dependent or species dependent has not been determined.

The ozone oxidation performed here resulted in the formation of an intensely red-brown solution that has been observed in the oxidation of Am(III), Am(IV), or Am(V) in aqueous 2 M carbonate solutions [10]. Spectral features of Am(VI) in $HClO_4$ and carbonate solution are drastically different. These spectra have been reproduced in <u>The Chemistry of the Actinide and Transactinide Elements</u> [19] from the original publication [28]. The Am(VI) characteristic peaks at 666 and 996 nm can be used to determine concentration. However, these peaks are not the major feature of Am(VI) in carbonate solution. The major feature is composed of a single broad absorbance and is similar to the feature observed in Figure 5 with uranyl peroxy carbonate, $UO_2(O_2)(CO_3)_2^{4-}$ [21,29,30].
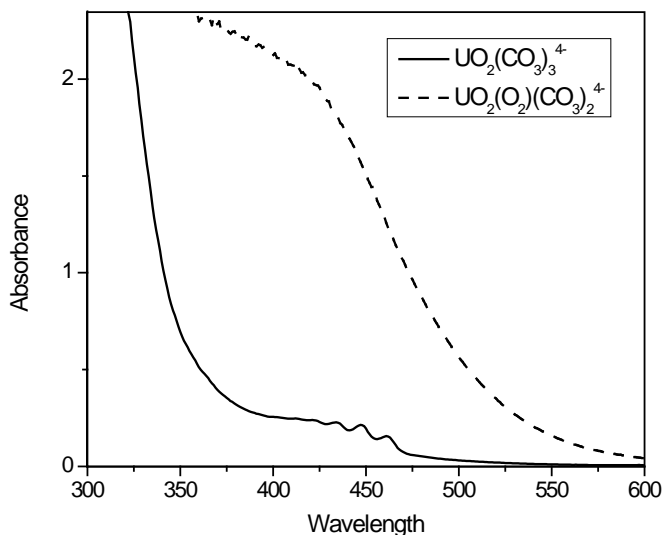
Figure 5: Spectra of $UO_2(CO_3)_3^{4-}$ and $UO_2(O_2)(CO_3)_2^{4-}$. $[UO_2CO_3)_3^{4-}] = 0.005$ M, $[H_2O_2] = 0.05$ M. Both solutions have been made using 0.1 M Na_2CO_3.

This feature is not only observed with UO_2^{2+} but also NpO_2^{2+} and PuO_2^{2+} [21]. Due to the appearance of the broad feature in the americium oxidation by ozone in carbonate solution shown in Figure 3, the presence of $AmO_2(O_2)(CO_3)_2^{4-}$ is suggested.

Conclusion

Through the use of ozone on a $M(OH)_3$ (M = Am, Cm and Ln's) in a 1 M Na_2CO_3 solution $\geq$ 50% separation of americium from curium and the lanthanides has been achieved in a single stage. Multi-stage efficiency has not been evaluated. Incorporation of this separation into current separation schemes could be done after UREX where uranium and technetium are separated first. NPEX would normally occur next however it would be possible for TRUEX to follow UREX. TRUEX was originally envisioned to separate the f-element from waste fission products such as Pd, Ru, Rh and Ag. The separation described in this paper would then follow TRUEX where trivalent species will be precipitated through the addition of NaOH. A portion of the actinide elements would remain in the solution. Any actinide remaining in the solution would be oxidized to their pentavalent or hexavalent state after the solid has been slurried in $NaHCO_3$ by bubbling O_3 through the slurry. The trivalent lanthanides and curium would remain a solid with the Am and any remaining Np or Pu being separated as a soluble species. The Am, Np and Pu could then be used together as targets in a fast reactor with the solid lanthanide and curium precipitate being sent to a repository.

Acknowledgements

References

1. Kelly, J.; Savage, C.: *Advanced Fuel Cycle Initiative (AFCI) Program Plan* 2005.

2. Weaver, B.; Kapplemann, F. A.: TALSPEAK: A New Method of Separating Americium and Curium from the Lanthanides by Extraction from an Aqueous Solution of an Aminopolyacetic Acid Complex with a Monoacidic Organophosphate or Phosphonate. In *Oak Ridge National Laboratory Report – 3559*, 1964.

3. Belova, E. V.; Egorov, G. F.; Nazin, E. R.: Thermochemical Oxidation of Components of Extraction Solutions and the Boundary Conditions of Thermal Explosion: 2. Effect of Radiolysis and Hydrolysis Products of TBP on the Kinetics of Gas Evolution in Thermal Oxidation of TBP with Nitric acid. Radiochem. **42(3)**, 257 (2000).

4. Mincher, B. J.; Martin, L. R.; Schmitt, N. C.: Tributylphosphate Extraction Behavior of Bismuthate-Oxidized Americium. Inorg. Chem. **47(15)**, 6984 (2008).

5. Thompson, S. G.; Seaborg, G. T.: Bismuth phosphate process for the separation of plutonium from aqueous solutions. US 2785951 19570319. 1957.

6. Seaborg, G. T.; Wahl, A. C.: The chemical properties of elements 94 and 93. J. Am. Chem. Soc. **70**, 1128 (1948).

7. Hermann, J. A.: *United States Atomic Energy Commission Unclassified and Declassified Reports* (Atomic Energy Commission and Its Contractors) 1956.

8. Stephanou, S. E.; Penneman, R. A.: Curium valence states; a rapid separation of americium and curium. J. Am. Chem. Soc. **74**, 3701 (1952).

9. Proctor, S. G.; Conner, W. V.: Separation of cerium from americium. J. Inorg. Nuc. Chem. **32(11)**, 3699 (1970).

10. Coleman, J.S.; Keenan, T.K.; Jones, L.H.; Carnall, W.T.; Penneman, R.A. Preparation and properties of americium(VI) in aqueous carbonate solutions. Inorg. Chem. **2(1)**, 58 (1963).

11. Shilov, V. P.; Yusov, A. B.: Oxidation of Americium(III) in Bicarbonate and Carbonate Solutions of Neptunium(VII). Radiokhimiya **37(3)**, 201 (1995).

12. Sullivan, J. C.: Reactions of Plutonium Ions with the Products of Water Radiolysis. In: *Plutonium Chemistry*, 1983 p.141.

13. Clark, D. L.; Hobart, D. H.; Neu, M. P.: Actinide Carbonate Complexes and Their Importance in Actinide Environmental Chemistry. Chem. Rev. **95**, 25 (1995).

14. Guilinger, T. R.; Schechter, R. S.; Lake, L. W.; Price, J. G.; Bobeck, P.: Factors Influencing Production Rates in Solution Mining of Uranium Using Basic Lixivants. Min. & Metall. Process. **2(1)**, 60 (1985).

15. Mason, C. F. V.; Turney, W. R. J. R.; Thomson, B. M.; Lu, N.; Longmire, P. A.; Chisholm-Brause, C. J.: Carbonate Leaching of Uranium from Contaminated Soils. Environmental Science and Technology **31(10)**, 2707 (1997).

16. Yamamura, T.; Kitamura, A.; Fukui, A.; Nishikawa, S.; Yamamoto, T.; Moriyama, H.: Solubility of U(VI) in Highly Basic Solutions. Radiochimica Acta **83(3)**, 139 (1998).

17. Maya, L.:Hydrolysis and Carbonate Complexation of Dioxoneptunium(V) in 1.0M $NaClO_4$ at 25 °C. Inorg. Chem. **22**, 2093 (1983).

18. Gelis, A. ; Vanysek, P.; Jensen, M. P.; Nash, K. L.: Electrochemical and Spectrophotometric Investigations of Neptunium in Alkaline Media. Radiochimica Acta **89(9)**, 565 (2001).

19. Runde, W. H.; Schulz, W. W.: *The Chemistry of the Actinide and Transactinide Elements*, 3rd ed., Morss, L.R.; Edelstein, N.M.; Fuger, J.; Katz, J.J.; Eds., Springer, 2006, Vol. 2, p. 1265.

20. Silva, R. J.; Bidoglio, G.; Rand, M. H.; Robouch, P. B.; Wanner, H.; Puigdomenech, I.: *Chemical Thermodynamics of Americium*, Elsevier, New York 1995.

21. Thompson, M. E.; Nash, K. L.; Sullivan, J. C.: Complexes of Hydrogen Peroxide with Dioxoactinide(VI) Species in Aqueous Carbonate and Bicarbonate Media. Israel J. Chem. **25**, 155 (1985).

22. Newton, T. W.; Sullivan, J. C.: In *Handbook on the Physics and Chemistry of the Actinides*; Freeman, A. J.; Lander, G.H., Eds.; North-Holland: Amsterdam, 1985, Vol. 3, p. 387.

23. Martinot, L.; Fuger, J.: Standard potentials of the actinides. Stand. Potentials Aqueous Solution. p. 631 (1985).

24. Martell, A. E.; Smith, R. M.: NIST Standard Reference Database 46 version 8.0, 2004.

25. Vercouter, T.; Vitorge, P.; Trigoulet, N.; Giffaut, E.; Moulin, C.: $Eu(CO_3)_3^{3-}$ and the Limiting Carbonate Complexes of Other M^{3+} F-elements in Aqueous Solutions: A Solubility and TRLFS Study. New J. Chem. **29**, 544 (2005).

26. Rao, R. R.; Chatt, A.: Studies on Stability Constants of Europium(III) Carbonate Complexes and Application of SIT and Ion-pairing Models. Radiochimica Acta. **54(4)**, 181 (1991).

27. Chemical Thermodynamics, Vol. 1. *Chemical Thermodynamics of Uranium*. North-Holland, New York. 1992.

28. Penneman, R. A.; Asprey, L. B.: Proceedings of the International Conference on the Peaceful Uses of Atomic Energy. **7**, 355 (1956).

29. Runde, W.; Brodnax, L. F.; Peper, S. M.; Scott, B. L.; Jarvinen, G.: Structure and stability of peroxo complexes of uranium and plutonium in carbonate solutions. Special Publication - Royal Society of Chemistry 305 (Recent Advances in Actinide Science), 174 (2006).

30. Goff, G. S.; Brodnax, L. F.; Cisneros, M. R.; Peper, S. M.; Field, S. E.; Scott, B. L.; Runde, W. H.: First Identification and Thermodynamic Characterization of the Ternary U(VI) Species, $UO_2(O_2)(CO_3)_2^{4-}$, in UO_2-H_2O_2-K_2CO_3 Solutions. Inorg. Chem. **47(6)**, 1984 (2008).

Chapter 7

Conclusion

Background

Removal of americium from used nuclear fuel is required when attempting to minimize the requirement of a long-term storage of wastes in a geological repository since it is the greatest contributor to radiotoxicity of the waste in the 300 - 70,000 year time frame after removal from the reactor. Being a long lived α-emitter, americium is an attractive target for transmutation. Unfortunately, the lanthanides, representing about 40% of the mass of fission products, are neutron poisons that will compete with Am for neutrons in any advanced transmutation process. Thus the mutual separation of Am from chemically similar lanthanides remains one of the largest obstacles to the implementation of advanced closed-loop nuclear fuel cycles that include Am transmutation. Two methods can be used to achieve the separation of Am and Cm from the lanthanides: 1) oxidation of Am to its pentavalent or hexavalent state to provide a different coordination environment for americium compared to the lanthanides or 2) the use of soft donors that will selectively complex the trivalent Am and not the trivalent lanthanide. Features of an oxidation/ precipitation separation as well as explorations of soft donor separations (TALSPEAK chemistry) have been presented with experiments ranging from acidic conditions to alkaline conditions. Studies performed under alkaline conditions were intended to evaluate the feasibility of a separation in a different realm than has typically been performed. Some aspects of TALSPEAK chemistry have been examined in systems containing acidic conditions.

Oxidation of americium and stability of the hexavalent state

Americium oxidation has been accomplished utilizing a variety of methods. Current literature claims that Am (V) and Am (VI) have been prepared through the use of ozone in

carbonate containing solution.[1] Temperature, flow rate and contact time are all significant parameters to be considered when optimizing this system. Without a consideration of the possible complexes that can be formed with americium, the oxidation of Am(III) could be described by the following equations.[2]

$$Am(III) + O_3 + 2OH^- \rightarrow AmO_2^+ + O_2 + H_2O \qquad (1)$$
$$AmO_2^+ + O_3 \rightarrow AmO_2^{2+} + O_3^- \bullet \qquad (2)$$
$$Am(III) + O_3^- \bullet \rightarrow Am(IV) + O_2 \qquad (3)$$
$$Am(IV) + O_3 + 2OH- \rightarrow AmO_2^{2+} + O_2 + H_2O \qquad (4)$$
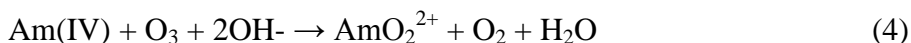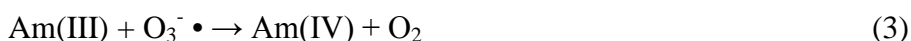
Experiments with 5 M K_2CO_3 verify the reaction mechanism seen in Equation 1, where the oxidation with ozone is accompanied by a replacement of the water molecule in the coordination sphere of the Am(III); however this experiment also demonstrated that an increased concentration of carbonate can sterically hinder the insertion of ozone resulting in an outer sphere process to form Am(IV).[2] The triscarbonato species has been shown to be a very stable soluble species. The terminal hexavalent complex, $AnO_2(CO_3)_3^{-4}$ ion, has been observed in U, Pu and Np and becomes the dominate species at relatively low carbonate concentrations between pH $\approx$ 7 and about 11.[3-5] It has been shown that the limiting species for Am(VI) in carbonate containing solution is $AmO_2(CO_3)_3^{-4}$.[6,7] The increased solubility of the ions formed through the complexation of the oxidized americium with carbonate would facilitate a separation of the lanthanides and curium from americium.

Asprey et al. and later Ward and Welch published a method to oxidize americium to the hexavalent state.[8,9] The oxidation of americium is thought to occur through two possible reaction paths. The first proposed path involves the Ag^+ being oxidized by persulfate. The oxidized silver then splits the persulfate into two sulfate radicals. The radical is thought to be responsible for the oxidation of the Am (III) to Am (VI). Following oxidation of the americium, the sulfate binds

with the lanthanide thus precipitating the sodium lanthanide salt. The second proposed path involves the direct interaction of oxidized silver with Am(III). Americium present as Am (III) is then oxidized by the divalent silver. The standard reduction potentials of silver and persulfate are:

$$Ag^{2+} + e^- \leftrightarrow Ag^+ \qquad\qquad E^o = 1.989V \qquad\qquad\qquad (5)$$

$$S_2O_8^= + 2e^- \leftrightarrow 2SO_4^= \qquad\qquad E^o = 2.01V. \qquad\qquad\qquad (6)$$
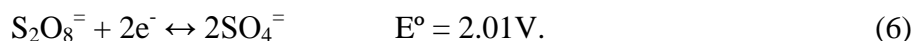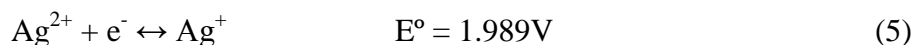
These show that both the Ag^{2+} and $S_2O_8^=$ both are sufficiently strong oxidants to oxidize the Am (III) to the hexavalent oxidation state. It is probable that both Ag^{2+} and $SO_4^- \cdot$ contribute to Am oxidation when silver is present. A possible complication arises in the decomposition of persulfate under acidic conditions. At acid concentrations $\geq$ 0.5 M, the peroxydisulfate is decomposed by a first order, acid-catalyzed path giving peroxy-mono-sulfuric acid which forms hydrogen peroxide.[10] The peroxide is known to reduce Am (VI). This should not be a concern within this system, as the persulfate should be stable under these conditions toward this possibly detrimental decomposition path. Silver nitrate has been used in all of the tracer studies given that the majority of the literature has used it in the oxidation of Am.[9,11] Penneman has been suggested that the use of silver nitrate as a catalyst is not necessary.[12] The apparent disagreement in the literature could be related to multiple pathways being utilized for the oxidation of americium using persulfate with (or without) silver.

Separation by oxidation of americium and precipitation of lanthanides

Although straight forward in theory, separations based on the oxidation of americium followed by precipitation of trivalent species proved to be challenging because of the heavy dependence on pH and general issues with reproducibility. Lanthanides and curium have been selectively precipitated while oxidized actinides remained in solution in both sulfate and

carbonate media. Solid lanthanide carbonates have been studied for many years, providing a wealth of information such as IR and crystal structures across the lanthanide series. These studies have shown that the degree of hydration is affected as the size of the metal decreases across the series. This lanthanide contraction will help demonstrate any systematic changes that could be possible that may increase or decrease the separation.

A fractional precipitation of americium and lanthanum oxalates was shown to provide a highly enriched americium precipitate and about 50% of the lanthanum being rejected at each stage.[13] Separation of americium and curium by oxidizing americium to the hexavalent state with peroxydisulfate followed by a precipitation of CmF_3 had been reported.[14] Separation of Am (VI) from large quantities of the lanthanides has also had been shown through precipitation of the lanthanide trifluorides.[15] These fluoride precipitations do achieve >90% separation; both employ 3 - 4 M HF as the precipitating agent. Use of HF for commercial reprocessing would be challenging due to its corrosive nature and general difficulty in handling HF solutions.

Separation in carbonate with ozone oxidation

Though many methods are available to facilitate the oxidation of Am from its most stable trivalent state, ozone was chosen initially to oxidize americium. The use of ozone was thought to allow for complete oxidation of americium without increasing the volume of waste inevitable in a reprocessing scheme. The oxidation was paired with carbonate to increase the solubility of americium as previously mentioned. Despite the presence of species favorable towards an Am/Ln separation over the pH range 8 - 12, it was determined that the best separation in the ozone oxidation in carbonate system was achieved at a pH ~ 9. This separation required the added step of an initial precipitation of the trivalent hydroxide followed by slurrying in a carbonate solution prior to oxidation. The ideal pH has been achieved through the use of a 1 M

160

NaHCO$_3$ solution to slurry the solid prior to oxidation with ozone. With the use of sodium bicarbonate, results were consistent day to day whereas sodium carbonate was not. This separation has been studied with an [Am]$_{tot}$ of 2 x 10^{-8} and 2 x 10^{-5}. At the higher concentration, a dual label experiment was utilized. This work has been performed at the Idaho National Lab.

Data obtained from the oxidation of americium at both concentrations in a 1 M NaHCO$_3$ solution are in good agreement when taking into account the errors, which are presented at $\pm$ 1σ. The percent americium remaining in solution after treatment with ozone was ~ 96%. This quantity of americium in the solution phase is interpreted to represent the completeness of americium oxidation under this set of conditions in the presented separation procedure. As predicted by the speciation calculations, the percent Eu remaining in the solution phase is low. Europium remaining in the solution phase after treatment was ~ 1 and 2% for work performed at INL and WSU respectively. Evaluation of this procedure with Cm afforded more insight into the capability of this procedure. As would be expected, the curium remaining in the solution phase in the bicarbonate system was in perfect agreement with the % Eu at 1% remaining in solution after treatment. Am/Eu separation factors have varied from 47 $\pm$ 2 to 160 $\pm$ 13 for 10^{-8} M ^{241}Am and 10^{-5} M ^{243}Am respectively. An Am/Cm separation factor of 96 $\pm$ 8 was also obtained.

Separation in sulfate with persulfate oxidation

As an alternative to ozone as the oxidizing agent persulfate (peroxydisulfate - S$_2$O$_8^=$) was studied believing that it could oxidize the americium in a carbonate containing solution. The extent of oxidation has been determined exclusively by the location of ^{241}Am or ^{243}Am following a separation. When using persulfate as the oxidizing agent, it was found that ~90% of the americium would remain in the solution phase after oxidation. The sulfate based separation was monitored using lanthanide ($^{152/154}$Eu) and actinide (^{233}U, ^{237}Np, ^{238}Pu, and ^{241}Am) radiotracers.

This separation resulted from a fortuitous observation during an attempt to oxidize Am in a carbonate solution. Before the exact conditions were found in the ozone/carbonate separation, it was decided to try persulfate as the oxidizing agent. The procedure had persulfate plus a small amount of silver added to the acid solution of an americium spiked sample with heating to 90 °C. After heating for 15 minutes, an aliquot of 1 M $NaHCO_3$ was added to precipitate the trivalent lanthanide. This seemed to work but in one experiment it was observed that a precipitate was formed prior to the addition of the carbonate solution. The separation was performed on this sample without addition of carbonate to find that the americium was in the solution and not precipitate.

The ^{233}U, ^{237}Np and ^{239}Pu have been used for comparison of redox behavior with americium. Since uranium is predominantly in the hexavalent oxidation state it can serve as the best analog for americium (VI) in this system. Monitoring uranium partitioning provides a clear picture of the extent of the precipitation and retention of hexavalent americium without need of first oxidizing the actinide. Neptunium and plutonium both also have accessible hexavalent oxidation state, but would are typically V and IV respectively prior to introduction to oxidizing conditions. Europium radiotracer, $^{152/154}Eu$, was used exclusively as a representative of the trivalent lanthanides.

The $^{152/154}Eu$ radiotracer demonstrated that 8.2% of the lanthanide will remain in solution after the precipitation has occurred. Longer times in the water bath and more persulfate did not aid in the completeness of the precipitation of the trivalent europium. Uranium, which did not require oxidation, had 93% remaining in the solution phase after precipitation occurred. From this, it is expected that this value is the essential separation capacity of the system. In comparison, neptunium and plutonium were in good agreement with the percent U(VI) retained,

though the neptunium retained was slightly reduced. Percent Np and Pu in solution amounted to 86 and 94% respectively. The extent of oxidation of the americium was inferred from the percent americium that was retained in the supernate phase of this separation system. From this, 94% of the americium was oxidized during the course of the experiment and therefore retained in the solution phase, presumably as a sulfate anionic species. This provides an actinide/europium separation factor $SF_{An/Eu}$ of ~ 11 for all systems.

TALSPEAK separation and chemistry

The TALSPEAK process[16], developed during the 1960s at Oak Ridge National Laboratory is, at present, considered the best option in the U.S. for the transmutation-enabling separation of trivalent Am and Cm from fission product lanthanides but does not separate Am from Cm. TALSPEAK relies on diethylenetriaminepentaacetic acid (DTPA) as a complexing agent to selectively retain Am and Cm in the aqueous phase while the lanthanides are extracted by bis(2-ethylhexyl)phosphoric acid (HDEHP) into the organic phase. The lanthanides behave as hard-acid cations in solution preferring hard-base donors such as oxygen and fluoride. Steric factors can force an interaction of nitrogen donors from some aminopolycarboxylic acid complexes. The actinides are slightly softer acid cations than the lanthanides which allows for the separation. Overall, it is a challenging process to control owing to the need for pH control in a narrow range, the enigmatic contribution from the buffer (lactic acid) and considerable strength of HDEHP balanced against DTPA. Depending on conditions, this process has provided single stage separation factors between the least extracted lanthanide, neodymium, and americium of 10-100.[16] The separation factors obtained in both precipitation separations show that these methods are comparable to the tried and true TALSPEAK.

Kinetics

The thermodynamics of a given system will provide information of only the energy required to move from one stable species to another. A viable Ln/Am separation can be based on species that have only transient stability, i.e., not based solely on thermodynamics, but rather based on kinetic factors. Transient species have been observed with the actinides in the presence of CO_3^{2-}, OH^-, and H_2O_2. Though not overly stable, they may be the key to a successful separation scheme in alkaline media. Stopped flow spectrophotometry can be used to evaluate stability through a study of complexation or de-complexation kinetics.

An important feature of the chemistry of the TALSPEAK process is the interaction of trivalent lanthanide and actinide cations with an aminopolycarboxylic acid holdback reagent (DTPA) for retention of trivalent actinides in lactic acid buffer systems. To improve our understanding of the mechanistic details of these processes, an investigation of the kinetics of lanthanide complexation by DTPA in concentrated lactic acid solution used in TALSPEAK has been performed. The interaction between the lanthanide and the holdback reagent could possibly hinder the separation under TALSPEAK conditions.

DTPA results

An important factor in TALSPEAK is that the lactate concentration has been shown to greatly influence the rate of the reaction.[17] This was also observed in the work presented here. Summation of the results and observations provide the overall rate law shown in Equation 7 below. The rate constants k_{form} and k_{diss} have been shown to be directly proportional to $[H^+]$ and inversely proportional to [Lactate].

Rate $= k_{form}$[Ln][DTPA]($k^1 + k^2$[H$^+$])

$$- k_{diss}\text{[Ln-DTPA]}(k^3 + k^4\text{[H}^+\text{])}/(1 + k'\text{[Lactate]}_{tot}) \qquad (7)$$

The [H$^+$] dependence was determined through an evaluation of the free lactate in the system. As the pH was increased, the concentration of free lactate also increased. Therefore, k_{form} is directly proportional to [H$^+$]. The k_{diss} was shown to be inversely dependent on the total lactate concentration. As [Lactate]$_{total}$ increased, k_{diss} decreases.

EDTA results

The extension of this data to EDTA provided information on changes in the backbone of the complexing ligands.

Rate $= k_{form}$[Ln][EDTA]/($1 + k'$[Lac]$_{free}$)

$$- k_{diss}\text{[Ln-EDTA]}/(1 + \text{k''[Lac]}_{tot}) \qquad (8)$$

The [H$^+$] dependence was determined through an evaluation of the free lactate in the system. As the pH was increased, the concentration of free lactate also increased. Therefore, k_{form} is directly proportional to [H$^+$]. The k_{diss} was shown to be inversely dependent on the total lactate concentration. As [Lactate]$_{total}$ increased, k_{diss} decreases.

The reactions proceeded with a first-order approach to equilibrium under all conditions. The results of these studies provide additional evidence that solvation and geometric constraints are major factors in the kinetics of lanthanide complexation by aminopolycarboxylate ligands. Negative values for ΔS* have been interpreted as an indication of an associative mechanism for both complex formation and dissociation of the Ln/EDTA complex though ΔS* for lanthanum k_{form} differs from the rest showing that it could be more of an associative interchange mechanism. With DTPA, ΔS* for lanthanum k_{form} is more negative than observed in EDTA making the La/EDTA unique. The addition of a surfactant did not affect the rate of complex

165

formation and only had a small effect on the rate of complex dissociation in both the EDTA and DTPA systems.

<u>Kinetics in alkaline conditions</u>

Although much work has been performed under acidic conditions, little work has been performed under basic conditions examining lanthanide complexation with aminopolycarboxylic acids. The complexation of the lanthanides with EDTA and DTPA, have been extended to alkaline solutions. A comparison of this work to the work performed in lactic acid media shows a considerable slowing of the reaction rate from acidic to basic conditions not observed in the lactate system. This slowing continued across the lanthanide series with the rate of Lu(III) + DTPA being the slowest reaction of all performed. Another difference comes from the unexpected appearance of Michaelis-Menton type kinetic behavior. This reaction pathway has been observed in previous studies and may be common in ligand displacement reactions of the M-M type when the metal affinities of the competing ligands are of comparable strength.[18] The rate law derived from this data is shown in Equation 9.

$$-d[\text{Ln-EBT}]/dt = k_2[\text{Ln-EBT}]_t[\text{L}]/((k_{-1} + k_2)/k_1) + [\text{L}]) \qquad (9)$$

The appearance of M-M kinetic features as well as the general speed of the reaction is thought to result from the strength of interaction of the indicator vs. the displacing ligand. The strength of the metal indicator complex increases across the lanthanide series, slowing the reaction. Observed rate constants decreased by a factor of nearly 1000 from La to Lu with the largest change occuring between La and Ce. From Ce, k_{obs} steadily decreases to Lu for both DTPA and EDTA.

What has been learned?

On December 2nd, 1942 the nuclear age began with operation of the first nuclear reactor. On July 16th, 1945 the awesome power of the atom was demonstrated with the detonation of the first atomic bomb. Robert Oppenheimer later said, "We knew the world would not be the same. A few people laughed, a few people cried. Most people were silent. I remembered the line from the Hindu scripture, the *Bhagavad-Gita*; Vishnu is trying to persuade the Prince that he should do his duty, and to impress him, takes on his multi-armed form and says, 'Now I am become Death, the destroyer of worlds.' I suppose we all thought that, one way or another."[19] With these occurrences, good and bad, the nuclear age had begun. The fallout of these earlier days still haunts us in the waste produced during weapons productions and the naïve idea put forth in the Carter administration that not allowing reprocessing would make the world safer. The need to reprocess is as important today as ever. Reprocessing legacy waste and used fuel will reduce the long term hazards associated with the peaceful use of atomic energy. The focus of this work was on a small but important piece of the puzzle where americium was separated from Cm and the lanthanides. The method chosen was a precipitation separation which has advantages over a solvent extraction technique but is not perfect. With any such endeavor, a comparison of similar techniques is required. The current U.S. selection for separation of trivalent actinides from lanthanides is not without issue.

The separation factors found in this work show that these separation approaches are competitive with the tried and true solvent extraction TALSPEAK.[16,20] A precipitation based approach does lack the ability to be performed in multiple stages; therefore, a higher separation factor may be required for separations with only one stage possible. However; with a pure enough americium phase as the supernate, the separation is viable. As a separation, the

precipitation methods described has been shown to work at the lab scale. Before a scale up could be performed, more tests should be performed. First, the introduction of known Am(VI) reducing agents such as H_2O_2 should be added testing the stability of the oxidized americium species $AmO_2(CO_3)_3^{4-}$ and $AmO_2(SO_4)_3^{4-}$. Second, a simulated fuel study with a mixture of probable lanthanides found in used fuel needs to be performed. Questions concerning the benefits in addition or removal of a metal catalyst could be evaluated more carefully with Ag as well as other metals such as ruthenium and rhodium already present in used fuel mixtures. The effects of radiolysis on the system components would have to be evaluated. Holding oxidants and contact times would need to be further evaluated. Finally, the ultimate question that has to be answered is: what is the best approach to handling radioactive solids?

The TALSPEAK process makes use of soft donors and slight differences in cation hardness to have a complete separation. The kinetic experiments presented herein add to the vast body of work related to TALSPEAK. The interaction of EDTA and DTPA with lanthanides under TALSPEAK like conditions has been studied. The work corroborated previous work, showing that there was a dependence on the lactic acid present. The lactic acid, which was used as a buffer, also acts as a weak complexing agent in the system. Since the DTPA is used as a holdback reagent for the trivalent actinides, the information provided here is useful in further optimizing the process with holdback reagents that have less interaction with lanthanides. Further work could find holdback reagents having less interaction with trivalent lanthanides. Ultimately, TALSPEAK works but a complete understanding has still not been achieved.

The extension of the EDTA/DTPA complexation kinetics to alkaline condition was primarily a fundamental study. The work demonstrated that the kinetic parameters for this system could be determined though the process was slow and arduous. The rate of complexation

with lanthanides was very slow with competition with the chosen indicator. Limits of the OLIS RSM 1000 were tested with this system and methods were found to complete an initial evaluation of the system. Further studies could profit from a re-evaluation of indicators, possibly finding one with less binding strength.

A world that has become increasing dependent on fossil fuels must make drastic changes in the near future in both the way it uses and produces electricity. An increase in energy production from nuclear power is the best means to meet current consumption in the US and the world while reducing the dependence on fossil fuels. A move away from fossil fuel, especially oil, in the US has a multiple benefits. Reducing our oil consumption will help maintain the wealth of our nation that too many people have come to expect. Second, we will set an example for the world by lowering our "carbon" footprint. Last of the benefits to be mentioned here is a preservation of national security when we reduce our dependence of fossil fuels from other countries.

References

1. Coleman, J. S.; Keenan, T. K.; Jones, L. H.; Carnall, W. T.; Penneman, R. A. Preparation and properties of americium(VI) in aqueous carbonate solutions. Inorg. Chem. **1963**, *2(1)*, 58-61.

2. Shilov, V. P.; Yusov, A. B. Oxidation of Americium(III) in Bicarbonate and Carbonate Solutions of Neptunium(VII). Radiokhimiya **1995**, *37(3)*, 201-202.

3. Chemical Thermodynamics, Vol.1. *Chemical Thermodynamics of Neptunium and Plutonium*. OECD Nuclear Energy Agency, Ed.; North-Holland, Elsevier Inc.: San Diego, Ca, 2001.

4. Sullivan, J. C. Reactions of Plutonium Ions with the Products of Water Radiolysis. In *Plutonium Chemistry*, Carnall, W. T., Choppin, G. R., Eds.; ACS Symposium Series 216; American Chemical Society: Washington, D.C., 1983; pp 241-249.

5. Clark, D. L.; Hobart, D. H.; Neu, M. P. Actinide carbonate complexes and their importance in actinide environmental chemistry *Chem. Rev.* **1995**, 95(1), 25-48.

6. Runde, W. H.; Schulz, W. W. Americium. In *The Chemistry of the Actinide and Transactinide Elements*; 3rd ed.; Morss, L. R., Edelstein, N. M., Fuger, J., Katz, J. J., Eds.; Springer: New York, **2006,** Vol. 2, pp 1265-1395.

7. Silva, R. J.; Bidoglio, G.; Rand, M. H.; Robouch, P. B.; Wanner, H. and Puigdomenech, I. *Chemical Thermodynamics of Americium*, Elsevier: New York (1995)

8. Asprey, L. B.; Stephanou, S. E.; Penneman, R. A. A new valence state of americium, Am(VI). *J. Am. Chem. Soc.* **1950**, 72(3), 1425-1426.

9. Ward, M.; Welch, G. A. The oxidation of americium to the sexavalent state. *J. Chem. Soc.* **1954**, 4038.

10. Kolthoff, I. M.; Miller, I. K. The Chemistry of Persulfate. I. The Kinetics and Mechanism of the Decomposition of the Persulfate Ion in Aqueous Medium. *J. Am. Chem. Soc.* **1951**, 73(7), 3055-3059.

11. Asprey, L. B.; Stephanou, S. E.; Penneman, R. A. A new valence state of americium, Am(VI). *J. Am. Chem. Soc.* **1951**, 73, 5715-5717.

12. Penneman, R. A.; Keenan, T. K. *The Radiochemistry of Americium and Curium*. NAS-NS-3006; United States Atomic Energy Commission [Unclassified and Declassified Reports], Atomic Energy Commission and Its Contractors: Los Alamos, NM, 1960.

13. Hermann, J. A. Coprecipitation of Am(III) with Lanthanum Oxalate. LA-2013; United States Atomic Energy Commission [Unclassified and Declassified Reports], Atomic Energy Commission and Its Contractors: Los Alamos, NM, 1957.

14. Stephanou, S. E.; Penneman, R. A. Curium valence states; a rapid separation of americium and curium. *J. Am. Chem. Soc.* **1952**, *74*, 3701-3702.

15. Proctor, S. G.; Conner, W. V. Separation of cerium from americium. *J. Inorg. Nuc. Chem.* **1970**, *32(11)*, 3699-3701.

16. Weaver, B.; Kapplemann, F. A. *TALSPEAK: A New Method of Separating Americium and Curium from the Lanthanides by Extraction from an Aqueous Solution of an Aminopolyacetic Acid Complex with a Monoacidic Organophosphate or Phosphonate.* Oak Ridge National Laboratory Report– 3559: Oak Ridge, TN, 1964.

17. Kolařík, Z.; Koch, G.; Kuhn, W. The rate of Ln(III) extraction by HDEHP from complexing media. *J. Inorg. Nucl. Chem.* **1974**, 36, 905-909.

18. Friese, J. I.; Nash, K. L.; Jensen, M. P.; Sullivan, J.C. Interactions of Np(V) and U(VI) with Dipicolinic Acid. *Radiochim. Acta.* **2001**, *89*, 35-41.

19. J. Robert Oppenheimer on the Trinity test (1965). Atomic Archive. http://www.atomicarchive.com/Movies/Movie8.shtml (accessed February 25, 2010).

20. Nilsson, M.; Nash, K. L. A Review of the Development and Operational Characteristics of the TALSPEAK Process. *Solvent Extr. Ion Exch.* **2007**, 25, 665-701.

Appendix

Kinetics with Lactic Acid

The rate constants determined in Chapters 2 and 3 for the kinetics of Ln^{3+} with DTPA and EDTA in a lactic acid buffer are presented in Table A1. These values were determined from a plot of k_{obs} vs. [DTPA] or [EDTA] which yields a slope = k_{form} ($M^{-1}s^{-1}$ x 10^3) and a y-intercept = k_{diss} (s^{-1}). These values have been intentionally left to two decimal places for the benefit of anyone looking at this data at a future date. Conditions were set at $[Ln^{3+}] = [AAIII] = 1$ x 10^{-4}, [DTPA] and [EDTA] = varied, I = 0.3 M ($NaClO_4$), [Lac] = 0.3 M and pH = 3.6.

As with many other studies involving lactic acid, in this work the lactic acid proved problematic/interesting. The lactic acid definitely takes part in the system but question of "How?" has not been fully or satisfactorily answered, if it even can be. In the end, two additional possibilities will have to be considered with more studies. These possibilities for EDTA include:

$$M(Lac)_n^{3-n} + H_2EDTA^{2-} \rightarrow Products \qquad\qquad (1)$$

Vs.

$$M(H_2O)_n^{3+} + H_2EDTA^{2-} \rightarrow Products. \qquad\qquad (2)$$

Additional experiments have been performed or envisioned that could aid in determining the extent of the role lactate plays in the kinetics. The first set of experiments made an attempt to control [Lactate]$_{free}$ at 0.15 M while changing the pH of the system. Basic experimental technique has been described previously in Chapters 2 and 3. Conditions are such that $[Ln^{3+}] = [AAIII] = 1$ x 10^{-4} and I = 0.3M ($NaClO_4$). To set [Lactate]$_{free}$ at 0.15M while changing the pH required changes in the total lactate of the system. At pH 3.2, the total lactate in the system is 0.86 M to maintain the free lactate at 0.5 M. In this solution, the characteristic blue observed in the Ln-AAIII solution is not present, replaced by a more purple solution that would not change

upon addition of the ligand. The experiment did behave "normally" at pH 3.7, 4.2 and 4.8 where the [Lactate]$_{total}$ = 0.33 M, 0.19 M and 0.16 M respectively. Plots of k_{obs} vs. [Ligand] are shown in Figures A1 and A2. Results of this experiment were inconclusive with only k_{diss} (s^{-1}) for DTPA increasing rather linearly with increase in [H$^+$]. The observation that k_{diss} (s^{-1}) for DTPA shows a dependence on [H$^+$] in this experiment is contrary to the results of Chapter 2 where k_{diss} was essentially constant upon changes in pH. Based on the findings in this experiment, the initial findings presented in Chapter 2 and 3 should be favored over results in these most recent experiments.

One more experiment has been envisioned to possibly shed some light on the role of lactate in this system. The experiment will be performed at variable ionic strengths. This might be instructive as the 2nd reaction above will have a greater z$^+$/z$^-$ effect than the 1st. Any other experiments will be performed prior to publication of material in Chapters 2 and 3 and will not be included in this dissertation.

Table A1: Compilation of rates constants determined in Chapters 2 and 3. All values have intentionally been presented to two decimal places for both k_{diss} (s^{-1}) and k_{form} (M^{-1}s^{-1} x 10^3)

	EDTA					
	k_{diss} (s^{-1})			k_{form} (M^{-1}s^{-1} x 10^3)		
La	5.75	±	0.05	7.91	±	0.06
Ce	4.70	±	0.28	6.40	±	0.37
Pr	4.33	±	0.41	8.43	±	0.41
Nd	3.54	±	0.14	7.81	±	0.16
Pm	--	--	--	--	--	--
Sm	6.78	±	0.25	8.56	±	0.27
Eu	7.31	±	0.30	9.78	±	0.34
Gd	4.89	±	1.02	17.88	±	1.14
Tb	3.77	±	0.82	13.02	±	0.92
Dy	0.65	±	0.35	11.80	±	0.38
Ho	0.24	±	0.43	11.70	±	0.49
Er	0.47	±	0.56	9.87	±	0.64
Tm	0.67	±	0.28	6.43	±	0.31
Yb	0.62	±	0.46	4.97	±	0.52
Lu	0.33	±	0.42	4.85	±	0.45

	DTPA					
	k_{diss} (s^{-1})			k_{form} (M^{-1}s^{-1} x 10^3)		
La	9.59	±	0.31	14.46	±	0.35
Ce	9.68	±	0.54	10.38	±	0.65
Pr	6.34	±	0.34	10.55	±	0.37
Nd	6.08	±	0.74	8.42	±	0.79
Pm	--	--	--	--	--	--
Sm	3.13	±	0.43	11.09	±	0.48
Eu	5.10	±	0.99	9.69	±	1.13
Gd	2.99	±	1.25	13.49	±	1.36
Tb	2.24	±	0.56	10.01	±	0.58
Dy	0.85	±	0.42	11.86	±	0.43
Ho	0.08	±	0.08	10.62	±	0.08
Er	-0.81	±	0.46	9.95	±	0.53
Tm	-0.54	±	0.46	9.00	±	0.50
Yb	-0.78	±	0.29	7.24	±	0.32
Lu	0.34	±	0.03	4.55	±	0.03
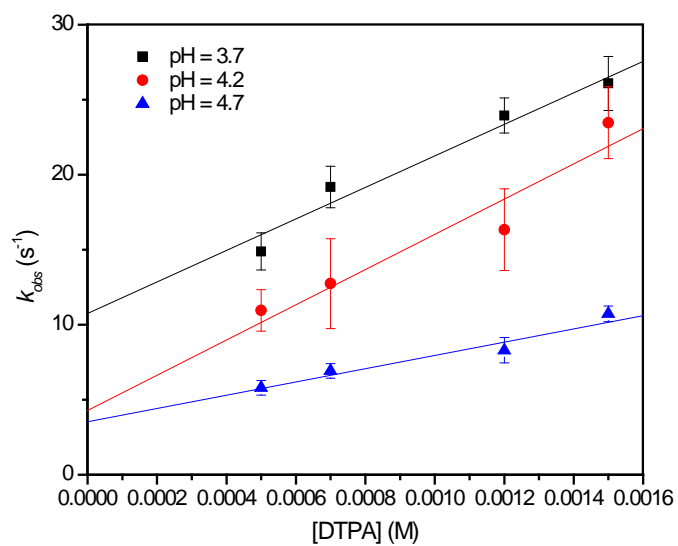
Figure A1: Plot of k_{obs} vs. [DTPA] at constant free lactate concentration. $[Ln^{3+}]$ = [AAIII] = 1 x 10^{-4}, I = 0.3M (NaClO$_4$), [Lactate]$_{free}$ = 0.15 M and T = 25 °C.
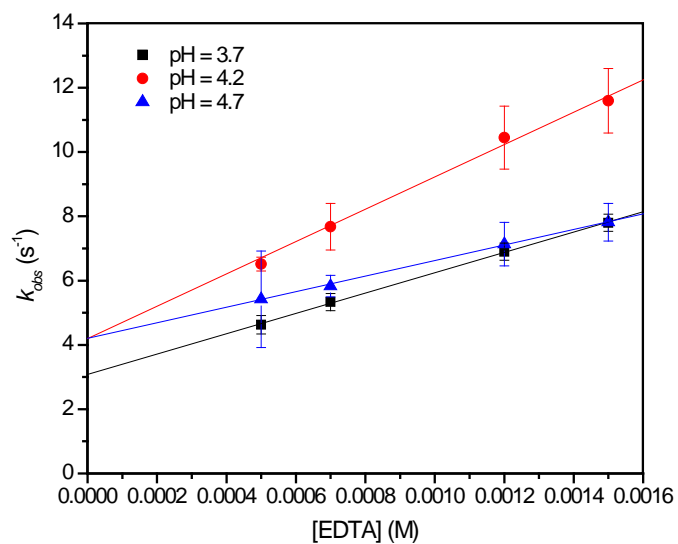
Figure A2: Plot of k_{obs} vs. [EDTA] at constant free lactate concentration. $[Ln^{3+}]$ = [AAIII] = 1 x 10^{-4}, I = 0.3M (NaClO$_4$), [Lactate]$_{free}$ = 0.15 M and T = 25 °C.

Table A2: Rates constants determined in pH study holding free lactate constant. All values have intentionally been presented to two decimal places for both k_{diss} (s^{-1}) and k_{form} ($M^{-1}s^{-1}$ x 10^3). $[Ln^{3+}] = [AAIII] = 1$ x 10^{-4}, $I = 0.3M$ ($NaClO_4$), $[Lactate]_{free} = 0.15$ M and T = 25 °C.

DTPA		
pH	k_{diss} (s^{-1})	k_{form} ($M^{-1}s^{-1}$ x 10^3)
3.7	10.76 ± 1.58	10.50 ± 1.45
4.2	4.29 ± 2.85	11.74 ± 2.63
4.7	3.54 ± 0.9	4.42 ± 0.83

EDTA		
pH	k_{diss} (s^{-1})	k_{form} ($M^{-1}s^{-1}$ x 10^3)
3.7	3.08 ± 0.06	3.16 ± 0.06
4.2	4.20 ± 0.39	5.03 ± 0.33
4.7	4.20 ± 0.04	2.42 ± 0.05

Table A3: Values of k_{obs} with 1σ absolute error for Ln series complexation to EDTA or DTPA at T = 25 °C, [Ln^{3+}] = [AAIII] = 10^{-4} M, [Lac]$_{tot}$ = 0.3 M, I = 0.3 M.

[EDTA]	La			Ce			Pr			Nd			Sm		
0.0012	15.2	±	2.5	12.4	±	0.1	14.3	±	2.2	12.9	±	1	17	±	3
0.0010	13.7	±	2.4	11.2	±	1.8	13	±	1.8	11.3	±	1.7	15.3	±	1.2
0.0007	11.3	±	1.9	9	±	1	10.3	±	0.8	9.2	±	0.8	13	±	2.1
0.0005	9.7	±	1.6	7.7	±	1	8.3	±	0.7	7.5	±	0.6	10.8	±	0.4
0.0002	7.3	±	1	6.3	±	0.6	6.1	±	0.1	5	±	0.8	8.3	±	0.8

[EDTA]	Eu			Gd			Tb			Dy			Ho		
0.0012	19	±	3	27	±	3	19	±	6	15	±	1.2	14.4	±	1.2
0.0010	17	±	3	22	±	3	17	±	6	12.2	±	0.9	11.7	±	0.9
0.0007	14.4	±	2.4	17.5	±	2.4	13.6	±	5.5	8.9	±	0.7	8.8	±	0.7
0.0005	12.3	±	2	13.5	±	2	9.7	±	4	6.2	±	0.4	5.7	±	0.9
0.0002	8.8	±	0.8	9.5	±	0.8	6	±	1.7	3.3	±	0.5	2.9	±	0.5

[EDTA]	Er			Tm			Yb			Lu		
0.0012	12.4	±	1	8.5	±	1	6.9	±	1	6.4	±	1
0.0010	10	±	1	7.1	±	1	5.2	±	0.9	4.9	±	0.8
0.0007	7.9	±	1	4.9	±	0.8	4.1	±	0.6	3.5	±	0.5
0.0005	5	±	0.8	3.9	±	0.7	2.9	±	0.6	2.7	±	0.4
0.0002	2.5	±	0.4	2.3	±	0.3	2	±	0.4	1.7	±	0.3

[DTPA]	La			Ce			Pr			Nd			Sm		
0.0012	27	±	2	22	±	1	19	±	2.2	16	±	1	16.5	±	1.1
0.0010	24	±	1.6	20	±	1.5	16.7	±	1.2	14.5	±	1.15	14	±	1
0.0007	19.8	±	1	17	±	1.5	14	±	1.1	12.4	±	1	11	±	0.85
0.0005	16.4	±	1	15.4	±	1.2	11.8	±	1	10.1	±	0.4	9.2	±	0.5
0.0002	12.8	±	0.8	11	±	0.6	8	±	0.5	6.2	±	0.1	4.9	±	0.4

[DTPA]	Eu			Gd			Tb			Dy			Ho		
0.0012	16.5	±	1	18.6	±	1.5	14	±	1.1	15.2	±	1.2	12.8	±	0.6
0.0010	14.3	±	0.6	16.7	±	1.5	12.7	±	0.6	12.3	±	0.6	10.7	±	0.5
0.0007	12.8	±	1	13.6	±	1.1	9.5	±	0.4	9.4	±	0.4	7.6	±	0.3
0.0005	10	±	0.5	9.4	±	0.5	7.4	±	0.3	6.9	±	0.3	5.4	±	0.4
0.0002	6	±	0.4	4.5	±	0.5	3.7	±	0.25	3.1	±	0.2	2.1	±	0.15

[DTPA]	Er			Tm			Yb			Lu		
0.0012	11.5	±	0.45	10.5	±	1	8	±	0.5	5.8	±	0.5
0.0010	8.8	±	0.5	8	±	0.7	6.3	±	0.5	4.9	±	0.4
0.0007	6.1	±	0.5	5.9	±	0.5	4.5	±	0.35	3.5	±	0.3
0.0005	4	±	0.3	3.8	±	0.4	2.5	±	0.2	2.6	±	0.2
0.0002	1.6	±	0.2	1.5	±	0.3	0.8	±	0.2	1.3	±	0.1

Table A4: Hydrogen ion dependence of La-EDTA/DTPA complexation for $[La^{3+}] = [AAIII] = 10^{-4}$ M, T = 25 °C and $[Lac]_{tot} = 0.3$ M. Observed rate constants.

[EDTA]	pH = 3			pH = 3.3			pH = 4			pH = 4.5		
0.0012	16.8	±	1.5	13.0	±	1.0	10.3	±	0.7	10.3	±	0.7
0.0010	14.6	±	1.1	11.0	±	0.8	9.2	±	0.5	9.2	±	0.5
0.0007	10.9	±	0.9	8.5	±	0.5	6.9	±	0.5	6.9	±	0.5
0.0005	8.5	±	0.5	6.6	±	0.5	5.4	±	0.4	5.4	±	0.4
0.0002	4.8	±	0.3	3.8	±	0.4	3.5	±	0.2	3.5	±	0.2

[DTPA]	pH = 3.3			pH = 3.5			pH = 4.3		
0.0012	27	±	1.2	27	±	1.2	21.5	±	2
0.0010	24	±	1	24	±	1	19.4	±	1.5
0.0007	19.8	±	0.7	19.8	±	0.7	16	±	0.65
0.0005	16.4	±	0.55	16.4	±	0.55	14.3	±	0.6
0.0002	12.8	±	0.4	12.8	±	0.4	11.2	±	0.9

Table A5: Dependence of reaction rate on lactic acid concentration at T = 25 °C and pH = 4 for La-EDTA system with $[La] = [AAIII] = 10^{-4}$ M. Observed rate constants.

[EDTA]	0.1 M Lac			0.2 M Lac			0.3 M Lac		
0.0012	14.8	±	1.0	12.5	±	0.5	10.3	±	0.7
0.0010	13.2	±	0.6	10.0	±	0.8	9.2	±	0.5
0.0007	11.6	±	0.5	8.6	±	0.5	6.9	±	0.5
0.0005	10.3	±	0.9	7.6	±	0.5	5.4	±	0.4
0.0002	8.0	±	0.5	5	±	0.4	3.5	±	0.2

[DTPA]	0.1 M Lac			0.2 M Lac			0.3 M Lac		
0.0012	51.8	±	1.5	41.0	±	1.0	34.0	±	2.0
0.0010	48.3	±	1.0	36.8	±	0.8	30.0	±	3.0
0.0007	42.5	±	1.0	32.0	±	0.8	25.0	±	2.0
0.0005	38.4	±	1.0	26.2	±	0.5	20.4	±	1.5
0.0002	32.3	±	0.8	22	±	0.5	14	±	1